2009

Peak Mitotic Cyclin Permits Mitotic Exit

Benjamin Drapkin

Peak Mitotic Cyclin Permits Mitotic Exit

A Thesis Presented to the Faculty of

The Rockefeller University

in Partial Fulfillment of the Requirements for

the degree of Doctor of Philosophy

by

Benjamin Drapkin

June 2009

Peak Mitotic Cyclin Permits Mitotic Exit

Benjamin Drapkin, Ph.D.
The Rockefeller University 2009

In eukaryotes, DNA replication, mitosis, and cytokinesis are all regulated by Cyclin-dependent kinase (Cdk). Cyclin/Cdk complexes promote replication origin firing and mitotic entry, and conversely, inhibit pre-replication origin loading and exit from mitosis. Cyclin synthesis and degradation, Cdk phosphorylation and Cdk inhibitors are controlled such that Cdk activity oscillates once per cell cycle.

Little is known about the quantitative relationship between the level of Cdk activity and the occurrence, rate, and coordination of cell cycle events. We have addressed this question in *Saccharomyces cerevisiae* by introducing titrated levels of undegradable mitotic B-cyclin (Clb2kd) in cells prior to release of a metaphase block. We calibrated single-cell Clb2kd levels to the peak level of endogenous Clb2 attained in a normal cell cycle and examined the ability of differing amounts of Clb2kd to affect completion of mitosis and initiation of the next cell cycle.

Clb2kd delays mitotic exit, and interferes with α-factor response and bipolar spindle assembly in the subsequent cell cycle. Distinct cell cycle events have different B-cyclin inhibitory thresholds; significantly, an amount of Clb2kd equal to the peak endogenous Clb2 level attained in a normal cell cycle only marginally restrains any aspect delays most aspects of mitotic exit.

Genetic experiments and *in vitro* kinase assays suggest that post-translational regulation of Cdk activity has only modest effects on these results; thus, Clb2kd levels are reliable indicators of Clb2kd/Cdk activity.

The ability of Cdk to both activate and inhibit sequential processes, combined with the oscillation of cyclin/Cdk activity, suggested 'ratchet' models to explain cell cycle ordering. If the Cdk activating threshold for the first event is greater than the inhibitory threshold for the second, then these thresholds form an activity ratchet that couples the sequence to Cdk oscillation. These models account for considerable data, but they have generally been tested by contrasting absence of Cdk activity to gross overexpression. We found that the normal peak level of Clb2 promotes efficient mitotic entry but cannot stably restrain mitotic exit or subsequent DNA replication. These results challenge ratchet models, and suggest that Cdk activity oscillation is insufficient to explain ordering of cell cycle events.

This thesis is dedicated to my grandparents,

Eli Drapkin and Frances Miller.

Acknowledgements

I gratefully acknowledge all of the help I have received from the members of the Cross and Rout labs. This work would not have been possible without a tremendous amount of cooperation on everybody's part.

A few people helped me a whole lot, and deserve special consideration. Andrea Geoghegan and Ying Lu performed a substantial number of the experiments presented here. Andrea performed all of the *swi5Δ* threshold measurements, and graciously allowed me to present her work to this thesis. She also assisted me in the SPB duplication and metaphase spindle measurements, and we have collaborated throughout the development of this work.

Ying Lu developed a novel method for monitoring Cdc14 release by time-lapse microscopy. He used this method to monitor Cdc14 release in cells pulsed with undegradable Cyclin B. This powerful method is as yet unpublished, and it is with his permission that I present the results here. His work is critical to my interpretation of my results, and I am grateful for its inclusion. In addition, Ying performed the four-color analysis of the effects of persistent cyclin B on the mitotic spindle.

Benjamin Timney wrote custom MATLAB software for the specific purpose of segmenting cell fields. Without this contribution, none of the threshold measurements would have been possible. Additionally, he assisted with the design of the threshold measurement method, and provided invaluable advice.

Lea Schroeder provided significant technical assistance for several experiments. And she taught me how to do a western blot. And she made the lab fun. Nick Buchler provided the plasmids and technical assistance that made it possible to derive a method to pulse undegradable Cyclin B at normal concentrations. Conversations with Jan Skotheim and Stefano D'Italia provided invaluable insight into a quantitative approach to my project in particular and the cell cycle in general. Their advice has undoubtedly shaped not only my thesis but also my future career in research, whatever the topic. Additionally, Stefano provided technical assistance for the time-lapse microscopy.

Mario Neipel, Caterina Strambio-de-Castillia, and Mike Rout assisted with development of the cell fixation method, and advice early on in the project. Additionally, Mike allowed me to keep attending his lab meetings and eating all his chocolate. Even earlier, Vincent Archambault taught me the basics protocols of yeast genetics and introduced me to the lab.

Finally, every experiment presented here is the product of Fred Cross's teaching, guidance, and support. And patience. Over the past few years, he has formed my entire approach to science, my chosen career. I don't know how to thank him enough.

Table of Contents

List of Figures

Introduction

Chromosome duplication and partition requires specific regulation.

The cell theory, a tenet of modern biology, states that all cells come from pre-existing cells by division (Schwann, 1847). The cell cycle describes the mechanism that underlies cell theory: the sequence of events by which a parent cell duplicates its components and divides them into two daughter cells capable of repeating the process (Hartwell et al., 1974). Most of these sub-cellular components are present in such large numbers that they partition equally without special regulation. However, the copy number of some essential components is too low for chance alone to guarantee their adequate distribution. Among the components of least abundance are chromosomes, the hereditary material, which may be present in as few as one copy per cell. Chromosomes provide instructions, both directly and indirectly, for the synthesis of all cellular components. To ensure complete transmission of these instructions to each generation, chromosome replication and segregation are highly regulated processes.

Chromosome transmission during cell division occurs in a sequence of discrete steps.

When external and internal prerequisites, such as sufficient size and nutrient availability, have been met, a cell initiates a program that leads to chromosome

replication and segregation. This commitment is termed START (Hartwell et al., 1974). Chromosomes replicate during an interval subsequent to Start, called S-phase. After DNA replication is complete the spindle segregates duplicated chromosomes to opposite ends of the cell during mitosis, or M-phase. Each cell receives one pole of the spindle (a microtubule-organizing center), and duplication of this pole in the next cell cycle is required to allow another bipolar spindle to form. Spindle poles are another critical component in single copy that must be duplicated exactly once, in this case to avoid multipolar or unipolar spindles, which would seriously disrupt accuracy of chromosome transmission in mitosis.

The intervals between S phase and M phase are referred to as G1 (gap 1, between M and S) and G2 (gap2, between S and M). The critical Start commitment event occurs in mid-G1. The final stage of the cell cycle, called mitotic exit, involves disassembly of the spindle, partitioning of the cytoplasm by cytokinesis, and steps to prepare the cell for G1 of the next cell cycle. The latter events include reloading of replication origins to prepare for DNA replication; preparation of spindle poles for duplication, and complete proteolysis of mitotic cyclins; the nature and regulation of these events is described in detail below.

In vitro DNA replication requires only helicase activity to unwind double-stranded DNA and a suite of enzymes to polymerize dNTPs into a copy of each strand (Kleppe et al., 1971). If unrestrained, these reactions would result in continuous DNA synthesis, which would render maintenance of gene copy

number impossible. In living cells, initiation of DNA polymerization requires prior licensing at specific locations, called origins of replication. In eukaryotes, the replication license is a DNA-bound multi-protein assembly called a pre-replicative complex (pre-RC) (Diffley et al., 1994). Once bound, the pre-RC must be activated to recruit the enzymes that polymerize DNA. Activation of the Pre-RC "fires" the origin, and DNA replication forks progress bi-directionally. Once DNA synthesis begins, the Pre-RC disassembles and cannot reassemble until after cell division.

Once chromosomes have been replicated, the spindle ensures that each daughter cell receives a complete genome. The spindle is composed of dynamic polymeric cables (microtubules), chromatid anchors (kinetochores), and polar anchors (centrosomes, or SPBs in yeast). Spindle microtubules extend from a centrosome to either the kinetochores or to microtubules emerging from the opposite centrosome. Kinetochore-attached microtubules are responsible for pulling forces that send chromosomes toward the centrosome. Attachment of sister chromatids to opposite centrosomes, called bi-orientation, generates tension at the kinetochores because the pulling forces are opposed by the cohesion complex, which binds sister chromatids (Michaelis et al., 1997). Simultaneous tension at every kinetochore is a prerequisite for cohesin cleavage by separase, a cysteine-directed protease (Orr-Weaver, 1999; Uhlmann et al., 1999; Uhlmann et al., 2000); this prerequisite is likely due to checkpoint control (see below). Cleavage of cohesin permits migration of sister chromatids toward

centrosomes, known as anaphase A (Straight et al., 1997). Microtubules that connect centrosomes, called pole-to-pole microtubules, push centrosomes to opposite ends of the cell in a process called anaphase B.

A contractile ring composed of actin and type II myosin mediates the cleavage of the cell into two daughter cells (cytokinesis) (Bi et al., 1998). Concentration of chromosome sets at distantly separated centrosomes allows cytokinesis between the poles to produce two daughter cells with complete genetic information and a single spindle pole.

The experiments presented here were performed in the budding yeast *Saccharomyces cerevisiae*. In this organism, formation of the actomyosin ring that mediates cytokinesis occurs just after Start. Thereafter most of the increase in cellular mass is transmitted through this ring, forming a bud that becomes the cell body of the 'daughter' cell. Unlike in animal cells, the yeast nuclear envelope does not break down during mitosis. Consequently, budding yeast SPBs are embedded in the nuclear envelope.

Several mechanisms, both intrinsic and extrinsic, could enforce the sequence of steps that lead to chromosome transmission.

Description of the molecular machinery that executes DNA replication, mitosis, and cytokinesis has been a major accomplishment of recent years, but leaves important questions about coordination and ordering unanswered. Centrosomes must be duplicated once and only once per cell division so that a

bipolar and not a multipolar or monopolar spindle will form (the latter two will result in aneuploidy). Replication origin licensing must be prevented during the interval between origin firing and completion of anaphase so that re-replication, either of individual origins or of the entire genome, does not occur before separation of the replicated genome. There must be enough time between origin firing and cohesin cleavage for bipolar spindle formation (since otherwise absence of tension between replicated sisters will result in random segregation to the two poles, with resulting aneuploidy (Michaelis et al., 1997). Spindle disassembly must not occur until anaphase is complete, and cytokinesis must not occur until spindle disassembly is complete. Finally, the molecular events of Start should be dependent on completion of mitosis, in order to prevent complete or partial cell cycle reinitiation before the ongoing cycle is complete.

These criteria define a strict order for the steps of cell division. Deviation from this order can lead to chromosome loss or re-replication, fragmenting of chromosomes by the cytokinetic furrow (the 'cut' phenotype, well known in fission yeast cell cycle mutants), and other disastrous outcomes. The temporal regulation of these events may be intrinsic, meaning that the nature of the events themselves dictates the order, or extrinsic, meaning that a signaling network controls the order of events.

The most straightforward type of intrinsic regulation is mechanical dependency, or a 'substrate-product' relationship: one process generates the substrate for a subsequent process, analogous to a linear metabolic pathway or

assembly of some multi-protein complexes, such as in bacteriophage assembly (Hartwell et al., 1974; Murray and Kirschner, 1989b). Clear examples of mechanical dependency certainly exist, such as the relationship between centrosome duplication and spindle elongation or, in *Saccharomyces cerevisiae,* bud formation and cytokinesis. Recent work has shown that centrosome duplication depends on prior centrosome separation (Simmons Kovacs et al., 2008). However, mutations and chemicals can relieve several dependencies necessary for cell division, including the dependency of mitosis on DNA replication, which implies that a substrate-product relationship does not govern these events (Gerhart et al., 1984; Weinert and Hartwell, 1989).

As an alternative to mechanical dependence, a pair of processes could have co-evolved rates such that they are completed in the correct order. For example, DNA replication could be intrinsically faster than spindle assembly, which in turn could be faster than actomyosin ring assembly. This type of control would only require one extrinsic regulatory step to start all the processes at the same time. This idea is difficult to evaluate, because it is in general unknown whether processes run at their intrinsic maximum rates *in vivo*, or are under regulatory controls.

However, these intrinsic rates could be surprisingly fast; for example, the cell cycles in the Drosophila blastoderm require less than 10 min for DNA replication, spindle formation and function, and resetting for the next cell cycle. These cells

lack membranes, so this situation does not provide a lower limit for time required for cytokinesis.

A third possibility is that ordered sequences of steps could derive from neither mechanical dependency nor intrinsic timing, but through surveillance mechanisms (commonly called 'checkpoints') that prevent one process until another is complete. In response to DNA damage or inhibition of DNA replication, *S. cerevisiae* cells do not initiate chromosome segregation. Similarly, spindle defects such as unattached kinetochores block anaphase and subsequent exit from mitosis. These dependencies can be eliminated by disruption of well-characterized signal transduction pathways that sense DNA damage or spindle deficiencies, and thus clearly do not derive from mechanical dependencies (Elledge, 1996). However, these surveillance systems are not required for normal alternation of replication and mitosis in yeast, since the signal transduction systems are genetically dispensable for viability; therefore, these mechanisms are not responsible for order in the unperturbed cell cycle, but instead function in the case of rare errors.

Cyclin dependent kinase (Cdk) regulates most of the events of cell division.

The best-established model for extrinsic control of cell division is based on cyclin-dependent kinase (Cdk). During the 1970s and 1980s, three independently discovered cell cycle regulators, *CDC28* in budding yeast, *cdc2-*

cdc13 in fission yeast, and MPF in amphibian oocytes, were found to oscillate in activity, once per division, and to be essential for Start, DNA replication and mitosis (Murray and Hunt, 1993). MPF oscillation in oocytes is independent of the execution of either replication or mitosis (Gerhart et al., 1984). These findings suggested than an extrinsic timer could control cell cycle events (Murray and Kirschner, 1989b).

Characterization of these regulators converged on a heterodimeric protein kinase composed of cyclin B and Cdk subunits (Beach et al., 1982; Gautier et al., 1988; Lohka et al., 1988). Cdk enzymatic activity absolutely requires cyclin binding. Both budding and fission yeasts possess a single major cell-cycle-regulatory Cdk (*CDC28* and *cdc2,* respectively); other organisms have multiple Cdks. Most organisms contain multiple cyclin genes, which in many cases exhibit considerable functional diversity (Bloom and Cross, 2007a).

Cdk could bind different cyclins to regulate each cell cycle event. Control of cyclin synthesis and degradation is gene-specific, and each cyclin has different substrate affinities (Bloom and Cross, 2007a). However, not all cyclin genes are essential. In fact, a single cyclin B gene is sufficient for replication and mitosis in both organisms: *CLB2* in *S. cerevisiae* and *cdc13* in *S. pombe* (Fisher and Nurse, 1996; Hu and Aparicio, 2005). In *S. pombe,* the cdc2-cdc13 complex is sufficient for all cell cycle events, but *S. cerevisiae* still most likely requires G1 cyclins (Clns) for Start as well as a B-type cyclin for DNA replication and mitosis.

Three mechanisms control Cdk activity: binding of an activating cyclin, binding of Cdk inhibitors (CKI's) to cyclin-Cdk complexes, and inhibitory phosphorylation of the kinase. Cyclins activate the Cdk catalytic subunit by altering its conformation, and contribute to the substrate specificity of the kinase, and cyclins are tightly regulated at the levels of transcription and protein stability (Bloom and Cross, 2007a; Miller and Cross, 2001; Morgan, 1996; Morgan, 1997). Cyclins are degraded by the 26S proteasome, and are targeted for degradation by ubiquitination (Zachariae and Nasmyth, 1999). In budding yeast, CKI's and regulators of cyclin expression and proteolysis, as opposed to Cdk phosphorylation and dephosphorylation are primarily responsible for the oscillation of Cdk activity (Amon et al., 1992).

Cyclin B / Cdk inhibits mitotic exit.

In frog egg extracts, Cyclin B synthesis is both necessary and sufficient to promote nuclear envelope breakdown and chromosome condensation in sperm nuclei, both early mitotic events (Murray and Kirschner, 1989a; Murray et al., 1989). Furthermore, Cyclin B is rate limiting for mitotic entry (Murray et al., 1989). Within these extracts, Cyclin B concentration oscillates, and the nuclei cycle accordingly.

In the same extracts, if an N-terminally truncated allele of Cyclin B (CYCΔ90) is added, mitotic entry occurs, but nuclear envelopes do not re-form and chromosomes do not de-condense. The extract does not cycle because unlike

wild-type cyclin B, CYCΔ90 is not degraded. These findings suggested that Cdk activity both promotes mitosis and blocks mitotic exit.

Degradation of Cyclin B is mediated by poly-ubiquitination of the N-terminus (Glotzer et al., 1991). Within the N-terminal domain, a 9 amino acid sequence, called the "destruction box" (D-box) is required for this ubiquitination. In *S. cerevisiae*, overexpression of a B-cyclin lacking the destruction box (Clb2Δdb) induces a telophase arrest with large-buds, an elongated spindle and segregated chromosomes (Surana et al., 1993). Thus, in both cell extracts and living cells, B-cyclin is necessary for mitotic entry and can inhibit mitotic exit if it cannot be degraded.

D-box dependent ubiquitination of Cyclin B requires an ubiquitin ligase called the anaphase-promoting complex (APC) (Irniger et al., 1995; King et al., 1995). In the absence of APC activity, endogenous Cyclin B is not degraded and over-accumulates (Irniger et al., 1995; Zachariae and Nasmyth, 1996). In an interesting case of coordination, the APC is also required for the D-box-dependent degradation of securin (Pds1 in budding yeast), which prevents breakdown of the cohesin complex and ensuing anaphase, because Pds1 inhibits the separase protease that cleaves the Mcd1 subunit of cohesin (Ciosk et al., 1998; Cohen-Fix and Koshland, 1999; Irniger et al., 1995). Thus, in the absence of APC activity, anaphase does not occur; but if the APC requirement for anaphase is bypassed (for example by *PDS1* deletion), absence of APC activity still yields cell-cycle-arrest, but in telophase, and this arrest is dependent

on accumulation of undegraded cyclin B (Shirayama et al., 1999; Thornton and Toczyski, 2003; Wäsch and Cross, 2002).

The requirement for Cyclin B degradation can be bypassed by overexpression of Cdk inhibitors, or by drug-mediated Cdk inhibition (Potapova et al., 2006; Thornton and Toczyski, 2003; Wäsch and Cross, 2002). Thus cyclin degradation is required for mitotic exit. Combined with the mitosis-promoting function, a model emerges in which a single oscillation of Cyclin B / Cdk activity defines the order of mitosis and mitotic exit (King et al., 1994). This model (which we term a 'ratchet' model) is discussed in detail below.

Cyclin B / Cdk inhibits Pre-RC formation.

Cell fusion experiments demonstrate that the cytoplasm from an S-phase cell promotes DNA replication in nuclei from G1 cells but not in nuclei from G2 cells (Rao and Johnson, 1970). This finding is clarified by the characterization of Pre-RCs, which are present in G1 cells but are disassembled during DNA replication (Diffley et al., 1994). The presence of Pre-RCs in G1 cells renders their chromosomes permissive for DNA replication, and Pre-RC absence after S-phase renders G2 chromosomes non-permissive (Wuarin and Nurse, 1996).

Cdk activity directly inhibits Pre-RC formation. Cdk phosphorylation inactivates several Pre-RC components, either through resultant degradation, nuclear export, or conformational change (Nguyen et al., 2001). Mutation of these phosphorylation sites results in over-replication, implying that these Cdk-

dependent phosphorylations are specifically inhibitory and do not contribute to initiation of replication.

Cdc6 is a highly unstable component of the Pre-RC, and upon its depletion, replication does not occur (Piatti et al., 1995). If Cdc6 is restored in these cells before expression of Cyclin B, Pre-RCs form and DNA replication occurs. If Cdc6 is expressed after Cyclin B accumulates, Pre-RCs cannot form. Furthermore, if Cyclin B expression is delayed by deletion of S-phase cyclins *CLB5* and *CLB6*, the window during which Pre-RCs can form is extended (Piatti et al., 1996). This series of experiments suggests that endogenous levels of cyclin B-Cdk activity can prevent pre-RC formation.

After replication, some Cyclin B-Cdk complexes bind specifically to fired origins of replication, forming a post-replicative complex which is likely to enhance local negative control of pre-RC formation (Wilmes et al., 2004; Wuarin et al., 2002).

Cyclin-Cdk complexes are required for pre-RC firing to initiate DNA replication.

Formation of the pre-RC is referred to as 'licensing' the origin, since a fully loaded pre-RC is competent to initiate replication. However, pre-RC formation is not sufficient for replication. In contrast to the inhibitory effect of cyclin-Cdk on pre-RC formation, which is required for origin firing, fully loaded and competent ('licensed') pre-RCs will not initiate replication in the absence of cyclin-Cdk (in

yeast, B-type cyclin-Cdk) (Schwob et al., 1994). This is due at least in part to the requirement for Cdk phosphorylation of essential replication factors for replication to initiate (Tanaka et al., 2007; Zegerman and Diffley, 2007).

Manipulation of Cdk activity can change the order of cell cycle events.

In a series of beautiful genetic experiments in *S. pombe*, Paul Nurse and colleagues demonstrated that normal Cdk function is necessary to prevent mitosis before the completion of replication and, reciprocally, that Cdk is required to prevent re-replication. Analogous experiments have been performed in budding yeast, with generally similar outcomes.

Hydroxyurea (HU) treatment prevents dNTP synthesis, which in turn prevents DNA replication. HU arrests wild-type cells prior to mitosis. However, a mutant *cdc2* allele, *cdc2-3w*, was isolated that allows cells to undergo mitosis in the presence of HU (Enoch et al., 1991). Furthermore, in cells that cannot replicate DNA because of Pre-RC depletion, simultaneous overexpression of wild-type *cdc2* and *cdc13* drives mitosis without prior replication (Hayles et al., 1994). A similar experiment performed in budding yeast results in mitosis without cyclin overexpression. Inhibition of Cdk activity in these cells prevents aberrant mitosis (Piatti et al., 1995). Together, these results imply that Cdk activity is necessary to enforce dependency of mitosis on prior replication.

To investigate control of DNA replication, *cdc2* mutants were generated that underwent an extra round of replication without an intervening mitosis. The

existence of these mutants suggests that normal Cdk function prevents re-replication under such conditions (Broek et al., 1991). Furthermore, overexpression of *rum1*, a cdc2 inhibitor, causes multiple rounds of DNA replication in G2 cells (Correa-Bordes and Nurse, 1995; Moreno et al., 1994). Finally, cells in which *cdc13* has been deleted undergo multiple rounds of DNA replication without mitosis, presumably because the other S-phase cyclins, *cig1* and *cig2*, complex with *cdc2* but cannot promote mitosis (Hayles et al., 1994). In analogous experiments in budding yeast, Cdk oscillation without mitosis has been shown to cause endo-reduplication of DNA (Dahmann et al., 1995; Noton and Diffley, 2000). These experiments demonstrate that normal Cdk function is necessary for proper ordering of replication and mitosis.

Bipartite regulation of DNA replication by cyclin-Cdk.

The combination of inhibition of pre-RC formation and promotion of pre-RC firing by the same cyclin-Cdk enzymatic activity suggested a model in which a single oscillation of cyclin-Cdk activity would allow a single cycle of replication, beginning and ending with loaded pre-RCs. Note the similarity of this situation to the role of cyclin-Cdk in both promoting mitotic entry, and blocking mitotic exit, discussed above.

Spindle pole body licensing

Experiments in budding yeast examining the control of SPB duplication, separation and function revealed similar controls. After mitosis, when each newborn cell inherits a single SPB, this SPB is 'licensed' for duplication; cyclin B-Cdk activity inhibits this licensing step. Later, licensed SPBs will duplicate, separate and form a bipolar spindle; these activities require cyclin-Cdk activity (Fitch et al., 1992). The identity of the cyclin involved has significant consequences for the results; G1 cyclins are sufficient for SPB duplication, whereas the multiple B-type cyclins have differential roles in regulating licensing, maturation and functioning of the SPB (Haase et al., 2001). Despite these refinements, the overall shape of the regulatory loop is similar as for mitotic exit and DNA replication: cyclin-Cdks blocking licensing of SPBs for duplication and function, but also, later on, promoting the duplication and function of the licensed SPBs.

Budding, cell morphogenesis and cyclin-Cdk control.

As discussed above, early in the cell cycle (right after Start), budding yeast produce a bud, which initially grows apically (elongating at the tip); later in the cell cycle growth switches to isotropic growth in which both mother and daughter cell bodies grow by enlarging evenly in all directions (Lew and Reed, 1993). These processes are tightly coupled to cyclin-Cdk: G1 cyclin-Cdk is thought to promote

apical bud growth, while B-type-cyclin-Cdk inhibits initial bud formation and promotes isotropic bud growth. Thus, while again there are some refinements in the picture, overall, cell morphogenesis follows the rule that an early step (bud emergence) is inhibited, while a later step (isotropic growth, which could be considered bud maturation) is promoted by B-type-cyclin-Cdk.

Ratchet models for Cdk control of cell division.

The evidence discussed above indicates multiple cases where B-type cyclin-Cdk activity inhibits one step and promotes another step in a cell cycle process (DNA origin loading and firing, mitotic exit and entry, SPB licensing and maturation, bud emergence and maturation). In addition, B-type cyclin-Cdk activity oscillates once per cell division cycle (which was, indeed, the basis for discovery of cyclins) (Evans et al., 1983; Minshull et al., 1989). These observations have been combined in models that parsimoniously explain ordering of events in the cell cycle (Nasmyth, 1996; Stern and Nurse, 1996; Zachariae and Nasmyth, 1999).

In such models, one regulator, cyclin-Cdk activity, triggers or inhibits each step in cell division. A single process, such as DNA replication, is separated into mechanically coupled elements: a licensing step that is inhibited by low regulator level, and an execution step that requires a higher regulator level, or vice versa **(figure 1A)**. One oscillation of the regulator defines two non-overlapping intervals for licensing and execution. If the regulator rises and falls once per cell

division, then the process occurs once per division (Stern and Nurse, 1996). Mechanically separate processes, such as mitosis and cytokinesis, can be ordered similarly by arranging their regulatory thresholds for execution and inhibition **(figure 1B)**. When regulator level is high, the regulator-activated process occurs, and the inhibited process is not permitted until the regulator level drops.

Fine-tuning of the order of events may occur through successively increasing excitatory thresholds, or decreasing inhibitory thresholds. For example, if replication origin firing were promoted by a lower level of regulator than mitosis, then DNA replication would precede mitosis as the regulator rose (Stern and Nurse, 1996).

We refer to these models as “Ratchet” models. A ratchet is a device that restricts motion to a single direction through coupling to a toothed wheel and pawl. Similarly, these ratchet models define the temporal direction of cell cycle events in response to oscillating Cdk activity.

The Ratchet model suggests that the trajectory of Cdk activity defines the order of cell cycle events. Recently work tested this prediction in vertebrate cells using potent and specific chemical inhibition of Cyclin B degradation and Cdk activity (Potapova et al., 2006). Addition of a proteasome inhibitor prevented the degradation of securin and Cyclin B, which in turn inhibited anaphase and mitotic exit, respectively. However, prophase and metaphase events occurred. In metaphase-arrested cells, chemical inhibition of Cdk activity then caused mitotic

Figure 1. Ratchet models for control of DNA replication, mitosis and mitotic exit. A model is depicted for extrinsic control of DNA replication **(A)**, or mitosis and mitotic exit **(B)** by an oscillating master regulator. X-axis = time; Y-axis = regulator level. Horizontal lines denote thresholds for processes activated (blue) or inhibited (red) by the regulator. Vertical lines of the same color extend to the X-axis from the intersection point of the regulator trajectory (black) and the process. The result of these intersections, depicted on the X-axis, is the orderly progression of cell cycle events, entrained to regulator oscillation. Anaphase (vertical arrow) signals the peak regulator level.

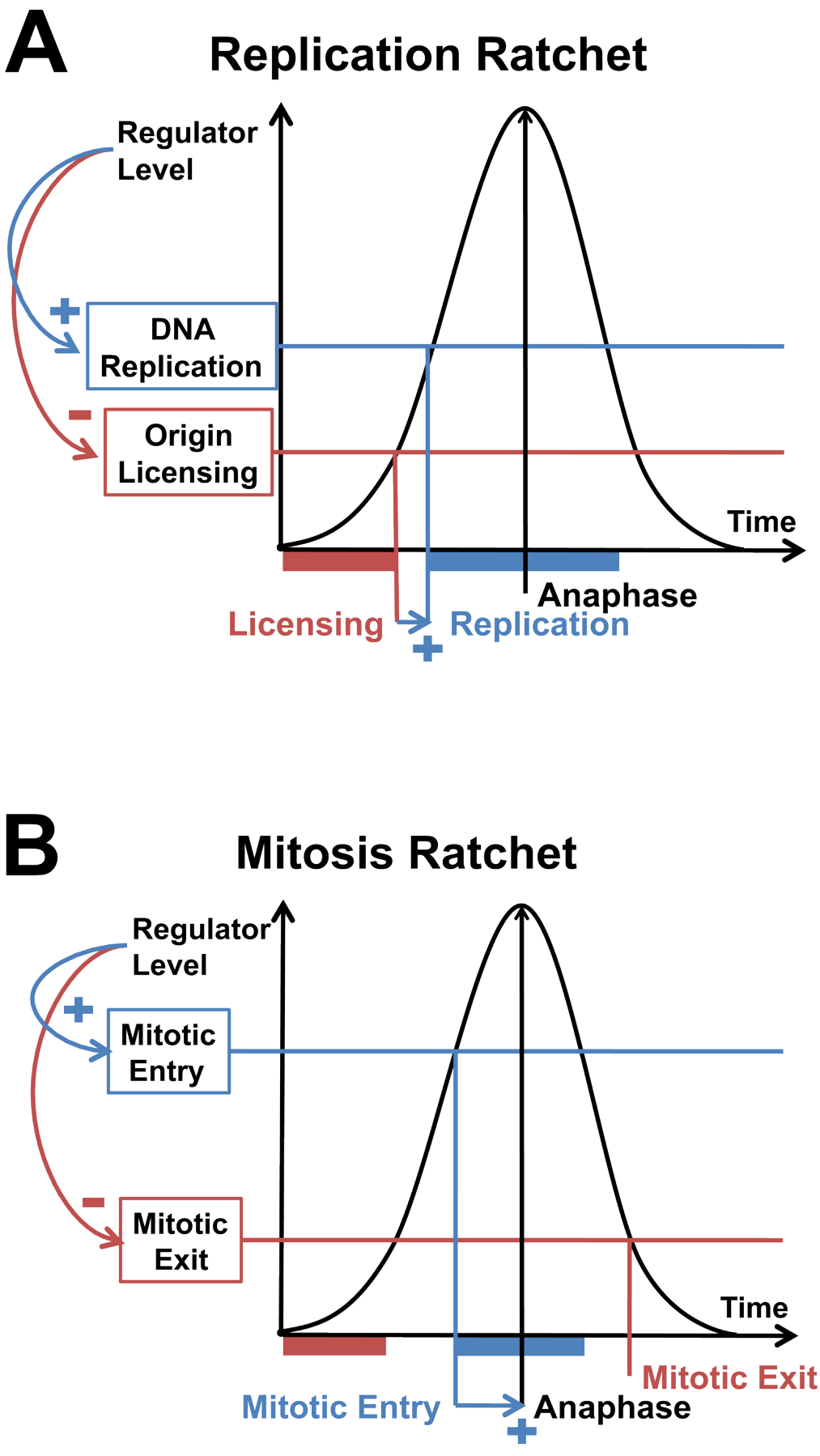
A
Replication Ratchet
Regulator Level
DNA Replication
Origin Licensing
Time
Anaphase
Licensing
Replication
B
Mitosis Ratchet
Regulator Level
Mitotic Entry
Mitotic Exit
Time
Mitotic Exit
Mitotic Entry
Anaphase

exit without anaphase: chromosome decondensation, spindle breakdown and nuclear envelope formation. Cytokinesis commenced, but could not complete because chromosome segregation was still prevented by the proteasome inhibitor. Remarkably, when the Cdk inhibitor was washed free, all of the mitotic exit events reversed and the cells returned to metaphase. Unlike Cdk inhibition, Cyclin B degradation is irreversible. Therefore, the authors concluded that Cyclin B degradation provides directionality for mitotic exit. The reversibility of mitotic exit by manipulation of Cdk activity supports the Cdk ratchet model.

Ratchet models vary by specific unit of regulation and regulatory frame of reference.

Cyclins activate Cdks; subject to additional regulatory controls such as Cdk phosphorylation or Cdk inhibitors, cyclin-Cdk then phosphorylate substrate proteins. Specific and non-specific phosphatases then can remove phosphates from these targets. Cyclin oscillation is controlled by regulated synthesis and degradation; inhibitory Cdk phosphorylation and accumulation of Cdk inhibitors can be independently controlled, and phosphatases are also under independent regulation. Cdk activity oscillation is a complex result of cyclin oscillation, enzymatic regulation, and stoichiometric inhibition. The rise and fall of Cdk-dependent protein phosphorylation is controlled by both Cdk oscillation and, at least in *S. cerevisiae*, periodic phosphatase activity (Cdc14) (Shou et al., 1999). Although Cdc14 has been described primarily as an indirect inhibitor of Cyclin B /

Cdk complexes, recent work suggests that Cdc14 acts to reverse Cdk substrate phosphorylation, as well (Bloom and Cross, 2007b).

Cyclin concentration, Cdk activity, and net Cdk phosphorylation potential (that is, the balance of kinase and opposing phosphatase, which could be different for each substrate due to differences in kinase or phosphatase affinity or subcellular localization) each are likely to rise and fall once per division. Therefore, a ratchet model could be formed based on any or all of these mechanisms of control.

Furthermore, each regulator has a specific and dynamic sub-cellular localization. B-cyclin localizes to the nucleus, and specifically to the centrosomes and spindle (Bailly et al., 2003). Cdc14 phosphatase localizes to the nucleolus when inactive, then to the nucleus during early anaphase release, and finally to the cytoplasm and bud neck (D'Amours and Amon, 2004). At least in animal cells, the Cdk inhibitory kinase (Wee1) and counteracting phosphatase (Cdc25) undergo complex cell-cycle-regulated nucleo-cytoplasmic traffic that may control their access to Cdk. Therefore the relevant frame of reference for regulator level may be the whole cell (global) or a sub-cellular compartment (local).

We test the global cyclin concentration and Cdk activity ratchets.

The ratchet models make several assumptions about the level of Cdk regulatory activity necessary to promote or inhibit cell cycle events – the models clearly work most effectively if thresholds for activating and inhibiting steps are set appropriately (to avoid, for example, a low concentration of cyclin-Cdk

promoting replication initiation without simultaneously inhibiting reformation of pre-RCs) (Figure 1; (Stern and Nurse, 1996)). However, little quantitative data exists for the Cdk activating and inhibiting thresholds in living cells.

Recent work addresses these quantitative relationships. Using exogenous constitutive expression of the wild-type mitotic B-type cyclin Clb2 in cycling cells allows an estimate that the inhibitory concentration of B-cyclin for mitotic exit is near the maximum level of accumulation during an unperturbed cell cycle (Cross et al., 2005). In the absence of Cdk inhibitors, this threshold is significantly lower.

Here we expand on this work by titrating undegradable B-cyclin in cells arrested prior to mitotic exit, then releasing these cells from arrest and correlating phenotype with B-cyclin concentration. This strategy allows us to measure the B-cyclin inhibitory threshold for mitotic exit. We calibrate this threshold to the peak level of B-cyclin expression during an unperturbed cell cycle. By measuring this threshold, we directly test the global cyclin concentration ratchet for mitosis and mitotic exit. In order to indirectly evaluate the global Cdk activity ratchet, we test the contribution of Cdk inhibitors to these thresholds.

These measurements are performed in *S. cerevisiae* and require control of Cyclin B / Cdk activity. Therefore, we must take into account the endogenous regulation of Cyclin B and Cdk in this organism. The following is a summary of this regulation.

Regulation of Cyclin-Cdk activity in *S. cerevisiae*

S. cerevisiae has nine cyclins and one cyclin-dependent kinase, Cdc28. With one exception, Cln3, all budding yeast cyclins are present in homologous pairs, a result of the duplication of the *S. cerevisiae* genome (Wolfe and Shields, 1997). The cyclins are designated Cln (G1 cyclins) or Clb (B-type) (S/M cyclins). There are three Clns, numbered 1 – 3, and six Clbs, numbered 1 – 6 (Nasmyth, 1996). The homologous pairs of cyclins (Cln1/2, Clb1/2, Clb3/4, Clb5/6) exhibit strongly overlapping functions and similar timing of expression and degradation. Further functional studies suggest that Cln3 is primarily a transcriptional activator of Cln1/2; Cln1/2 serve to allow accumulation of active Clb proteins; Clb5/6 primarily promote DNA replication, and Clb1,2,3,4 primarily promote entry into mitosis.

Cln3 expression is relatively constant, but rises slightly during and shortly after mitosis (MacKay et al., 2001; Wittenberg et al., 1990). Cln1/2 expression peaks in late G1, before initiation of DNA replication (Tyers et al., 1993). Clb5 and Clb6, the S-phase cyclins, are expressed coincident with Cln1/2, and initiate DNA replication (Epstein and Cross, 1992; Schwob and Nasmyth, 1993).

Clb1 – 4, the mitotic B-type cyclins, are expressed later than the S-phase cyclins and govern entry into mitosis. Expression of Clb1/2 peaks just before anaphase and then drops precipitously (Surana et al., 1991). *CLB3/4* mRNA levels rise earlier than those of *CLB1/2*, at initiation of replication, and fall simultaneously with *CLB1/2* mRNA levels in anaphase (Fitch et al., 1992).

The architecture of the cyclin-Cdk-control network is highly complex, with many interlocking controls. One simplification that has been hypothesized is to organize this architecture into two coupled biochemical oscillators, each capable of independent function (Cross, 2003). Both rely on the periodic expression, proteolysis and/or inhibition of cyclins. In both systems, Sic1p is the principal Cyclin-Cdk inhibitor (Dirick et al., 1995), and the anaphase-promoting complex (APC) controls B cyclin proteolysis. APC activity requires one of two substrate-specific activators: Cdc20 or Cdh1 (Visintin et al., 1997), which are differentially regulated.

The Relaxation Oscillator

A relaxation oscillator defines two steady states of Clb-Cdk activity. In G1, Clb-Cdk activity is minimal, and the activity of Clb antagonists is high. In G2/M the reverse is true. Mutual antagonism of Clbs and CKIs + Cdh1 (only Clb1/2) establishes these states.

Several mechanisms contribute to the stability of the Clb-low state. APC^{Cdh1}-mediated ubiquitination of Clb1 and Clb2 is responsible for Clb degradation in mitotic exit and G1 (Schwab et al., 1997; Visintin et al., 1997). Sic1 is a stoichiometric inhibitor of Clb-Cdks (Schwob et al., 1994). Cdc6 can also bind and inhibit Clb-Cdk complexes, but is not as strong an inhibitor as Sic1 (Archambault et al., 2003; Calzada et al., 2001; Elsasser et al., 1996). The G1 low-Clb state is less stable in the absence of either Sic1 or Cdh1, and the

genotype *cdh1Δ sic1Δ* is not viable (Schwab et al., 1997; Tyers, 1996; Visintin et al., 1997).

The Clb-high steady state of the relaxation oscillator is self-reinforcing. Mitotic cyclins positively regulate their own expression (Amon et al., 1993) and inhibit Sic1 and Cdh1. Mitotic cyclin-Cdk complexes phosphorylate Cdh1, which prevents Cdh1 binding to the APC (Jaspersen et al., 1999; Zachariae et al., 1998) and phosphorylate Sic1, targeting it for ubiquitination and subsequent degradation (Verma et al., 1997). Thus, in G2/M, mitotic cyclins both stimulate their own expression and inhibit their inhibitors.

Transitions from low-Clb to high-Clb and from high-Clb to low-Clb states occur sequentially and irreversibly. The first transition (called 'Start') occurs when the cell has attained sufficient mass to initiate a transcriptional positive feedback, driving irreversible commitment to DNA replication (Di Talia et al., 2007; Skotheim et al., 2008), and the second occurs at exit from mitosis (Visintin et al., 1998). The following is a description of these transitions.

Low→High

Cell size homeostasis requires the coupling of continuous mass increase to discrete rounds of chromosome replication and segregation. The transition at Start is ultimately stimulated by the acquisition of "critical mass" (Nasmyth, 1996) and commits the cell to progression through mitotic division and prohibits conjugation.

Cln3 and Bck2 are the earliest known components of the size homeostasis mechanism (Cross, 1988; Cross et al., 2002; Nash et al., 1988). Cln3-Cdc28 acts upstream of Cln1/2 (Tyers et al., 1993), and the principal function of Cln3 is to induce *CLN1/2* expression (Dirick et al., 1995). Cln3-Cdc28 executes this function by activating SBF, a transcription factor responsible for the expression of *CLN1* and *CLN2* (Dirick and Nasmyth, 1991) Cln3-Cdc28 activates SBF in two ways: directly by excitatory phosphorylation, and indirectly by inhibitory phosphorylation of Whi5, a functional homologue of the mammalian Rb protein that inhibits SBF (Costanzo et al., 2004; de Bruin et al., 2004). Recent work has demonstrated that most size homeostasis occurs during the interval between cytokinesis and the inactivation of Whi5 (Di Talia et al., 2007).

Once Cln3 reaches a critical concentration, *CLN1/2* transcription is activated (Schneider et al., 1996). Cln2 then reinforces its activity through positive feedback on *CLN2* expression, which commits the cell to a round of mitotic division (Cross and Tinkelenberg, 1991; Dirick and Nasmyth, 1991; Skotheim et al., 2008). In addition to its effects on the cell cycle control network, Cln2 also directly promotes bud formation.

Transit from low-Clb to high-Clb after Start is mediated by the Clns. Cln1/2 antagonize the CKIs and Cdh1 by phosphorylating them. Cdh1 phosphorylation inhibits its association with the APC, and Sic1 phosphorylation promotes its proteolysis. Importantly, Cln1/2 are not themselves inhibited by Sic1 or Cdh1 (Schwob et al., 1994; Verma et al., 1997). Hence they can switch the system

from a low Clb state to a high Clb state. However, the Cln switch is self-limited. Clb1/2 negatively regulates SBF (Amon et al., 1993), and the negative feedback of Clb-Cdk activity on Cln-Cdk activity renders the high-Cln state unstable.

High→Low

Transit from the high-Clb to the low-Clb state is mediated by the phosphatase Cdc14. Cdc14 reverses Cdk-mediated phosphorylation of Swi5, Sic1, and Cdh1. Each of these Cdc14 substrates inhibits Clb-Cdk activity (Jaspersen et al., 1999; Visintin et al., 1998). Swi5 is a transcription factor and induces *SIC1* and *CDC6* expression (Knapp et al., 1996; Piatti et al., 1995; Toyn et al., 1997). Phosphorylation of the Swi5 NLS by CDK promotes its exclusion from the nucleus (Moll et al., 1991).

From G1 until mitosis, Cdc14p remains bound to two nucleolar proteins, Net1p and Sir2p, forming the RENT complex (Regulator of Nucleolar silencing and Telophase). Formation of the RENT complex sequesters Cdc14 to the nucleolus in an inactive form (Shou et al., 1999; Visintin et al., 1999). The release of Cdc14 is controlled by two pathways: the Mitotic Exit Network (MEN) and the FEAR (Cdc-14 early anaphase release) pathway. The particular signals that trigger these pathways have not been fully defined, but Cdc14 is not released until after cohesin cleavage.

The Negative Feedback Oscillator

The Clb1/2 – Cdc20 negative feedback oscillator is less complex than the relaxation oscillator, and can be summarized by two reactions: Clb2-Cdk activates the APC^{Cdc20}, and the APC^{Cdc20} targets mitotic cyclins for degradation. This transition occurs in mitosis.

APC^{Cdc20} targets include Pds1, Clb5, and Clb2 (Shirayama et al., 1999; Yeong et al., 2000). In budding yeast, the initiation of anaphase requires degradation of an inhibitor of sister chromatid separation, Pds1 (securin), by the APC^{Cdc20} (Cohen-Fix et al., 1996; Holloway et al., 1993; Shirayama et al., 1999). Cdc20-mediated degradation of mitotic cyclins facilitates mitotic exit. Failure to degrade Clb2, but not Clb5, results in telophase arrest (Wäsch and Cross, 2002). However, in the absence of Cdc20, Clb5-Cdk activity is lethal, probably because it inhibits Cdh1-mediated degradation of Clb2 (Huang et al., 2001; Shirayama et al., 1999; Wäsch and Cross, 2002).

APC^{Cdc20} activity is regulated in at least four ways. Cdc20 expression is cyclic and peaks in G2/M. Cdc20 is targeted for degradation by the APC (Shirayama et al., 1998). In response to unattached kinetochores, Cdc20 is inhibited by the spindle checkpoint (Hwang et al., 1998). The fourth mechanism is indirect. Three subunits of the APC, Cdc16, Cdc23 and Cdc27 are phosphorylated by Cdc28. This phosphorylation is necessary for Cdc20-mediated APC activity, but is not required for Cdh1 activity (Rudner et al., 2000; Rudner and Murray, 2000).

Cdc28-mediated phosphorylation of the APC completes the Clb1/2 – Cdc20 negative feedback loop.

Summary of Introduction.

Correct ordering of cell cycle events is essential. Potential mechanisms for ordering include:

(i) mechanical dependency (e.g., one step provides a critical substrate for a subsequent step);

(ii) intrinsic timing control (steps that must be completed later intrinsically take longer than steps that should be completed earlier);

(iii) surveillance or checkpoint controls (signal transduction systems that detect failure of completion of an early step, and block execution of a later step);

(iv) and 'ratchet' models, where a global regulator, that rises and falls in a regular oscillation, is coupled to inhibition and promotion of alternating steps in a cell cycle process.

There is clear evidence for (i) (indeed, some examples are almost trivial, such as the need for bud emergence for cytokinesis). (ii) is hard to evaluate *in vivo* because one can never be sure that all extrinsic controls have been lifted so that a process is going at its maximal possible rate. The surveillance mechanisms

that form the basis of (iii) are well established, but these systems seem to function almost exclusively in rare cases of aberrant damage, or in response to exogenous insults (such as X-rays or spindle poisons), and contribute little to endogenous cell cycle timing or ordering.

The ratchet models in (iv) fit very well with a great deal of cell cycle biology and biochemistry, for multiple cell cycle processes. The key requirements for these models are:

(a) A mechanism for periodic rise and fall of a regulator (cyclin-Cdk) with a period at least long enough for completion of all cell cycle events;

(b) Appropriate coupling of thresholds, both inhibitory and excitatory, between cyclin-Cdk activity and the regulated events.

(c) These models are differentiated based on the level of control. The simplest models would employ cyclin abundance as the main regulator. A more sophisticated model would consider instead cyclin-Cdk enzymatic activity, taking into account cyclin, Cdk inhibitors, and Cdk inhibitory phosphorylation. Finally, ratchet models could be proposed taking into account not only Cdk activity, but also localization of active Cdk, phosphatase, and the localization and specificity of each substrate for cyclin-Cdk and phosphatase.

In this thesis, I undertake to provide data that will allow a clear test of the first two versions of the ratchet model. Specifically, I have developed a method to introduce titrated amounts of stable B-type mitotic cyclin Clb2 in metaphase-arrested cells, followed by release of the arrest, and correlation of the execution of multiple steps of mitotic exit and the subsequent cell cycle to the level of stable Clb2 in individual cells. Measurement of enzymatic activity suggests that in this experimental context, cyclin abundance is a sufficient indicator of cyclin-Cdk activity level.

To provide information relevant to testing the ratchet models, and in general to provide a relevant biological metric, our basic 'unit' will be the maximum amount of Clb2 attained in a normal cell cycle, since this amount is demonstrably sufficient to drive occurrence of many events; we are then interested in whether this amount is sufficient to inhibit subsequent events.

Owing to the flexibility of the third class of ratchet models, it is impossible to test them except case by case, as the biochemistry of each substrate becomes clear. This is beyond the scope of this thesis, although we have determined initial information about the interaction of the phosphatase Cdc14 with the introduction of different levels of pulsed stable Clb2.

It is important to point out that the data in this thesis are not of interest solely as tests of the ratchet models. In general, many cases are known in biology where the complete absence of a protein yields one result (i.e. the 'null phenotype'), which is frequently contrasted to simple presence of the protein, or

indeed to its gross overexpression. In cases where a high level of a protein gives one outcome and absence gives another, it is of interest to know what happens as the level is titrated down. Are there sharp thresholds (that is, levels above which the event occurs exactly on schedule and below which it never occurs) or does the regulator smoothly affect rate? For a regulator such as cyclin-Cdk that affects multiple processes, do all the processes respond at the same level (suggesting either global regulation or co-evolution), or does each process have its own dose-response? And how do the critical levels compare to the endogenous level?

Materials and Methods

Strains and Plasmids

a) Standard yeast methods for strain and plasmid construction were used throughout.

b) Plasmids

   i) pRS406::*SIC1*

   ii) pRS406::P_{GAL1}→*CLB2Δdb,ken1,2* (Wäsch and Cross, 2002)

   iii) pRS404::*CFP-TUB1* plasmid (gift from Elmar Schiebel)

   iv) pRS406::P_{ADH1}→*GAL4-rMR* (gift from Nick Buchler)

Quantitative PCR

RNA and DNA extraction was as performed in (Cross and Tinkelenberg, 1991). For RNA purification we used the RNeasy Kit (Qiagen). Reverse transcription was performed using the Quantitect RT Kit (Qiagen), and quantitative PCR was performed using SYBR green (Qiagen).

How to measure a Clb2 inhibitory concentration threshold:

The following describes in generic fashion the method used to measure Clb2kd concentration thresholds for cell cycle events that occur after anaphase. The strain background was *cdc20::MET-CDC20 GAL4-rMR CLB2::*P_{GAL1}→*CLB2Δdb,ken1,2-YFP*, with a variety of CFP or mCherry-tagged alleles for phenotypic analysis. Section I describes the time course protocol

depicted in **figure 2**, as well as initial sample collection. Section II describes measurement of the ratio of the mean Clb2kd-YFP pulse to peak Clb2-YFP by quantitative western blot. Section III describes single-cell YFP fluorescence measurement and phenotypic annotation. Section IV describes Clb2kd inhibitory threshold calculation from the data generated in sections II and III. Section V describes the treatment of samples not used to measure thresholds directly. In cases where GFP or YFP-tagged alleles were employed, the untagged P_{GAL1}→*CLB2Δdb,ken1,2* was substituted, and thresholds based on single-cell Clb2kd concentrations were not measured.

I) Time Course Protocol

1) Cells were inoculated into synthetic complete media supplemented with 3% raffinose and all amino acids except methionine (SCR-M). The culture was shaken at approximately 250 rpm at 30º until it reached a density of approximately $1x10^7$ cells/ml. This density allowed one round of division during Cdc20-depletion arrest (step 2) without culture overgrowth.
2) The culture was then arrested by addition of 2mM methionine (15x normal concentration) for at least 3.5 hours to prevent Cdc20 synthesis. 2.5 hours after methionine addition, the culture was split into a control culture (no-pulse) and a Clb2kd induction culture (+pulse). At this point over 95% cells were budded, although not all cells were arrested with short spindles

(the characteristic arrest due to Cdc20 depletion). Clb2kd induction in budded cells had little effect on progression of cells to cdc20-arrest.

3) 10 μM deoxycorticosterone (dCort) was added to the +pulse culture to induce Clb2kd synthesis from the *GAL1* promoter via Gal4-rMR activation. 25-30 minutes after dCort addition, synthesis was rapidly arrested by addition of 1:2 volumes ice and 3% glucose. dCort was washed from the +pulse cells by repeated centrifugation and resuspension in ice-cold SC medium supplemented with 3% glucose and 2 mM methionine (SCD+M). The same protocol was applied to the no-pulse culture, except for hormone addition.
4) Both cultures were resuspended in SCD+M at 30º for 45 minutes to allow YFP maturation without release of the *cdc20* block.
5) Cells were then collected by centrifugation, washed with ice cold SCD-M to remove all traces of methionine, and resuspended in SCD-M at 30º to induce Cdc20 synthesis (t=0'). For the experiments described in figures 19, 20, 21A, and 24, α-factor was added to 100 nM at t=0'. Strains for these experiments contained the *bar1Δ* mutation to prevent α-factor degradation. For all other time courses measuring the post-anaphase effects of Clb2kd, 2 mM methionine was added at t=45' post-release to re-deplete Cdc20, resulting in capture of cells that complete one mitosis at a second metaphase arrest. The 45' time was settled on because earlier methionine addition risks cdc20 depletion before every cell has undergone

Figure 2. A method to measure the post-anaphase response of single cells to persistent Clb2p.

This cartoon describes the protocol for a synchronized cdc20 time course following a Clb2kd-YFP pulse. Cells of strain background *CLB2::P_{GAL}→CLB2Δdb,ken1,2-YFP P_{ADH1}→GAL4-rMR cdc20::P_{MET3}→HA_3-CDC20* are grown overnight to early log phase in methionine-free medium containing raffinose, driving expression of the essential Cdc20 from the methionine-repressible *MET3* promoter (raffinose neither induces nor represses relieves the *GAL1* promoter, and lacking methionine, which permits expression of Cdc20. The culture is then synchronized at metaphase by addition of methionine for 150 min to block Cdc20 expression. (1) After arrest, undegradable Clb2 fused to YFP (Clb2kd-YFP) is induced by addition of deoxycorticosterone (dC), which activates the Gal4-rMR fusion protein (Gal4 DNA binding domain fused to the mineralocorticosteroid-binding domain). Induction is terminated after 30 minutes by washout of mineralocorticosteroid and resuspension in methionine-containing medium with glucose, to repress the *GAL1* promoter. Metaphase arrest is maintained for an additional 45 minutes to allow YFP maturation, then Cdc20 expression is re-induced by suspension in methionine-free medium. (2) Cdc20 induction promotes a synchronous anaphase, which is not affected by undegradable Clb2 protein, and synchronous progression through mitotic exit and the subsequent cell cycle; high levels of Clb2 are known to inhibit mitotic exit. Methionine is added back to the culture 45 minutes post-release to block divided cells at a second metaphase (Cdc20-depletion) arrest. (3) Peak [Clb2-YFP] and steady state [Clb2-YFP] at metaphase arrest define the relevant concentration ranges for the hypothetical plot, [Clb2kd-YFP] versus process execution. The green box illustrates a hypothetical threshold (steepest decrease, passing through 50% completion) in units of peak [Clb2-YFP].

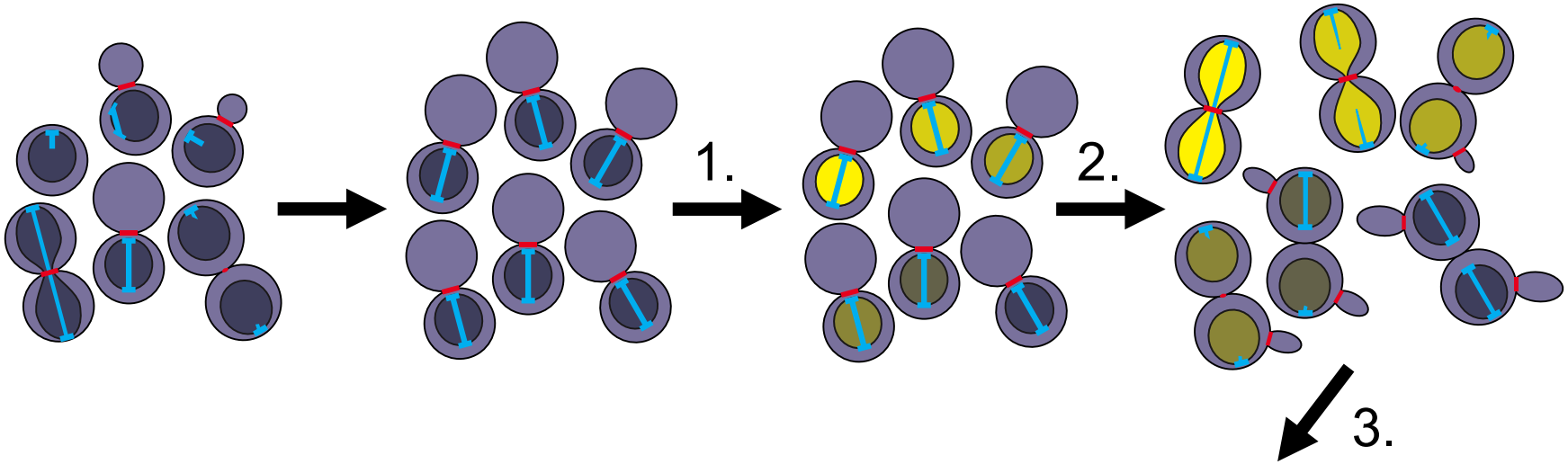

1. Pulse *cdc20*-blocked cells with stable Clb2kd-YFP

2. Release *cdc20* block

3. Correlate cell cycle progression with Clb2kd-YFP levels

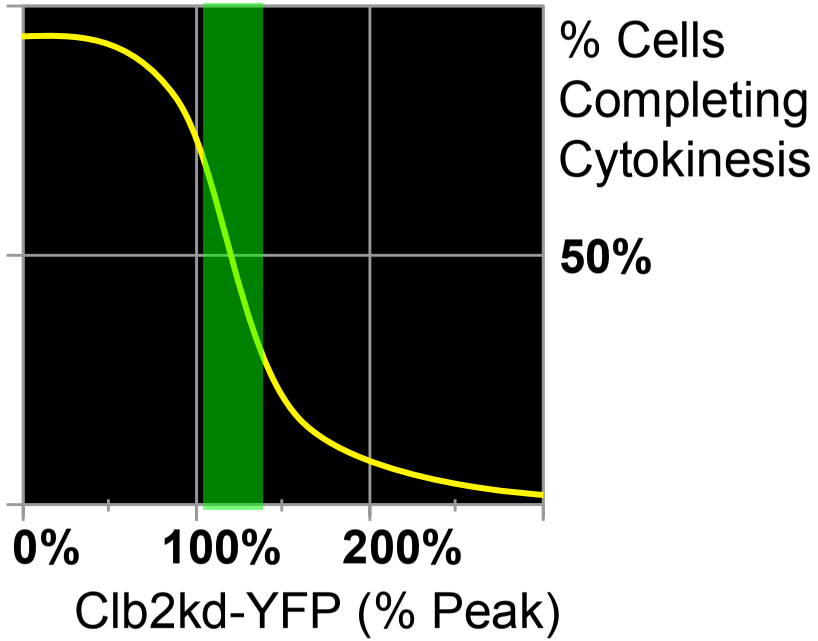

anaphase, and later addition risks allowing some cells to enter a second anaphase.

6) After resuspension in SCD-M, with or without methionine or α-factor, culture samples were collected at regular intervals for a variety of analyses, including protein concentration measurement by quantitative immunoblot, DNA content by flow cytometry of ethanol-fixed propidium-iodide-stained cells, fluorescence microscopy and kinase activity. For release to α-factor, samples were collected every 20 minutes for 60 or 80 minutes. For release to a second cdc20-arrest, samples were collected every 15 minutes for 90 minutes. Samples were added to tubes filled with ice and remained ice-cold until either lysed for protein extraction or fixed with 4% paraformaldehyde or 70% ethanol.

7) For peak Clb2 comparison to the pulse, a *MET-CDC20 clb1,3,4Δ CLB2-YFP bar1Δ* culture was arrested in SCD + 100nM α-factor for 2.5 hours, then released to SCD-M or SCD+M to inhibit any Clb2-YFP degradation (although this proved to be unnecessary). Samples were extracted every 10 minutes for western blotting and analysis of DNA content. The 60-minute post-release samples contained equal concentrations of Clb2-YFP, and the maximum concentration for SCD-M culture. This denatured protein sample was used to compare with the pulse Clb2kd concentration.

II) Quantitative Fluorescence Microscopy

1) Cells were collected by centrifugation and fixed no more than 1 hour after sample extraction to preserve spindles. Fixation was performed at room temperature for 3 minutes using a paraformaldehyde buffer (4% paraformaldehyde, 3.4% sucrose, 200 μM $MgCl_2$, 100 mM KPO_4, pH 7.5). Fixed cells were washed three times with Sorbitol-Phosphate buffer (1.2M sorbitol, 200 μM $MgCl_2$, 100 mM KPO_4, pH 7.5), and resuspended in a small volume (100 μL) of the same buffer for storage. No sonication or centrifugation above 8k was possible, because these treatments disturbed spindle morphology based on initial experiments. All cells were imaged within 5 days of fixation to preserve sub-cellular structures, again based on initial experiments. This fixation protocol does not affect total YFP fluorescence or spindle stability, when compared with live cell imaging. DAPI staining was performed by standard protocols.
2) Fluorescence and DIC images were acquired using an Axioplan 2 microscope (Carl Zeiss MicroImaging Corp.), with a 63x 1.4 numerical aperture Plan-Apochromat objective, coupled to a Hamamatsu C4742-95 CCD camera (Sciscope Instrument). Camera and microscope were interfaced with the OpenLab software (Improvision). Clb2-YFP, Clb2kd-YFP, and Spc29-YFP fluorescence were detected using a YFP filter, Myo1-mCherry was detected using an Cy3 filter, CFP-Tub1 and Spc29-

CFP were detected using a CFP filter, GFP was detected using a narrow band pass FITC filter, and DAPI was detected using a DAPI filter. For phenotypic analysis of Spc29-YFP, Spc29-CFP, CFP-Tub1, and Myo1-mCherry, and DAPI-stained nuclei, three-dimensional image stacks containing 3-5 0.3 μm optical sections were merged into two-dimensional maximum projections. Single exposures of Clb2-YFP or Clb2kd-YFP fluorescence were used for quantification to minimize photobleaching.

3) Phenotypic fractions for each time point for both the +pulse and no-pulse cultures were scored from contrast-enhanced tiffs exported by OpenLab using MatLab Cell Counter program developed by Fred Cross. Event thresholds were measured for time points at which the event had been completed in the no-pulse control but not in a significant fraction of the +pulse culture.
4) For +pulse phenotype correlation with YFP fluorescence, whole-cell masks were generated from tiff images depicting CFP-Tub1 or background CFP fluorescence, and segmented to distinguish single cells based on Myo1-mCherry fluorescence. The mask-making program was developed in MatLab by Ben Timney. It is important to note that due to the requirement to avoid sonication in this protocol to preserve spindle morphology, it was necessary to assume that completion of cytokinesis and separation of an initially budded cell into two was marked by disappearance of Myo1 signal from the bud neck. Thus, for example, cells

were scored as a single cell with a broken-down spindle if they contained two small tubulin foci in each cell body but maintained a Myo1 signal at the bud neck; similar images lacking the Myo1 signal were scored as two unbudded post-division cells, each with a monopolar tubulin focus (such as is observed in normal G1 cells).

5) For each fluorescence picture, using the segmented single cell masks in OpenLab, whole-cell mean YFP fluorescence was measured for individual cells after background subtraction (signal in unlabeled cells) to determine Clb2kd-YFP levels in each cell, and the phenotypes of these cells were annotated. Tables were generated designating the cell location, phenotype, and Clb2kd levels. To obtain sufficient data to reliably score the relationships between Clb2kd levels and phenotypes, Clb2kd levels were binned. These tables were exported as Microsoft Excel spreadsheets. 450 to 1700 cells were scored for each time point analyzed, depending on the number of event thresholds being measured and the desired fineness of binning of Clb2kd levels.

III) Quantitative Western Blotting

1) Yeast protein was extracted for western blot analysis in denaturing buffer using bead beater extraction, and immediately heated at 95 degrees. Samples were resolved by SDS-PAGE on 4-20% tris-glycine gradient gels and transferred onto PVDF membrane. Clb2-YFP 60-minute peak protein samples (section I.7) were loaded next to +pulse samples for direct

comparison. 2-fold dilution standards of Clb2kd-YFP to Clb2-YFP were loaded onto each gel for comparison of pulse to peak. Dilution standards were prepared from denatured protein extracts from *MET-CDC20* strains arrested in SCR+M, to which galactose had been added for 3 hours to induce expression from *GAL-CLB2kd-YFP* or *GAL-CLB2-YFP*. These extracts were diluted into *clb2Δ* extract of the same total protein concentration to avoid transfer artifacts due to differences in total protein transferred in the lanes.

2) The presence of Clb2kd-YFP and Clb2-YFP were detected using a 1:1000 dilution of mouse monoclonal anti-GFP (Roche) or a 1:10,000 dilution of rabbit polyclonal anti-Clb2 (Covance), raised against purified MBP-Clb2 (Courtesy of Fred Cross). Pgk1 was detected using a 1:10,000 dilution of mouse monoclonal anti-Pgk1 (Santa Cruz). Protein signal was detected by ECL, and imaged on Fujifilm DarkBox + CCD camera. Blots were imaged in trays filled with ECL solution, which improved the dynamic range
3) Quantification of pixel volumes for signal with local background subtraction was performed using MultiGauge software. Volumes for each band were tabulated and exported as Microsoft Excel spreadsheets.
4) Multiple western blot comparisons were performed for each time point at which a threshold was measured.

IV) Clb2kd inhibitory threshold calculation

1) Pulse/Peak: The ratio of Clb2 signal to Pgk1 was calculated to control for loading and total protein concentration of the extract. Clb2/Pgk1 was then interpolated onto the appropriate dilution curve. The ratio of Clb2kd-YFP to peak Clb2-YFP was then directly calculated. If peak and pulse values came from an anti-Clb2 blot, then a correction for the difference in antigenicity between the Clb2wt-YFP and Clb2kd-YFP proteins was applied. This correction was calculated from average ratio of dilution standard signals of each allele on anti-Clb2 versus anti-GFP blots. Clb2-wt typically yielded 2.5-fold more signal relative to the Clb2kd on blots probed with anti-Clb2 than on blots probed with anti-GFP. All calculated pulse/peak values are the average of at least two separately loaded bands.
2) Single-cell fraction pulse: Background YFP fluorescence from cell-free areas was subtracted for each cell. Non-specific cell background was then subtracted using the average fluorescence of the un-pulsed control for that time-point. For each annotated cell, this value was then divided by the average background-subtracted fluorescence of all cells measured.
3) Single-cell fraction peak: The fraction-pulse value for each cell was divided by the pulse/peak value derived from the quantitative western blots (IV.1)

4) Histograms of each phenotype were then generated for the pulsed cells. Bins were selected over the pulse range to contain 60 – 150 cells, depending on the number of phenotypes scored. The same bins were used for all phenotypes. The fraction of cells of each phenotype was then calculated and plotted versus the mid-bin fraction of peak Clb2 concentration. Event thresholds were then derived from these plots by summing the phenotypes that had completed an event. For example, the 60-minute post-release rebudding threshold was calculated from the sum of the fraction of all phenotypes that had rebudded, regardless of spindle morphology or degree of completion of cytokinesis (figure 14A).

V) Indirect assays of Clb2kd pulse activity and consequences

1) Measurement of YFP-associate Histone H1 kinase activity was performed as essentially as described in (Levine et al., 1996)**,** using polyclonal Rabbit anti-GFP at an empirically determined saturating concentration.

2) DNA flow cytometry performed as described in (Epstein and Cross, 1992).

3) Time-lapse microscopy of cells pulsed with either Clb2kd or Clb2kd-YFP was performed essentially as described in (Bean et al., 2006). Cells growing in synthetic liquid medium were seeded onto thin low-melt agarose slabs of the appropriate medium. Cell growth and division was observed with fluorescence time-lapse microscopy at 30 ºC using a Leica DMIRE2 inverted microscope with a Ludl motorized XY stage. Images

were acquired every 3 minutes with a Hamamatsu Orca-ER camera. Custom Visual Basic software integrated with ImagePro Plus was used to automate image acquisition and microscope control.

Chapter 1: Development of a Method to Measure the Post-Anaphase Response of Single Cells to Persistent Clb2p

Cyclin B concentration oscillates and exerts bipartite control over most cell cycle events (see Introduction). However, since the levels of Cyclin B that activate and inhibit each event are unknown, the significance of this bipartite control remains unclear. To address this question, we have developed a method to measure the post-anaphase response of individual cells to a spectrum of fixed Cyclin B concentrations, expressed as a fraction of peak endogenous concentration. This method is described in figure 2 and will be justified below. It involves the coordination of four related components:

a. Measurement of single-cell peak Clb2p concentration. The average peak Clb2p level attained in the course of a normal cell cycle will be the **standard unit** of Clb2 used throughout. Previous estimates (Cross et al., 2002) suggest that this may correspond to on the order of 10^4 molecules of Clb2 per cell. We will refer to this level as **peak-equivalent** throughout.

b. Induction of undegradable Clb2p, measurement of its concentration in individual cells, and comparison of this value to the peak.

c. Development of a method for induction of undegradable Clb2p during a defined interval during a late cell cycle block, followed by release of the block

d. Correlation of persistent Clb2p concentration with post-anaphase phenotype, as compared with control cells not exposed to undegradable Clb2p. Note that the phrase '**persistent Clb2**' will be used throughout to refer to Clb2 present before mitotic exit, and persisting due to lack of degradation independent of the execution of cell cycle events (in some cases well into the succeeding cell cycle).

There are several questions that we answer with this method. These are labeled with question marks in **figure 2**. What level of undegradable Clb2 is required to block mitotic exit events such as spindle disassembly and cytokinesis? What are the consequences of persistent undegradable Clb2p on bud formation and spindle synthesis in the subsequent cell cycle? How is degradation and synthesis of endogenous Clb2p affected by persistent undegradable Clb2p? In addition to the unknowns labeled in the figure, we also explored the consequences of persistent Clb2p on DNA replication, α-factor arrest, and Cdc14 phosphatase release.

We are most interested in focusing on the effects of levels of persistent Clb2p that are close to normal peak levels achieved in an unperturbed cell cycle, since this is the most clearly physiological 'high' level. As discussed in the Introduction, determination of the biological effects of **persistent** Clb2p at this

peak-equivalent level (definitions above) allows direct evaluation of the simplest form of the ratchet model for control of order in the cell cycle.

A First Attempt: A Wrong Way to Measure the B-Cyclin Inhibitory Threshold for Mitotic Exit, and what We Learned from Debugging this Error

Undegradable B-cyclin expressed at sufficient levels is lethal. Therefore, we required its expression to be conditional for our experiments. We chose the tightly regulated and reversible *GAL1/10* promoter because it had been reported to be titratable and homogeneously expressed in response to graded concentrations of galactose (Biggar and Crabtree, 2001).

The *GAL1/10* promoter activity is regulated by carbon source. It is rapidly activated by galactose, and is independently subject to repression by glucose. Other carbon sources such as raffinose are neither inducing nor repressing, and typically support a very low level of expression from this promoter that is still higher than that in glucose.

Galactose induction has been used to study the post-anaphase effects of undegradable Clb2. Amon et al. (1994) grew cultures of *cdc15-2* cells containing either *GAL-CLB2* or *GAL-CLB2Δdb* in raffinose, induced telophase arrest by inactivation of Cdc15 (an essential protein for mitotic exit) at non-permissive temperature, and induced synthesis of either wild-type Clb2p or undegradable Clb2Δdb (with its destruction box removed to prevent its degradation – see Introduction) by adding galactose (Amon et al., 1994). They then released cells

from telophase arrest by lowering the temperature to reactivate Cdc15, in glucose-containing media, inactivating the *GAL* promoter. The purpose was to assess mitotic exit following generation of a controlled pulse of stable Clb2. They measured mitotic exit by counting the fraction of cells with long spindles in the culture, imaged by anti-tubulin immunofluorescence **(figure 3A)**. (*cdc15*-arrested cells block with long spindles, which disassemble rapidly upon reversal of the block). They found that despite a substantial Clb2Δdb pulse, spindle disassembly occurred. Based on these findings, they concluded that cells could exit mitosis with a significant concentration of mitotic cyclin.

We initially employed a variant of the Amon protocol for measuring the Clb2 inhibitory threshold for mitotic exit, changing only the method of synchronization and the undegradable Clb2 allele. We abandoned synchronization by *cdc15-2* arrest in favor of hydroxyurea arrest (HU). We changed synchronization methods for two reasons. First, *cdc15-2* cells are severely delayed in actomyosin ring contraction upon release to permissive temperature, making both cytokinesis and subsequent DNA replication difficult to monitor. Second, HU synchronization could be conducted at 30°, which allows greater induction from the *GAL1/10* promoter. For undegradable Clb2, we used an allele lacking both *ken* boxes, targeting sequences for APC^{Cdh1}-mediated ubiquitination (Pfleger and Kirschner, 2000; Wäsch and Cross, 2002), as well as the destruction box that targets proteins to both APC^{Cdh1} and APC^{Cdc20} (*CLB2Δdb,ken1,2*, called *CLB2kd* below)

Figure 3. *GAL1* promoter activation by raffinose de-repression and galactose induction is not a suitable method for generating a pulse undegradable Clb2 pulse.

(A) The *GAL1* promoter has been used previously to study the effects of Clb2Δdb on mitotic exit. Reproduced from Amon et al 1994: "*cdc15-2* mutants lacking the endogenous *CLB2* gene either carrying *GAL-CLB2* (open circles) or *GAL-CLB2Δdb* (closed circles) were arrested at the restrictive temperature (37°) [in raffinose medium] for 120 min followed by galactose addition for another 60 min. Cells were released from the *cdc15-2* block by transfer to YEP medium containing raffinose plus glucose at 25° C (t = 0 min). (top) Amount of Clb2 protein. (bottom) The percentage of cells having anaphase spindles." **(B and C)** *CLB2::P_{GAL}→CLB2Δdb,ken1,2-YFP* cells were arrested with hydroxyurea in raffinose medium at 30° for 120 minutes. Galactose was added to 0.3% for 60 minutes, and cells were released to glucose medium lacking hydroxyurea. Samples were analyzed every 30 minutes for DNA content and Clb2kd-YFP protein concentration **(B)** and at 120 minutes post-release for YFP fluorescence **(C)**.

A

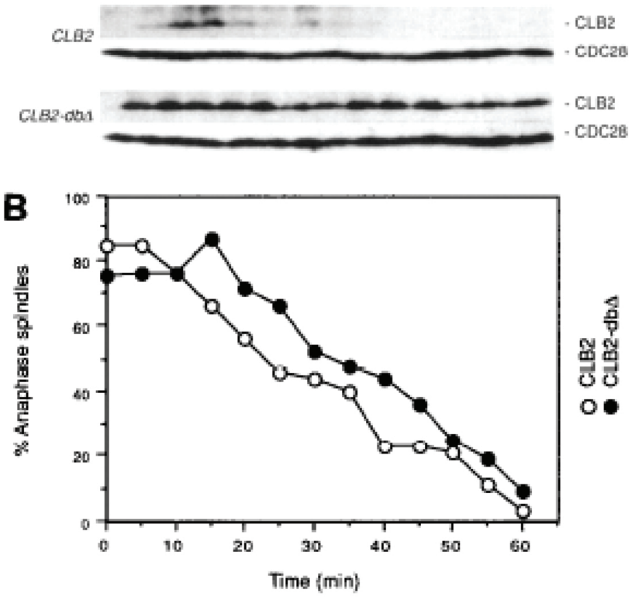

Amon et al 2004:

Arrest in Raff w/ ***cdc15-2***
→ Pulse w/ ***3% Gal*** for ***60 min***
→ Release into Glucose
→ Count long spindles

B

Arrest in YEPR + HU
→ Pulse w/ ***0.3% Gal*** for ***60 min***
→ Release into Glucose + α-factor

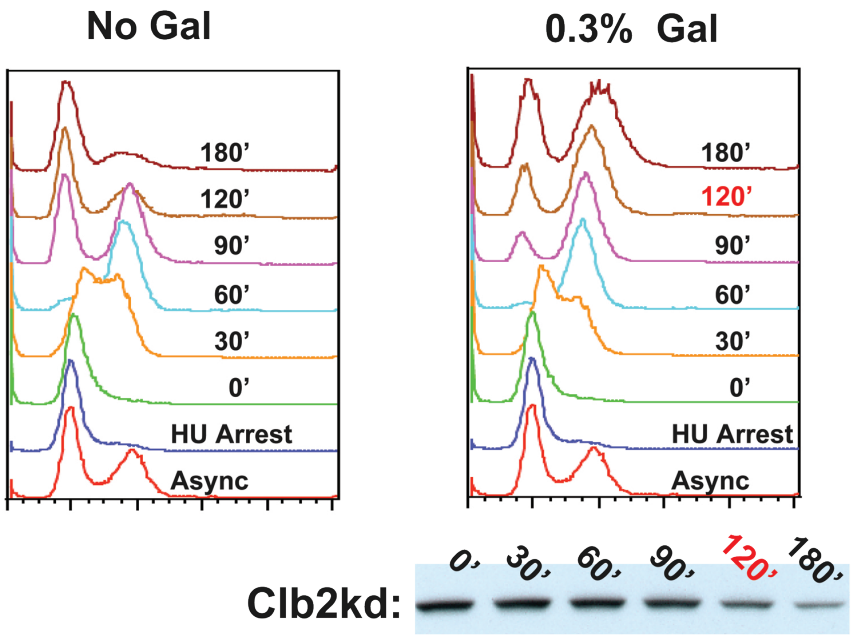

C

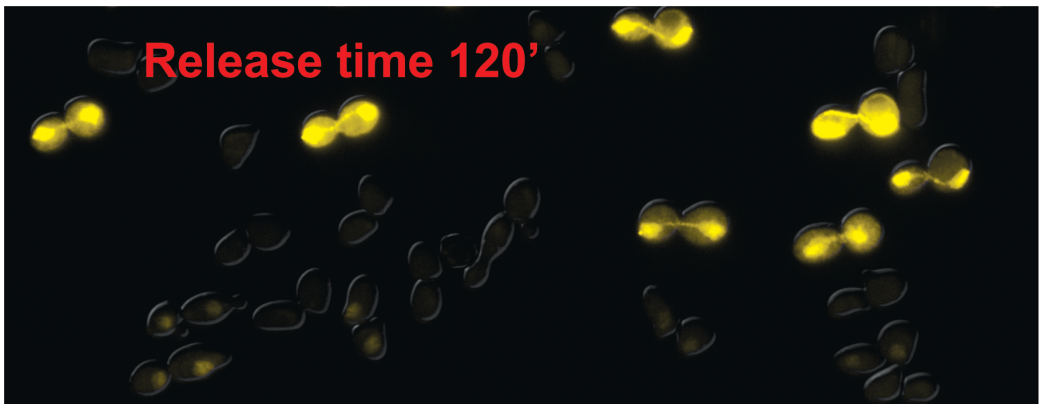

because this protein appears completely resistant to APC-mediated degradation (Pfleger and Kirschner, 2000; Wäsch and Cross, 2002).

We arrested cells in S-phase with hydroxyurea, pulsed with galactose for 1 hour, and released from HU arrest to media containing glucose and α-factor. Removal of HU permits DNA replication, glucose shut off *CLB2kd* expression, and α-factor trapped cells that were able to exit mitosis in G1 of the next cell cycle, allowing analysis of mitotic exit by accumulation of cells with 1C DNA content as measured by DNA flow cytometry **(figure 3B)**. We varied galactose concentration until roughly half the culture was prevented from exiting mitosis. Assuming a narrowly distributed pulse, the mean concentration of Clb2kd would approximate the mitotic exit threshold.

We compared our measured threshold to the peak concentration of Clb2p during an α-factor block-release-block time course. Our initial results indicated that only extreme hyper-accumulation of Clb2 could stably block mitotic exit. However, the phenotypic consequences were read in single cells as an all-or-none consequence of the pulse, but the pulse was measured as a population mean. We assessed the pulse distribution in individual cells by measuring the single-cell fluorescence of Clb2kd-YFP expressed from the *GAL1* promoter. Surprisingly, we found that the distribution of Clb2kd-YFP fluorescence following a 60-minute pulse with 0.3% galactose, which yielded approximately 50% mitotic exit, was nearly bimodal **(figure 3C)**. Further, it was clear that the cells undergoing mitotic exit were exclusively the cells containing very low levels of

Clb2kd-YFP. Therefore, all that could be concluded was that a very high level of Clb2p would block exit, and a very low level would not – little more than was known previously.

Finding a Method for Delivering a Uniform Pulse

The heterogeneity of the Clb2kd-YFP pulse was not a specific peculiarity of the $P_{GAL1/10}$→ *CLB2kd-YFP* allele but a general characteristic of galactose induction in raffinose. We verified this using $P_{GAL1/10}$→*GFP* or *YFP* constructs. Expression levels as measured by flow cytometry were extremely heterogeneous after short pulses with galactose. After 2 hours, galactose-induced expression became homogenous, suggesting that the heterogeneity of the pulse was due to asynchronous activation of the *GAL* promoter **(figure 4A)**.

While this situation was improved to some extent by pregrowth in glycerol-ethanol rather than raffinose **(figure 4B)**, basal expression of *GAL1-CLB2kd-YFP* in glycerol-ethanol was significant and toxic, and synchronization procedures worked poorly in this medium. For these reasons, we sought a pulse protocol that would yield low basal levels of expression, and that did not involve manipulations that induce a major change in metabolism or growth rate.

The *GAL1* promoter is normally activated by the Gal4 transcription factor. Gal80 binds to and inhibits Gal4 in the presence of glucose. A fusion of the Gal4 DNA binding domain to the hormone-binding domain of the rat mineralocorticosteroid receptor (Gal4-rMR) (Mattioni et al., 1994), lacking the

Figure 4. *GAL1* promoter activation is heterogeneous in raffinose and homogeneous in glycerol/ethanol.

P_{GAL1}→*GFP* cells were grown in either raffinose **(A)** or glycerol/ethanol **(B)**. Galactose was added to 3% (t=0) and samples were taken after 40 or 80 minutes. GFP fluorescence was analyzed by FACS and fluorescence microscopy.

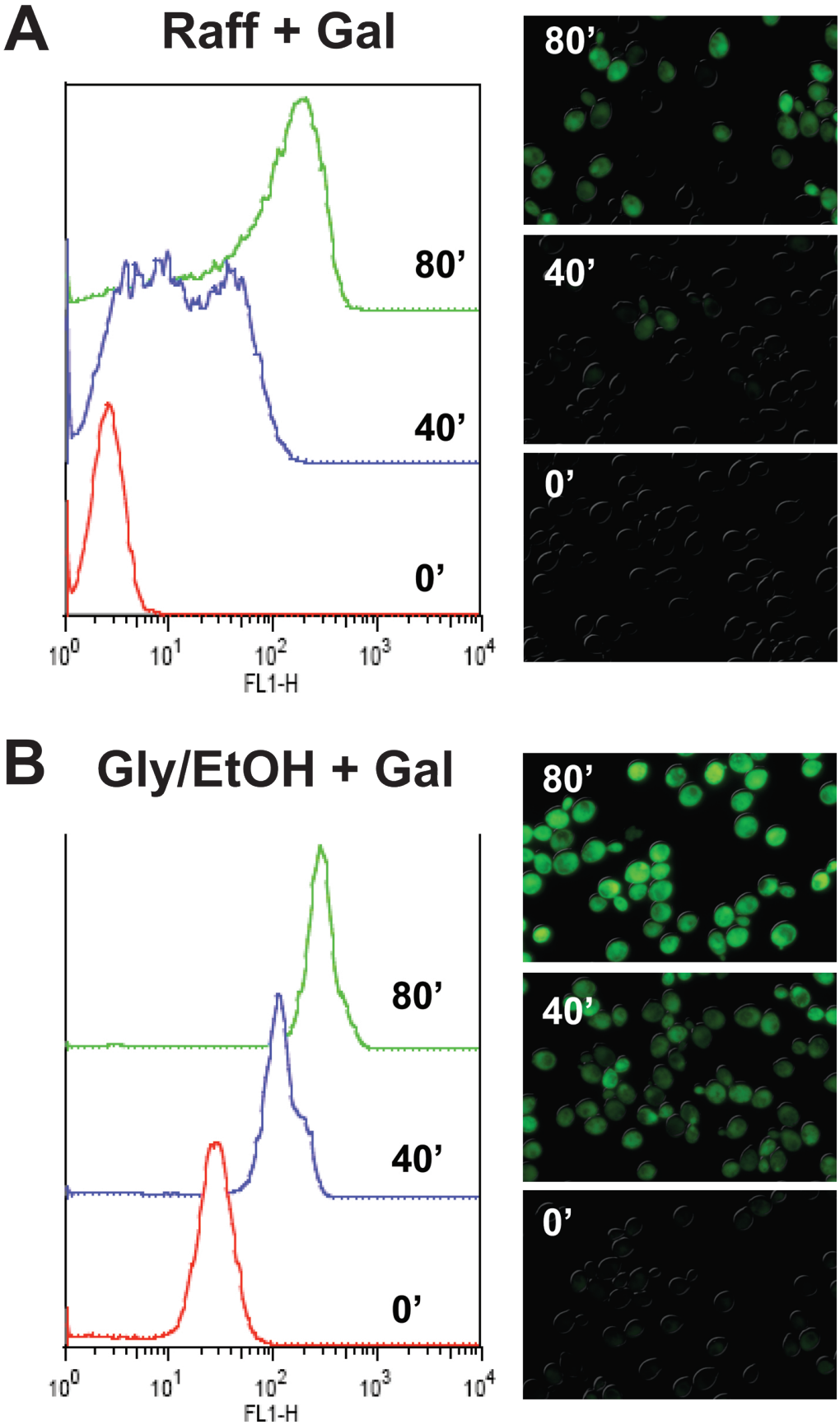
A
Raff + Gal
80’
40’
0’
10^0
10^1
10^2
10^3
10^4
FL1-H
80’
40’
0’
B
Gly/EtOH + Gal
80’
40’
0’
10^0
10^1
10^2
10^3
10^4
FL1-H
80’
40’
0’

Gal80 binding domain, was reported to drive effective induction of the *GAL1* promoter upon addition of deoxycorticosterone (dCort), a mineralocorticosteroid. Since the Gal4-rMR allele is not inhibited by Gal80, dCort induction of the *GAL1* promoter can be carried out in medium containing glucose.

When added to cells containing *GAL1-CLB2kd-YFP* and expressing Gal4-rMR, dCort induction provides a low and uniform pulse in glucose without detectible basal expression **(figure 5A)**. Shut off upon washout of hormone is comparable to glucose inactivation after galactose induction **(figure 5B)**. Surprisingly, this pulse of Clb2kd-YFP was too low to inhibit mitotic exit, even after a 90-minute induction. However, hormone-induced expression was enhanced by using raffinose as a carbon source, without broadening the pulse distribution **(figure 5C)**. This allowed an undegradable Clb2 pulse within a relevant range to study inhibition of mitotic exit.

Peak Measurement by Fluorescence

In order to calibrate the mean pulse fluorescence to peak B-cyclin concentration, we initially attempted measuring the maximum fluorescence of Clb2p tagged at its endogenous locus with YFP during an α-factor block-release-block time course. Western blot measurement of mean protein concentration revealed that Clb2-YFP began to accumulate 30 min post-release from α-factor arrest, reached peak concentration 60 min post-release, and was almost undetectable 90 minutes post-release.

It is notable how sharply Clb2p levels are cell-cycle-regulated in this protocol **(figure 6A);** this point becomes technically relevant later on. Clb2p levels represent only a portion of the total mitotic cyclin, because of the *CLB1,3,4* genes, which partially overlap in function with *CLB2* (Fitch et al., 1992; see Introduction). However, Clb2-YFP attained the same maximum concentration at the same time in the *clb1,3,4Δ* background as in a wt background **(figure 8A)**; this leads to the important conclusion that this level of Clb2 provides sufficient mitotic cyclin for timely mitosis, as evidenced by equivalent timing of cell division (indicated by the appearance of 1C DNA content cells) in the two strains in the α-factor block-release protocol **(figure 8B)**.

Peak Clb2-YFP fluorescence lagged behind the peak western level by 20 minutes, reflecting the known lag between Clb2-YFP synthesis and the maturation of the YFP to fluorescence. This lag was of a magnitude longer than that of critical events in the cell cycle (e.g., see timing of Clb2p accumulation and degradation, Figure 5). To work around the YFP maturation problem, we performed the same experiment in a strain in which the only functional *CDC20* allele is under the control of the methionine-repressible *MET3* promoter (*cdc20::*P_{MET3}*→*HA_3*-CDC20*, hereafter called *MET-CDC20*). Clb2p is stable in the absence of APC^{Cdc20} activity (see Introduction). We released an α-factor arrested culture of *MET3::CDC20 CLB2-YFP* cells into medium lacking α-factor, but containing methionine to deplete Cdc20 and prevent APC-mediated degradation of Clb2-YFP. At 60 minutes post-release, the time of peak western

Figure 5. *GAL1* promoter activation with deoxycorticosterone is homogeneous. **(A)** P_{GAL1}→*YFP GAL4-rMR* cells were grown in raffinose, glycerol/ethanol or glucose. The raffinose and glycerol/ethanol cultures were induced with galactose, and the glucose culture was induced with deoxycorticosterone (dCort). Induction times as indicated.
(B) P_{GAL1}→*YFP GAL4-rMR* cells were grown in raffinose and induced with galactose or grown in glucose and induced with dCort. Cultures were then resuspended in glucose medium lacking inducer. Samples were taken after removal of the inducer at the indicated times.
(C) P_{GAL1}→*CLB2kd-YFP GAL4-rMR MET-CDC20* cells were grown in glucose or raffinose, arrested with methionine, and induced with dCort for the indicated times.

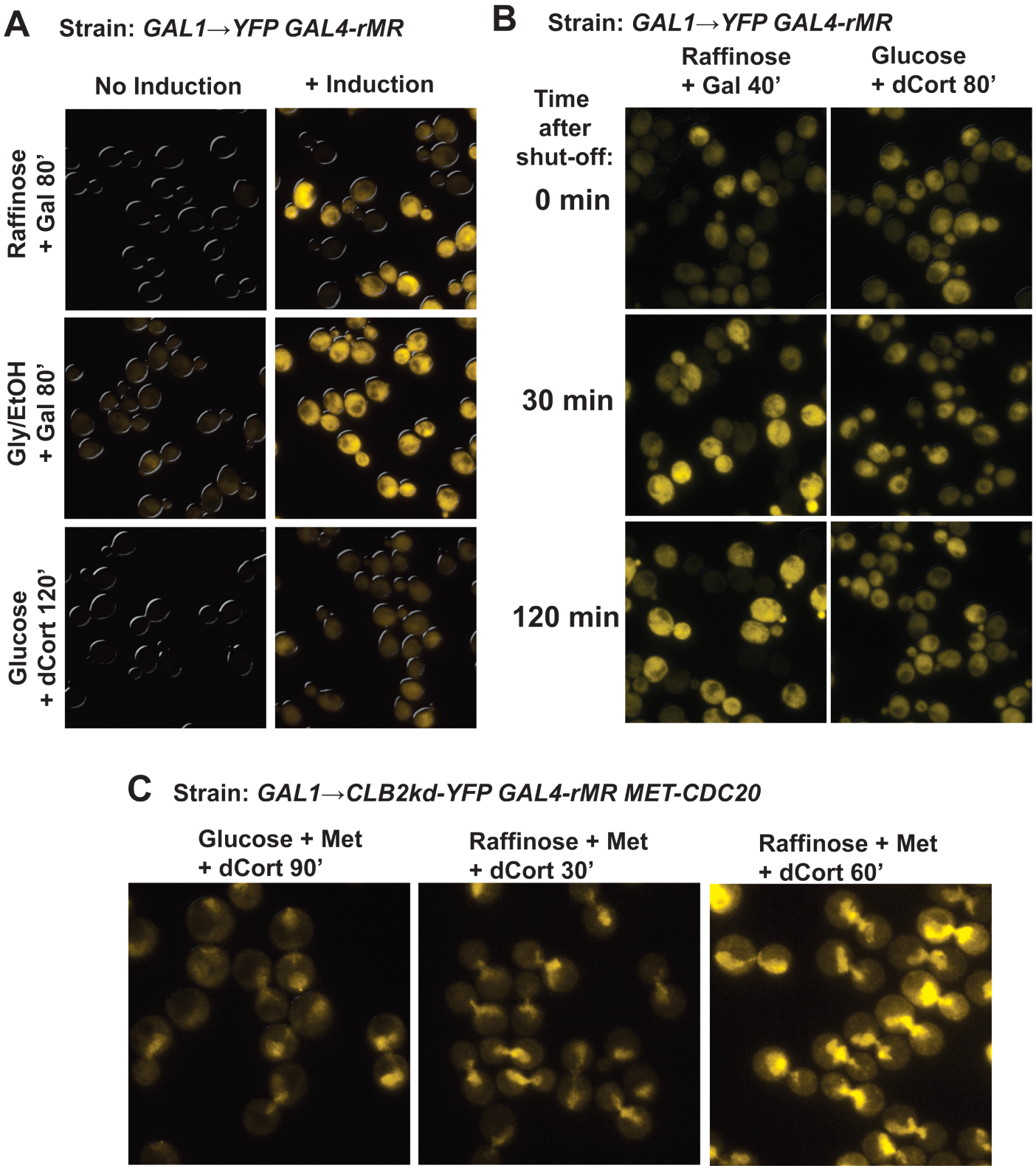
A
Strain: GAL1→YFP GAL4-rMR
No Induction
+ Induction
Raffinose + Gal 80'
Gly/EtOH + Gal 80'
Glucose + dCort 120'
B
Strain: GAL1→YFP GAL4-rMR
Raffinose + Gal 40'
Glucose + dCort 80'
Time after shut-off:
0 min
30 min
120 min
C
Strain: GAL1→CLB2kd-YFP GAL4-rMR MET-CDC20
Glucose + Met + dCort 90'
Raffinose + Met + dCort 30'
Raffinose + Met + dCort 60'

Figure 6. Peak Clb2-YFP fluorescence lags peak protein accumulation. **(A)** Cells expressing *CLB2-YFP* from the endogenous tagged locus were released from α-factor arrest, and α-factor was added back to the medium 45 minutes post-release. Samples were taken every 10 minutes and measured for DNA content by FACS and Clb2-YFP protein concentration by quantitative western blot. Pgk1p concentration was used as a loading control. **(B)** *CLB2-YFP* cells treated with α-factor as above. Samples were taken every 20 minutes and measured for Clb2-YFP protein concentration by quantitative western blot and fluorescence microscopy quantifying YFP fluorescence in individual cells. Pictures depict YFP fluorescence 60' and 80' post-release.

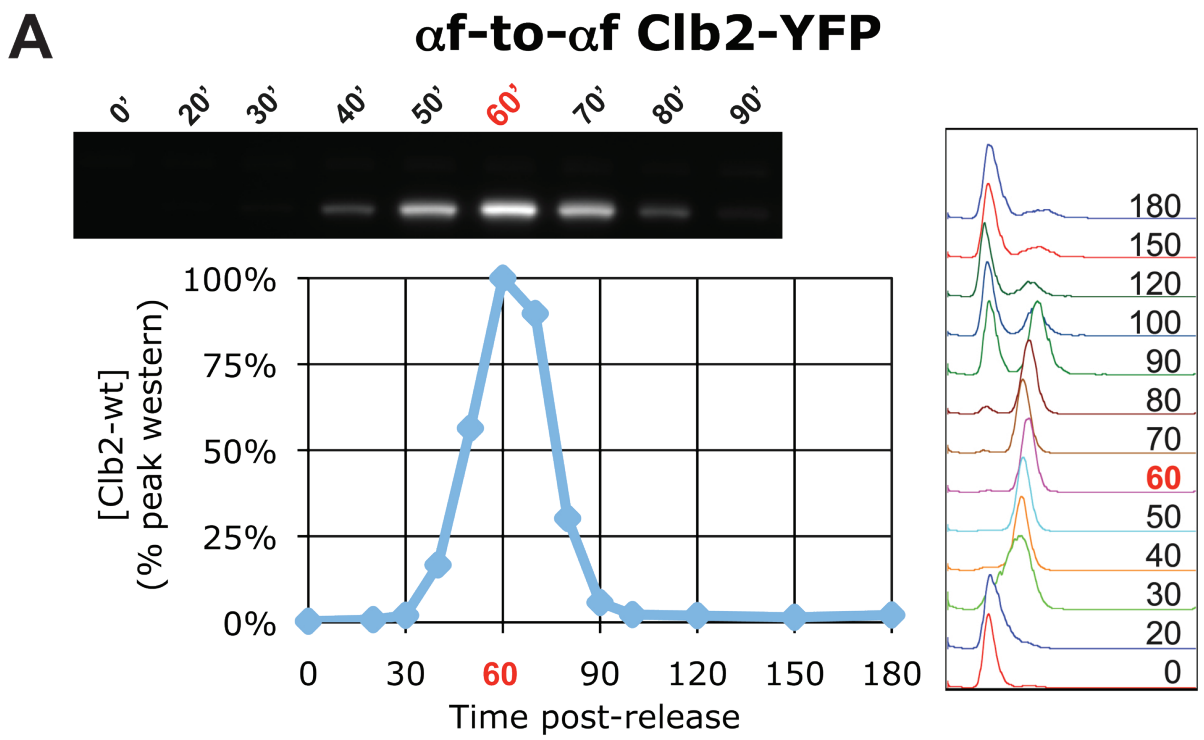
A
αf-to-αf Clb2-YFP
0'
20'
30'
40'
50'
60'
70'
80'
90'
100%
75%
50%
25%
0%
[Clb2-wt]
(% peak western)
0
30
60
90
120
150
180
Time post-release
180
150
120
100
90
80
70
60
50
40
30
20
0

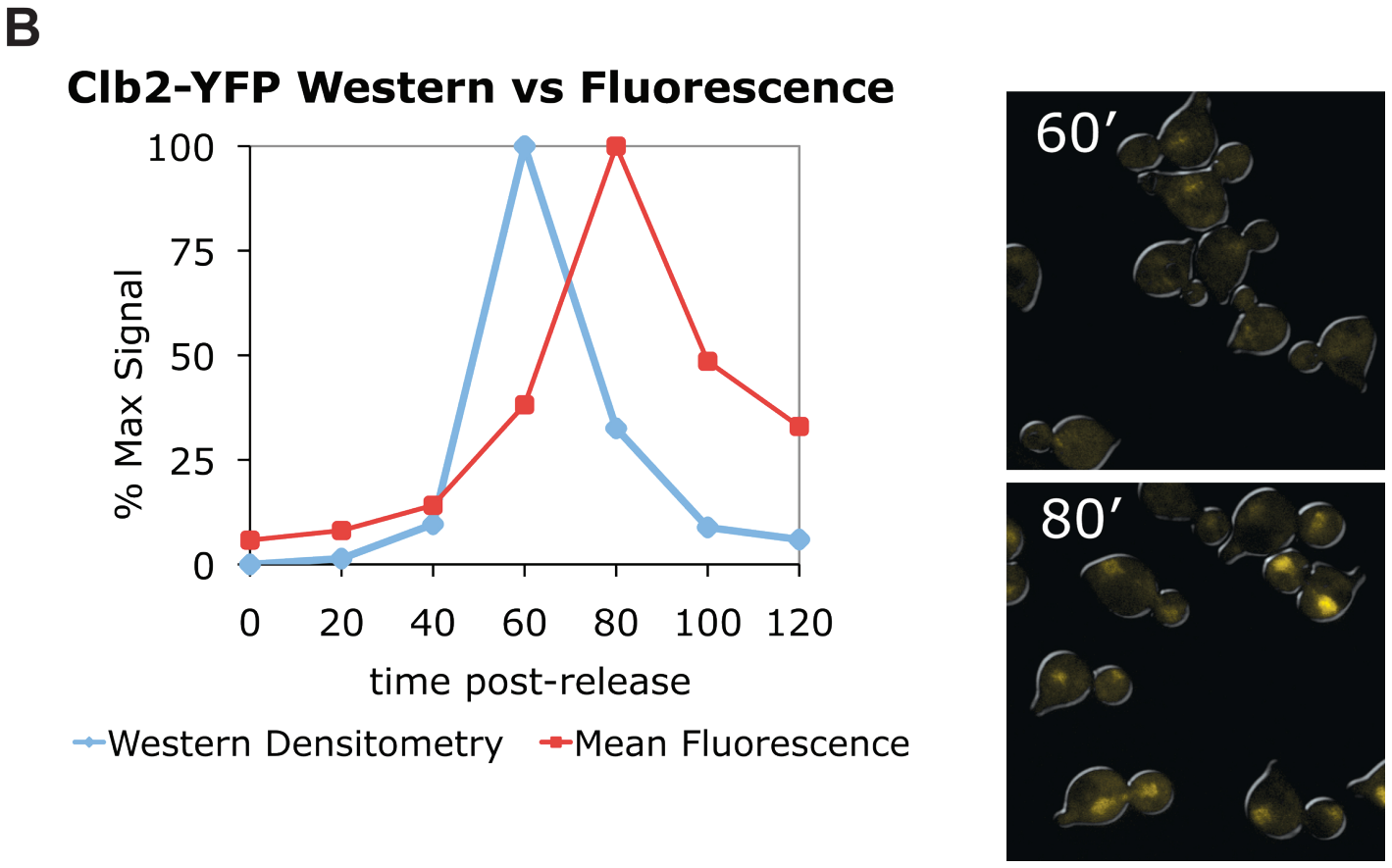
B
Clb2-YFP Western vs Fluorescence
100
75
50
25
0
% Max Signal
0
20
40
60
80
100
120
time post-release
Western Densitometry
Mean Fluorescence
60'
80'

signal in these time courses (Figure 5), we added the protein synthesis inhibitor cycloheximide to prevent continued Clb2-YFP synthesis. Under these conditions Clb2p should be neither synthesized nor degraded, and indeed a stable level was observed by Western blot (**figure 7A**). Unlike Clb2-YFP protein levels, Clb2-YFP fluorescence increased four-fold after cycloheximide addition, and reached a plateau after approximately 60 min after the block to new protein synthesis (**figure 7B**). Peak Clb2-YFP fluorescence was approximately normally distributed with a coefficient of variation of about 0.5 (**figure 7C**).

The average peak concentration of Clb2p in a synchronized time course closely approximates the single-cell maximum concentration.

The coefficient of variation of 0.5 in Clb2-YFP fluorescence in the *cdc20* cycloheximide protocol described above, once most or all Clb2-YFP had become fluorescent, could be interpreted as variation in the actual peak level, or could be due to asynchrony in the culture. Western blotting measures the average concentration of a protein in a cell population. With perfect culture synchrony, and if all cells make an identical level of Clb2 at each point in the cell cycle, the single cell Clb2-YFP maximum and population maximum would be identical. Increasing asynchrony in timing of onset of *CLB2* transcription or degradation would cause single-cell concentration curves to peak at different times, and

immunoblotting would then underestimate the true peak concentration **(figure 9A).** The peak level and timing is likely dependent on activation of Clb2p degradation by APC-Cdc20 (Yeong et al., 2000).

To assess the synchrony of the population, we released *MET-CDC20* cells from α-factor arrest into medium with or without methionine. We then compared the Clb2-YFP concentrations of the two cultures over time by western blot. Since the presence or absence of the other mitotic cyclins did not measurably affect Clb2-YFP accumulation or degradation, we performed this analysis in the *clb1,3,4Δ* background **(figure 8)**. If significant asynchrony in reaching the Clb2 peak made it appear artificially at a lower level in population measurements (where the average amount peaks at 60 min post release), then blocking Clb2 degradation by Cdc20 depletion would likely create an obviously higher level at this timepoint (**figure 9A**). However, we found that the Clb2-YFP accumulation curves are nearly identical up to 60 minutes post-release, whereupon the $Cdc20^{+}$ culture begins to degrade Clb2p, and the $Cdc20^{-}$ culture continues to accumulate Clb2-YFP to a plateau of approximately 2-fold the 60-minute peak (**figure 9B,C**). Importantly for later experiments, the timing of Clb2p accumulation in α-factor block-release experiments was very similar in wild-type cells and in *MET3-CDC20* cells maintained in –Met for continuous *CDC20* transcription (data not shown).

Figure 7. The average peak Clb2 concentration of a Distribution of peak Clb2-YFP fluorescence in a cell population.

To measure the distribution across a cell population of peak Clb2-YFP at its normal peak level, and with YFP fully matured, *MET-CDC20 CLB2-YFP* cells were released from α-factor to medium containing methionine to prevent Cdc20 accumulation; at the ensuing *cdc20* block Clb2 is completely stable (Wäsch and Cross, 2002). Cycloheximide (CHX) was added 55 min after release, at the time of peak Clb2 protein accumulation as estimated by Western blot, to prevent further Clb2-YFP synthesis. **(A)** Protein concentration (orange) and average YFP fluorescence (green) were monitored compared to the α-factor to α-factor time course described in **figure 6A** (blue). **(B)** YFP reaches full fluorescence 120 min post-release, ~65 min after cycloheximide addition. **(C)** The single cell distribution of Clb2-YFP 120 min post-release.

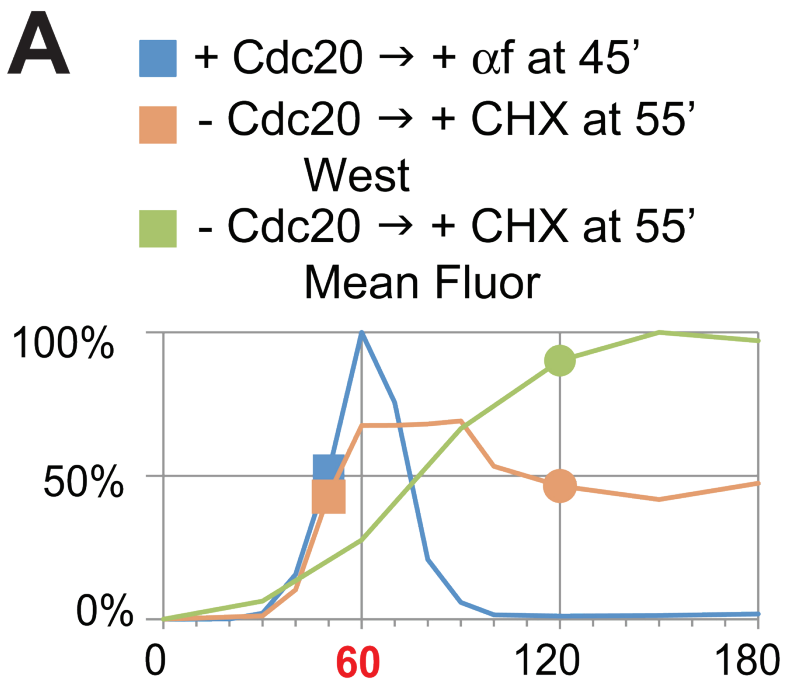
A
+ Cdc20 → + αf at 45’
- Cdc20 → + CHX at 55’
West
- Cdc20 → + CHX at 55’
Mean Fluor
100%
50%
0%
0
60
120
180

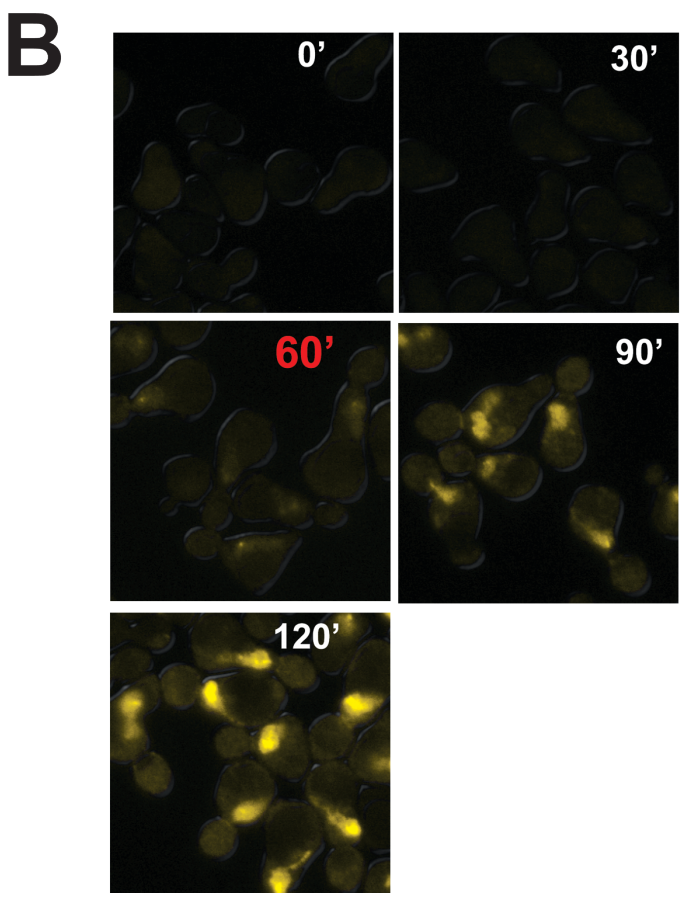
B
0’
30’
60’
90’
120’

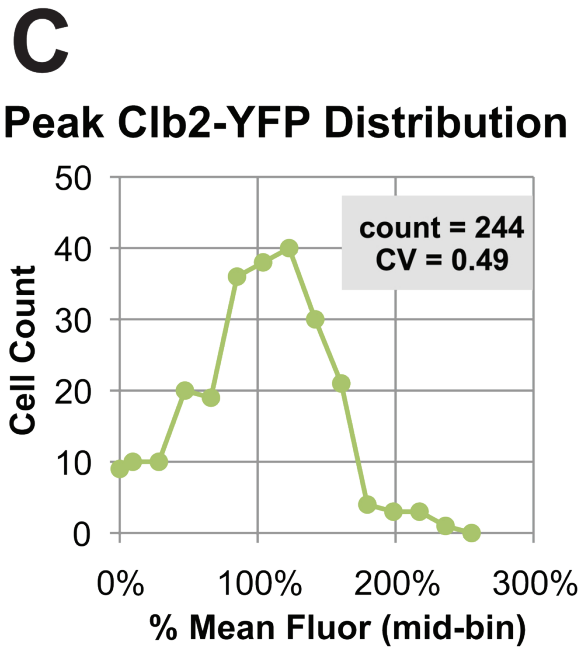
C
Peak Clb2-YFP Distribution
count = 244
CV = 0.49
Cell Count
50
40
30
20
10
0
0%
100%
200%
300%
% Mean Fluor (mid-bin)

Figure 8. Peak Clb2 concentration and timing of cell cycle events is not affected by deletion of other mitotic cyclins.

CLB2-YFP cells either containing (WT) or lacking (*clb1,3,4Δ*) the other mitotic cyclins were released from α-factor arrest; after release, α-factor was added back to block a second cycle. Samples were taken every 10 minutes and analyzed for DNA content **(A)** and protein concentration. Peak protein concentration occurred in both cases 60 minutes post-release. Peak samples were compared by quantitative western blot **(B)**.

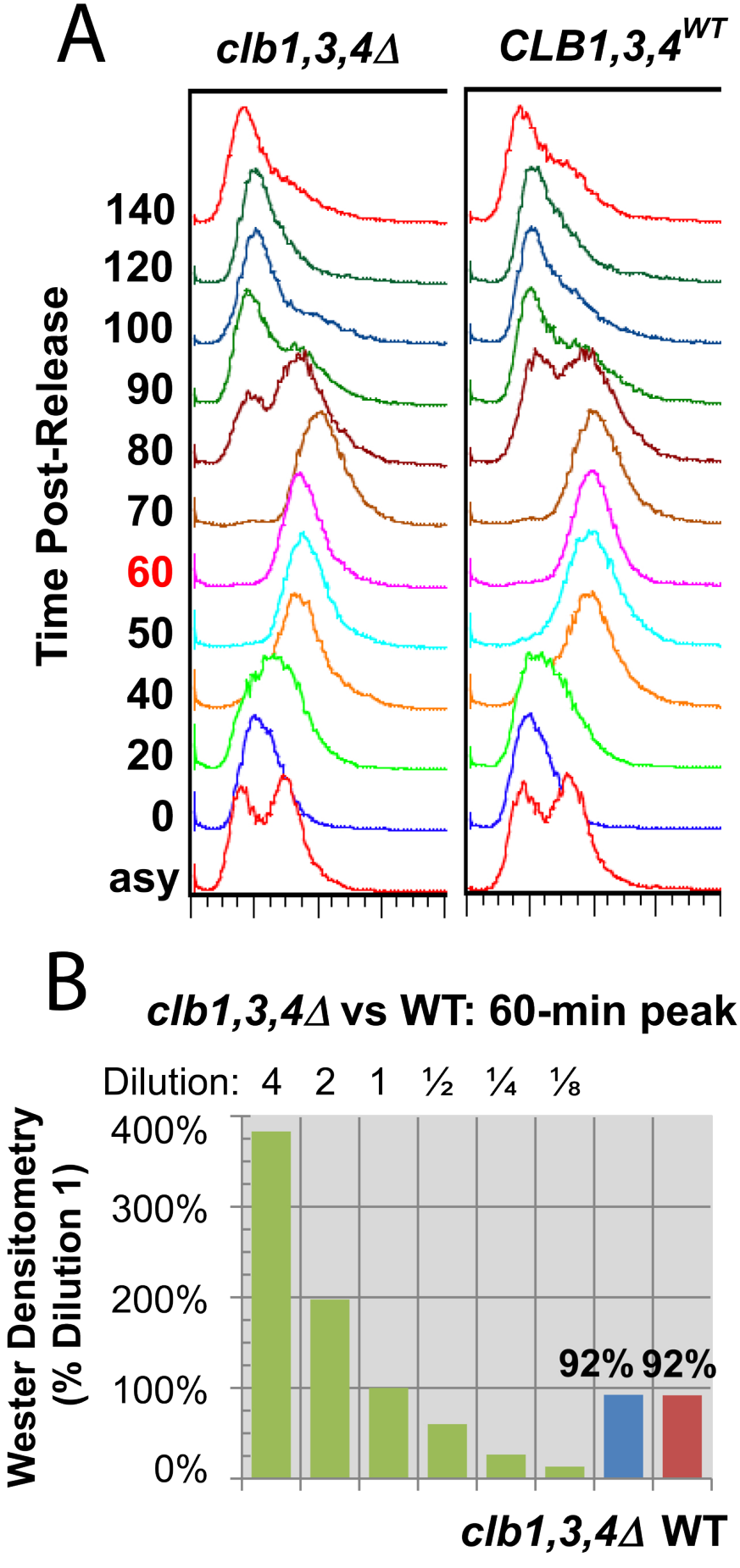
A
clb1,3,4Δ
CLB1,3,4WT
Time Post-Release
140
120
100
90
80
70
60
50
40
20
0
asy
B
clb1,3,4Δ vs WT: 60-min peak
Dilution: 4 2 1 ½ ¼ ⅛
Wester Densitometry (% Dilution 1)
400%
300%
200%
100%
0%
92% 92%
clb1,3,4Δ WT

Figure 9. synchronized culture closely approximates the average single-cell peak. (A) Models for synchronous or asynchronous protein concentration curves with or without APC^{Cdc20} activation. Single cell curves (yellow) and population averages (red) are depicted, as are the consequences of APC inactivation in either case. **(B and C)** *CLB2-YFP clb1,3,4Δ* cultures were synchronized with a-factor and released to either a cdc20 block or a second a-factor block. Clb2-YFP protein concentration was measured by quantitative western blot from samples taken every 10 minutes after release.

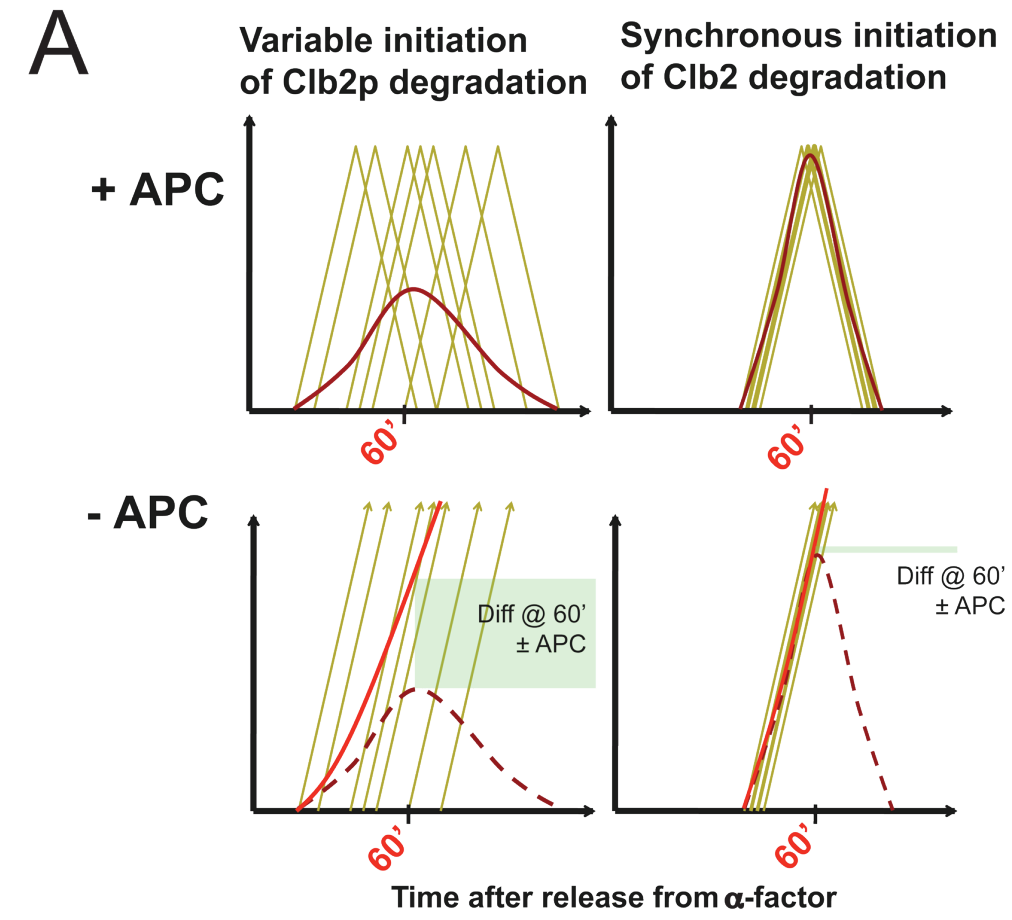
A
Variable initiation of Clb2p degradation
Synchronous initiation of Clb2 degradation
+ APC
- APC
60'
60'
60'
60'
Diff @ 60' ± APC
Diff @ 60' ± APC
Time after release from α-factor

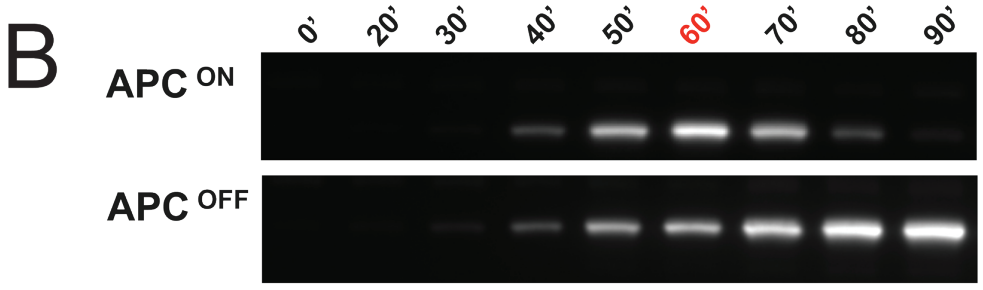
B
0'
20'
30'
40'
50'
60'
70'
80'
90'
APC ON
APC OFF

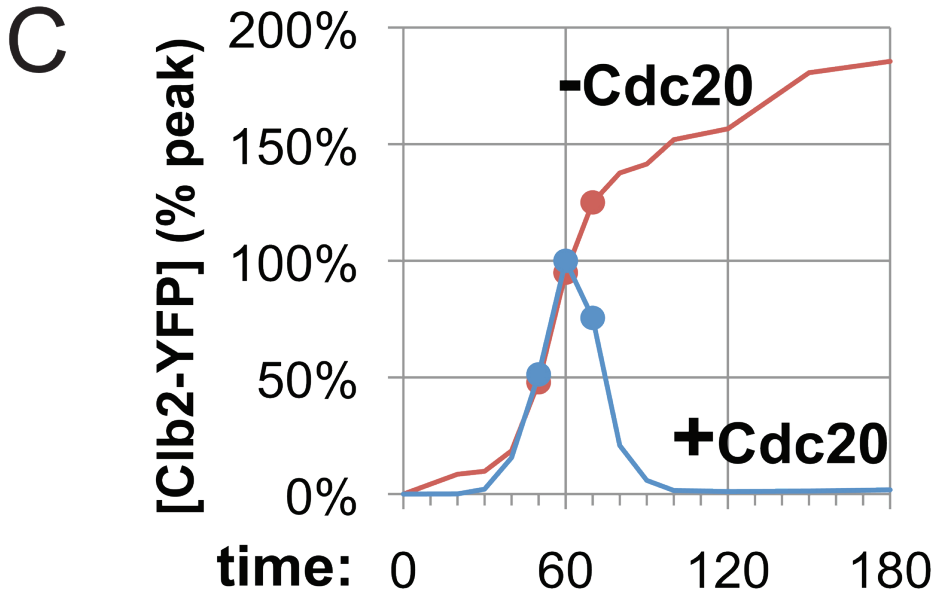
C
[Clb2-YFP] (% peak)
200%
150%
100%
50%
0%
-Cdc20
+Cdc20
time:
0
60
120
180

It is surprising that Clb2 appears to plateau at 2-fold the normal peak level in the absence of Cdc20, but this may be because *CLB2* transcript levels become very low at a *cdc20* block, for unknown reasons (Bean et al., 2005).

The finding that when a culture released from α-factor arrest reaches maximum Clb2p concentration, a culture released in parallel into conditions that prevent Clb2p degradation has the same Clb2p concentration suggests that the peak Clb2-YFP concentration of the α-factor-synchronized culture closely approximates the single-cell maximum concentration. There is significant variation in peak YFP fluorescence between individual cells (**figure 7C**); this implies that peak Clb2-YFP concentration varies from cell to cell, either because of duration or rate of Clb2 synthesis before Cdc20 activation.

Although the implications of this result for culture synchrony are specific to onset of Clb2-YFP degradation, other features of the α-factor time course also suggest a high degree of synchrony. DNA flow cytometry of samples taken at 10 min intervals demonstrates that DNA replication in the population is completed over a 20-minute interval **(figure 6A);** the shortest previous estimate for the time of replication based on execution point measurements and flow cytometry profiles of highly synchronized cultures is ~18 min (Epstein and Cross, 1992).

For the rest of this work, we will accept as an assumption that the apparent peak level of Clb2 attained in this time-course represents the normal peak level attained in an unperturbed cell cycle. Two caveats apply here: first, cell cycle synchrony is never perfect, so this measurement is likely to represent a slight

under-estimate of the true peak. Second, the measurement necessarily requires a block-release synchrony protocol, and this could affect Clb2 levels in some unknown way. We do not consider these to be major flaws but they need to be considered in evaluating the work overall.

Titration of Undegradable B-Cyclin to Endogenous Peak Concentration

We use the following protocol to measure the level of undegradable Clb2kd-YFP within single cells. We use cells of the genotype *MET3-CDC20 GAL1-CLB2kd-YFP ADH1- GAL4-rMR*, Before Clb2kd-YFP induction by addition of deoxycorticosterone (dCort), which activates the Gal4-MR fusion protein, *MET-CDC20* cultures are arrested at metaphase by Cdc20 depletion. The metaphase arrest induced by Cdc20 depletion provides an appropriate time for induction of undegradable Clb2kd for two reasons. First, Clb2p is already present at a high level in cdc20-arrested cells, and further overexpression does not disrupt spindle elongation or other mitosis-promoting CDK functions (Surana et al., 1993)**;** indeed, since we are typically aiming for approximately peak-equivalent concentrations of Clb2kd, the induced Clb2kd will represent a minority of the total Clb2p in these blocked cells. Second, all pre-anaphase cellular functions have been completed except for cohesin cleavage (Sullivan and Uhlmann, 2003), which is induced rapidly by Cdc20 activation (see Introduction). This avoids effects of excessive Clb2 on earlier events; for example, expression of high levels

of undegradable Clb2 in unbudded cells blocks bud emergence (Amon et al., 1994; Lew and Reed, 1993).

Brief activation with dCort via Gal4-rMR produces an approximately normally distributed pulse of Clb2kd-YFP; at appropriate pulse durations, a mean concentration can be obtained that is near the peak endogenous Clb2p level (i.e., a 'peak-equivalent' level of Clb2kd). Clb2kd-YFP synthesis is ended by washout of the hormone and resuspension in glucose-containing medium. No new Clb2kd-YFP is synthesized after the hormone is washed out, as demonstrated by comparison with cycloheximide-mediated termination of protein synthesis **(figure 10A**). Glucose may help further repress the *GAL1* promoter, and also provides the advantage that the rest of the experiment is carried out in rich glucose medium.

Cdc20 depletion is maintained for an additional 45' to allow the majority of Clb2-YFP to mature to fluorescence. At the conclusion of Clb2kd-YFP induction, which reaches 70% of its maximum at this time (**figure 10**). This timing agrees with the maturation time for endogenous Clb2-YFP with translation arrested by cycloheximide (see above). The F/W ratio in cells pulsed with Clb2kd-YFP reaches a maximum at 90' after dCort washout (45 min after release of the *cdc20* block), at which point control cells not containing *GAL1-CLB2kd-YFP* are completing mitotic exit. This is the first time point at which single-cell undegradable Clb2 concentration is measured. Attaining a maximum F/W ratio implies that essentially all of the pulsed Clb2kd-YFP is fully fluorescent. By

allowing completion of YFP folding to occur during the release of the *cdc20* block, we can minimize the time spent at the *cdc20* block, which reduces the artifactual increase in cell size in cells arrested at this block.

Measuring Single-Cell Undegradable B-Cyclin Concentration in Units of Endogenous Peak Concentration

The Clb2kd-YFP pulse is converted to peak-equivalent units as follows. First, we measure single-cell Clb2kd-YFP fluorescence. YFP fluorescence is determined as the average YFP-channel pixel intensity over a whole-cell mask. The single-cell fluorescence level is converted to concentration units of % mean pulse by dividing by the mean fluorescence of all the cells imaged in a given sample. Interestingly, Clb2kd-YFP fluorescence is not distributed evenly throughout the cell. Clb2kd-YFP concentrates in the nucleus, at the bud ring, and along the metaphase spindle, and is especially concentrated at the spindle pole bodies **(figure 10B)**. For simplicity, however, we measure only the total cellular Clb2kd-YFP; while this may discard some interesting information, including subcellular localization splits the data many more ways, thus requiring a large increase in sample size.

The peak Clb2-YFP western sample is treated as a close approximation of the average single-cell maximum for the reasons mentioned above. The pulsed Clb2kd-YFP western sample is treated as equivalent to the mean value of the pulse. Therefore, we convert single-cell Clb2kd-YFP concentration expressed as

Fiugre 10. Titration of undegradable B-cyclin to endogenous peak concentration and measurement in single cells.

(A – E) *P_{GAL1}→CLB2kd-YFP GAL4-rMR MET-CDC20* cells were grown in raffinose, arrested with methionine for 150 minutes, and induced with dCort for 30 minutes. **(A)** To test dCort induction shut-off, the culture was split into three. Cycloheximide (CHX) was added to the first. The second was resuspended in glucose + methionine (D+Met). The third was allowed to continue dCort induction for another 30 minutes. Samples were taken after 30 minutes and compared for YFP fluorescence. **(B – E)** After 30-minute dCort induction, cells were resuspended in D+Met for 45 minutes, then resuspended in D-Met. Samples were taken every 15 minutes for 90 minutes for quantitative western blot and fluorescence microscopy. Methionine was added back after 45 minutes. **(B)** Pictures: Clb2kd-YFP before and after hormone induction, 15 minutes before cdc20 release, and every 30 min after release from cdc20 arrest. Post-pulse time is in white, post-release time in red. **(C)** Western blots comparing 30' and 60' Clb2kd-YFP pulses to the 60-minute peak Clb2-YFP samples from *CLB1,3,4^{WT}* and *clb1,3,4Δ* time-courses (**figure 8**). Immunoblots using both anti-Clb2 and anti-GFP antibodies are shown. Protein levels are compared using 2-fold concentration standards of Clb2kd-YFP and Clb2^{WT}-YFP diluted into *clb2Δ* extract. **(D)** Mean Clb2kd-YFP pulse after release from cdc20-arrest, measured by western blot (blue) and YFP fluorescence (green). Fluorescence-to-western ratio is depicted (red). **(E)** Distribution of the Clb2kd-YFP pulse as a percentage of the average peak Clb2-YFP expression. For a single cell:

$$\%\ \text{peak} = \frac{F_{cell}}{\text{mean } F_{pulse}} \times \frac{W_{pulse}}{W_{peak}}$$

(F) Comparison of pulse and peak measurement by fluorescence and western. Clb2kd-YFP pulses are measured 60 minutes post-release from cdc20 arrest. Peak Clb2-YFP fluorescence is measured 60 minutes after addition of CHX.

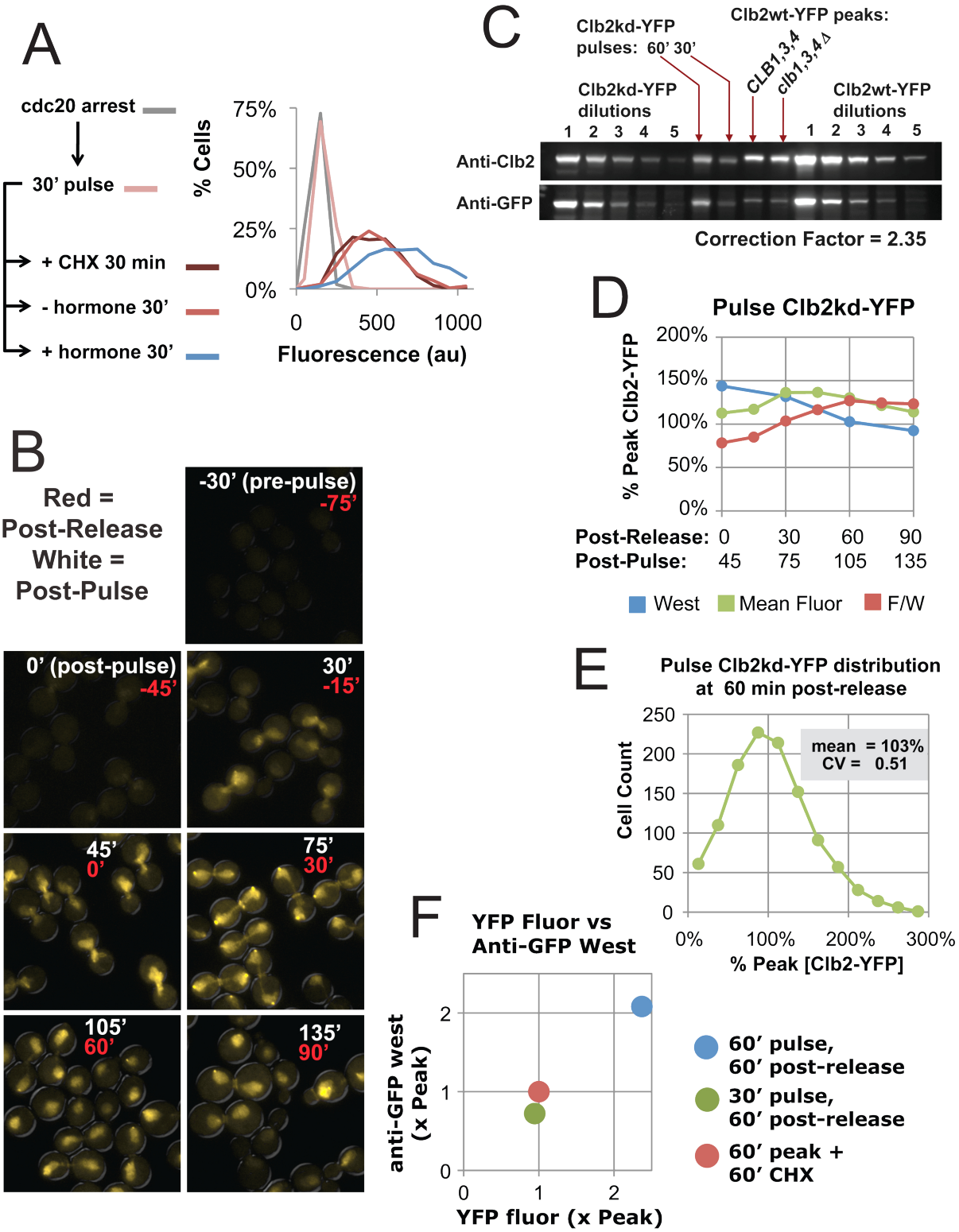
A
cdc20 arrest
30' pulse
+ CHX 30 min
- hormone 30'
+ hormone 30'
% Cells
75%
50%
25%
0%
0
500
1000
Fluorescence (au)
B
Red =
Post-Release
White =
Post-Pulse
-30' (pre-pulse)
-75'
0' (post-pulse)
-45'
30'
-15'
45'
0'
75'
30'
105'
60'
135'
90'
C
Clb2kd-YFP
pulses: 60' 30'
Clb2wt-YFP peaks:
CLB1,3,4
clb1,3,4Δ
Clb2kd-YFP
dilutions
Clb2wt-YFP
dilutions
1 2 3 4 5
1 2 3 4 5
Anti-Clb2
Anti-GFP
Correction Factor = 2.35
D
Pulse Clb2kd-YFP
% Peak Clb2-YFP
200%
150%
100%
50%
0%
Post-Release: 0 30 60 90
Post-Pulse: 45 75 105 135
West
Mean Fluor
F/W
E
Pulse Clb2kd-YFP distribution
at 60 min post-release
Cell Count
250
200
150
100
50
0
mean = 103%
CV = 0.51
0%
100%
200%
300%
% Peak [Clb2-YFP]
F
YFP Fluor vs
Anti-GFP West
anti-GFP west
(x Peak)
2
1
0
0
1
2
YFP fluor (x Peak)
60' pulse,
60' post-release
30' pulse,
60' post-release
60' peak +
60' CHX

a fraction of mean fluorescence in pulsed cells to peak-equivalent units by multiplying by the quantitative western blot ratio of pulse to peak **(figure 10C)**. For all quantitative western blots we use 2-fold dilution standards of both Clb2wt-YFP and Clb2kd-YFP into *clb2Δ* extract, preventing any non-linearity in the western blotting protocol due to differing amounts of total protein being transferred. For direct western comparison we use a monoclonal anti-GFP antibody, since $Clb2^{WT}$-YFP expressed from the endogenous *CLB2* promoter and exogenous Clb2kd-YFP expressed from the *GAL1* promoter contain the same C-terminal YFP fusion. We also use a polyclonal anti-Clb2 antibody. The anti-Clb2 antibody generates less background than the anti-GFP antibody, can be used at 10-fold lower concentration and detects untagged Clb2 as well as Clb2-YFP. Therefore the anti-Clb2 antibody allows greater precision in measurement. However, it generates a significantly stronger signal when exposed to $Clb2^{WT}$-YFP versus Clb2kd-YFP, as compared with the anti-GFP blot. This appears to be due to the KEN boxes and/or destruction boxes constituting major antigenic epitopes in the polyclonal anti-Clb2 antiserum available in the lab (data not shown). Therefore, when this antibody is used, a correction is derived for each blot by comparison of the ratios of the dilution standards with each antibody. For quantitative western blotting, we read the blots with a CCD camera, which gives a wide dynamic range and near-linear response through the signal intensities in these experiments (data not shown).

Using the protocol described above, a 30-minute induction with dCort results in a Clb2kd-YFP pulse that decreases from approximately 1.5× peak Clb2-YFP at the point of release from cdc20 arrest to slightly less than 1× peak at the conclusion of the time course, 90 minutes post-release (**figure 10D**). Since at all time points an equal amount of total cell protein is analyzed in this procedure, a decrease in Clb2kd-YFP level of approximately this magnitude is expected simply due to continued cell growth and dilution of previously synthesized Clb2kd-YFP. At 60 minutes post-release, this pulse reproduces the distribution of Clb2-YFP at its peak level: an approximately normal distribution of Clb2kd-YFP concentrations with a mean value of 103% peak and a coefficient of variation of 0.5 **(figure 10E).**

Convergence of Pulse/Peak Ratios by Fluorescence and Western Validates the Threshold Measurement

The measurement of single-cell Clb2kd-YFP level in terms of normal peak Clb2 level, described above, requires multiple measurements, each with associated but generally unknown inaccuracy. Fortunately, quantitative western blotting of protein extracts of cell populations and fluorescence microscopy of individual cells are independent methods that we can hope will have independent sources of error, that are unlikely to all point in the same direction. The observation that the ratio of pulsed Clb2kd-YFP to peak Clb2-YFP as measured

by western blot was similar to the ratio measured by mean YFP fluorescence (**figure 10F)** increases our confidence in the validity of these measurements.

Fluorescence as measured may slightly overestimate the pulse, since peak fluorescence is measured 60 minutes after cycloheximide addition, whereas pulse fluorescence is measured at least 75 minutes after cessation of translation. Indeed, the F/W ratio of the pulse reaches a plateau of approximately 1.2-fold peak **(figure 10D).** Since cycloheximide is not an innocuous treatment, we were reluctant to trust the results of longer incubations. However, as mentioned above, the western value closely approximates the single-cell peak. Therefore the mean fluorescence at peak Clb2-YFP accumulation is not necessary to calibrate the single-cell pulse concentration, although reassuringly, it does give a measurement close to that derived from the Western blotting procedure.

The process of reconciling fluorescence and western measurements revealed several sources of error that led to technical adjustments. These adjustments are detailed in the materials and methods, but in brief they include the choice of CCD camera over film, the use of dilution standards, correction of the anti-Clb2 antibody for increased binding to Clb2-wt vs. Clb2-kd, whole-cell masks to measure YFP fluorescence and provision of time for YFP maturation. The challenge of reconciling western and fluorescence results was the main driver for arriving at the protocol detailed in figure 2.

Mitotic exit and the subsequent cell cycle in unpulsed cells are highly synchronous after release from cdc20 arrest.

Since the YFP emission spectrum does not overlap with that of either CFP or mCherry, these channels may be employed, along with cell morphology, to correlate post-anaphase phenotype with increasing Clb2kd-YFP concentration. We follow the progression of cytokinesis, budding, and spindle dynamics in single cells using the fluorescent fusion proteins Myo1-mCherry (type-II myosin) and CFP-Tub1 (α-tubulin) **(figure 11A).** We score phenotype in units of original cell bodies rather than final cells: a pair of cell bodies deriving from an original budded cell, that have not completed cytokinesis (as indicated by persistence of Myo1-mCherry signal between them) is counted as two cells of a given phenotype. This avoids apparent over-representation of cells that have completed cytokinesis (for example, if 50% of cells complete cytokinesis and this correction is not applied, the result is 67% of cells scored as having completed cytokinesis, which is clearly misleading).

We found that spindle morphology was highly sensitive to sonication; therefore, the usual method of sonicating to disrupt cell clumps and assess cell division was not available for these experiments. Therefore, we use the Myo1-mCherry signal as a surrogate marker for cytokinesis; we assume that complete closure and disassembly of this ring correlates with cytokinesis (Bi et al., 1998).

We sample the cultures every fifteen minutes after restoration of Cdc20 synthesis by methionine removal. Sampling of the culture at 15-minute intervals

Figure 11. Phenotypic progression from cdc20 synchronization to a second cdc20 block.

(A) Cells are labeled with Tub1-CFP and Myo1-mCherry morphology, marking the spindle and bud ring, respectively. Spindles are distinguished as bar-shaped ('meta'), elongated ('long'), or dot-shaped ('brkdwn' or 'unipol' [unipolar], depending on old Myo1 ring disappearance). Old and new Myo1 rings are scored separately. Loss or contraction of old Myo1 rings reveal cytokinesis ('cytok') and are scored as fully intact (-), contracted (partial), or absent (complete). New Myo1 rings reveal new bud formation, and can be either absent (-) or present (rebud). **(B)** Percentages of cells with phenotype (left) and histograms of DNA content (right) versus time post-release are plotted.

A

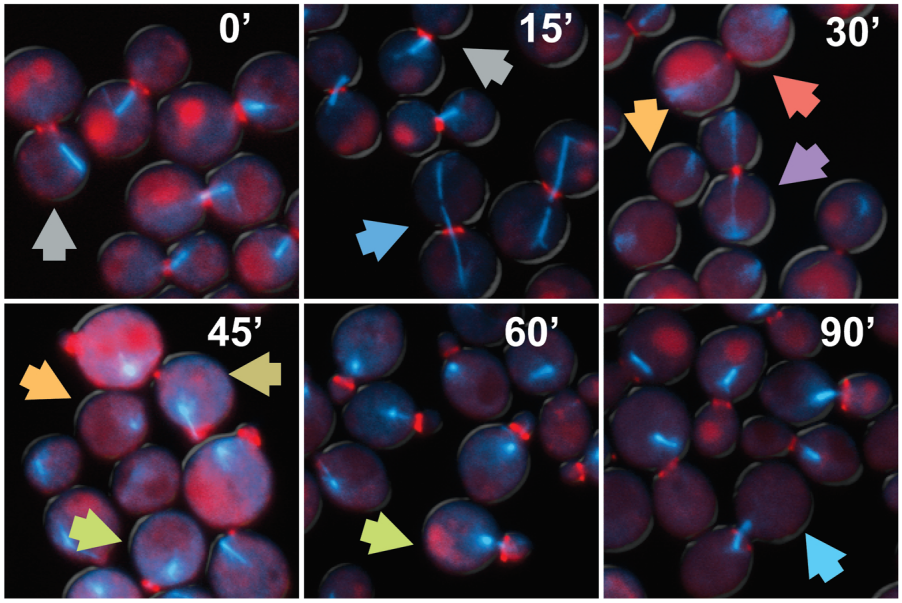

Spn	Cytok	Bud	Spn	Cytok	Bud
meta	-	-	brkdwn	partial	rebud
long	-	-	unipol	complete	-
long	partial	-	unipol	complete	rebud
brkdwn	partial	-	meta	complete	rebud

B

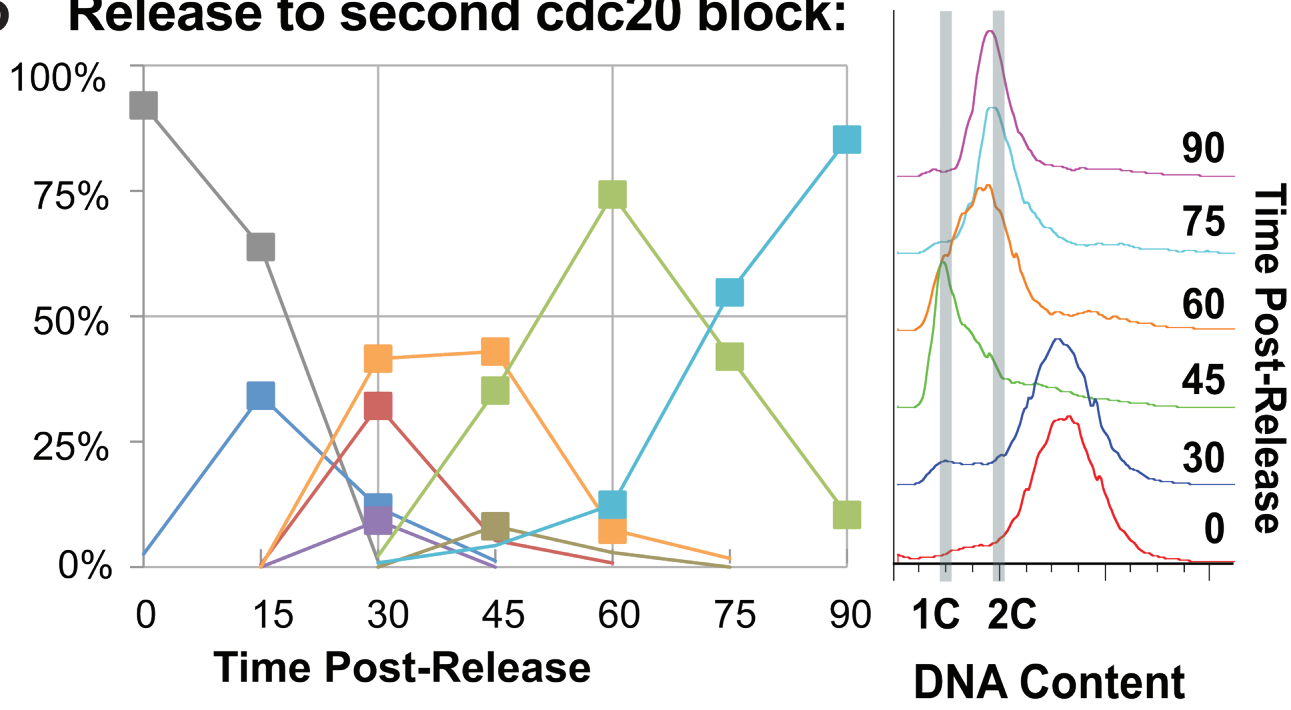

for 90 minutes is a sufficient period, with sufficient time resolution, to stage spindle elongation and disassembly, cytokinesis initiation and completion, budding, and in the succeeding cell cycle, DNA replication, and metaphase spindle formation. Methionine was re-added 45 min post release to catch cells that completed one round of mitotic exit at a second metaphase arrest. If Clb2kd is not expressed (i.e., in control unpulsed cells), the phenotypes progress as follows:

Anaphase spindles are observed 15 minutes after removal of methionine (release). At this time, the culture contains a mixture of large budded cells with metaphase and anaphase spindles that have not initiated actomyosin ring contraction. Cytokinesis can be observed beginning 30 minutes after release. At this time almost 90% of the original cells have initiated actomyosin ring contraction and 40% cells have no detectible Myo1 ring and are unbudded cells with unipolar spindles. Of the remaining 10% cells that have not visibly contracted Myo1 rings, all have anaphase spindles. Anaphase spindles persist in a quarter of the population.

At 45 minutes post-release, cytokinesis is complete in almost 90% of the population, and all cells have completed spindle disassembly. Rebudding is observed at 45 minutes in nearly 40% cells. Since most cells have completed cytokinesis, but few have initiated DNA replication (**figure 11B)**, a 1C DNA peak is observed by FACS.

A second round of budding has occurred in nearly 90% cells at 60 min post release. DNA replication is nearly complete, and the distribution of DNA content is unimodal, indicating a synchronous S-Phase in the culture **(figure 11B)**. Few cells (10%) have formed visible bar-shaped metaphase spindles. Metaphase spindles are observed in over half the population 75 min post-release. At this time all cells have 2C DNA content. Finally, at 90 minutes post release, the culture has reached a second cdc20 block, with 2C DNA content, large buds, and a metaphase ('bar') spindle.

The 15-min resolution of this time-course should allow detection of the persistence of a cell cycle phenotype 15 minutes after it should have progressed to a detectably different one (e.g., long anaphase spindle to disassembled late telophase spindle). Therefore, delays in execution of a given process induced by persistent B-cyclin can be measured if the induced delay is on the order of 15 min or longer. This amount of time is short enough (~1/6 of a cell cycle) that shorter delays, even if detected, might not be considered biologically significant. In addition, higher time resolution would yield diminishing returns due to asynchrony already detectable, for example, in timing of second spindle accumulation.

The preceding lengthy but necessary technical preamble sets the stage for the determination of the effects of varying levels of Clb2kd-YFP, in single cells, calibrated to normal peak levels of Clb2 attained in a normal cell cycle, on delay

or block of various events of mitotic exit. The results of this analysis form the subject of the next chapters.

Caveats for this method

The method described above allows accurate measurement of Clb2kd-YFP concentration thresholds for post-anaphase events in cells released from *MET-CDC20* arrest. However, we interpret the results of this method as the consequences of persistent Clb2 in cells exiting mitosis. Three obvious caveats to this interpretation must be discussed: the YFP tag, the deletion of *KEN* and destruction boxes, and the reversible cdc20-depletion arrest. All three are technically necessary but represent significant deviations from wild-type *CLB2* and *CDC20*. The YFP tag and the arrest are discussed below; potential biochemical and biological problems with Clb2kd will be discussed in chapter 3.

Our method depends strongly on the use of YFP-tagged Clb2, both wild-type and Clb2kd. The Clb2-YFP western signal per unit Pgk1 is about 2-fold higher than that of $Clb2^{WT}$, when measured with the anti-Clb2 antibody, and untagged Clb2kd requires about a 2-fold longer induction time than Clb2kd-YFP to cause a telophase arrest (data not shown). This suggests that by some means, the YFP tag may increase abundance or potentiate inhibitory activity. However, all threshold measurements were made comparing Clb2kd-YFP to $Clb2^{WT}$-YFP. Therefore the tag did not affect the pulse-to-peak ratios.

Furthermore, we compared asynchronous cultures of two *clb1,3,4Δ* strains, one containing *CLB2*^{WT} and one *CLB2-YFP*. Both grew exponentially at normal rates. Deletion of *CLB1,3,4* mildly decreased the 1C peak relative to the 2C peak in asynchronous DNA flow cytometry profiles for the *clb1,3,4Δ* strain, as previously reported (Epstein and Cross, 1992); this effect was identical with *CLB2* or *CLB2-YFP* (data not shown). Therefore *CLB2-YFP* does not grossly affect the duration of any cell cycle stage even when it is the sole source of mitotic cyclin. If Clb2kd-YFP is moderately potentiated relative to Clb2kd for inhibitory activity, this only strengthens one of our main conclusions, that it takes surprisingly high Clb2 levels to significantly inhibit many events of mitotic exit.

Our thresholds are measured after release from arrest by Cdc20 depletion. The extended cell cycle block results in an approximate doubling of cell size, although the protocol has been streamlined to arrest cells for as brief a time as possible. This increase is reflected in the shortened interval between cytokinesis and budding and a decrease in mother/daughter asymmetry compared to unperturbed cycling wild-type cells. We are measuring Clb2kd concentration rather than number of molecules per cell in all cases, making it more likely that cell size effects are neutralized (since the concentration of most other cell components are unlikely to change as cell size increases). However, ratios of number of Clb2 protein molecules to fixed-copy-number components such as spindle pole bodies or chromosomes will inevitably be increased in larger cells, at a constant Clb2 concentration. This could lead to an underestimate of the

inhibitory Clb2 threshold in smaller cells; once again, if this is so, it would only reinforce our conclusion that these thresholds are already surprisingly high.

In order to release cells from arrest, an HA-tagged version of Cdc20 is expressed from a reversible promoter; thus these cells are quite probably expressing unphysiological levels of Cdc20, a key mitotic regulator. However, we inactivate *MET-CDC20* as soon as possible after cells have undergone anaphase. Even without inactivation, HA_3-Cdc20 protein levels decrease after a brief spike during induction, likely due to Cdh1-dependent degradation of Cdc20 in G1 (Huang et al., 2001; Prinz et al., 1998). Therefore, we do not consider the brief induction of Cdc20 to be likely to perturb our results. In addition, the cell cycle kinetics and, critically, the timing of Clb2 degradation, in an α-factor to α-factor time course are not affected by replacement of $CDC20^{WT}$ with *MET-CDC20* (data not shown). Finally, it has been reported that in *S. cerevisiae* the only essential function of Cdc20 for progression from anaphase to the subsequent cell cycle and for Pre-RC formation is degradation of mitotic cyclin (Noton and Diffley, 2000; Thornton and Toczyski, 2003); since this has been ablated already in the case of Clb2kd, Cdc20 levels are likely to be irrelevant to the outcome of our experiments after its activation has led to cohesin cleavage and anaphase.

Chapter 2: Measurement of Clb2p Inhibitory Thresholds

In this chapter we measure inhibitory thresholds of persistent Clb2 for inhibition of post-anaphase processes.

Some comments on terminology: by our definition 'persistent Clb2' refers to Clb2 undegradable by removal of its destruction and KEN boxes, that is present from metaphase through anaphase and into the next cell cycle (if mitosis occurs). It is striking that the normal biology of the system is such that 'persistent Clb2' is effectively at a level of zero; these experiments take place against a very low background).

We refer to 'inhibitory thresholds', which raises several questions. First, are there true thresholds (i.e., levels below which nothing at all happens) or is the response graded all the way down? This issue can be addressed empirically in the course of these experiments. A related question is whether the response is best considered a block or a delay; in cases where multiple timepoints can be assessed, this also can be examined in these experiments. Second, is the correct measurement the concentration of persistent Clb2, or the total amount per cell? Practically, we measure the concentration, since all measurements are grounded on Western blotting of Clb2 standardized to total cell protein, and on average pixel intensity of Clb2kd-YFP across the cell area. However, because the cells increase in mass by considerably less than two-fold during the critical periods in these experiments, this distinction is not a critical one. Where

appropriate, we have tried to indicate concentration changes that might be significant.

We focus on post-anaphase processes that can be monitored with CFP-Tub1 and Myo1-mCherry: spindle disassembly and cytokinesis. Additionally, Myo1-mCherry assists in monitoring bud formation, the earliest morphological indication of entry into the subsequent cell cycle, since the Myo1 ring appears at the neck of even very tiny buds (Bi et al., 1998) **(figure 12)**. We then address the events of the subsequent cell cycle: bud formation, DNA replication, and bipolar spindle formation. We conclude by analyzing the effect of persistent Clb2 on α-factor arrest.

Our analysis of Clb2kd-mediated inhibition of individual events is based on three measurements in single cells: time of process execution in unpulsed cells, concentration of stable Clb2kd-YFP in the pulsed cell at some time at or after process execution in unpulsed cells, and state of execution of the process in the pulsed cell (complete, partial, or not initiated). To obtain sufficient data for clear conclusions, we bin cells by Clb2kd-YFP concentration (in units of peak Clb2 attained in a normal cell cycle, or 'peak-equivalent' units; see Chapter 1), and score the fraction of cells within each bin that have a particular phenotype. This generates a plot of Clb2 concentration versus percent process execution (complete, partial or uninitiated). We generate these plots starting at the first time point after release from *MET-CDC20* arrest at which a process has been completed in the majority of unpulsed cells, since this is the earliest time at which

failure of a process can reliably be attributed specifically to the presence of pulsed Clb2kd-YFP.

Correlation of process execution and Clb2kd-YFP concentration allows the determination of whether Clb2-dependent inhibition of the process is marked by a sharp threshold. A single timepoint will not clearly reveal whether Clb2 is imposing an all-or-none block to a process, or instead imposing a dose-dependent delay. Therefore, where possible, measurement of inhibitory thresholds was made at successive time points. By expressing Clb2kd-YFP concentration in peak-equivalent units, we can evaluate whether or not Clb2kd ever exceeds an inhibitory threshold during an unperturbed cell cycle, and consequently whether B-cyclin must be destroyed for a process to occur. For example, if Clb2kd-YFP only inhibits a process at a level far above the level ever achieved in a normal cell cycle, then there is no reason to believe that Clb2 inhibition of this process can occur in a normal cell cycle. Conversely, if a process is inhibited by a level of Clb2 significantly below the peak level attained in a normal cell cycle, then Clb2 may indeed inhibit this process during the course of a normal cell cycle. This determination therefore provides a direct and unambiguous test of the simplest form of ratchet model, one governed solely by mitotic cyclin level (see Introduction).

Figure 12. Mitotic exit after a Clb2kd-YFP pulse.

Phenotypic progression after Clb2kd-YFP release of a cdc20 block in cells preloaded with a pulse of Clb2kd-YFP; cells were released to a second cdc20 block as in Fig. 11. Left panels depict merged Myo1-mCherry and CFP-Tub1 fluorescence. Right panels depict Clb2kd-YFP fluorescence. Cells are categorized by spindle and bud ring morphology as in **figure 11**. Only phenotypes relevant to spindle disassembly, cytokinesis and bud formation are scored. Of note, cells that have disassembled spindles but have not begun cytokinesis (light blue), absent from the un-pulsed time course, are observed in the pulsed culture. Furthermore, cells that have formed new buds without completing cytokinesis (brown) are significantly more prominent in the pulsed culture.

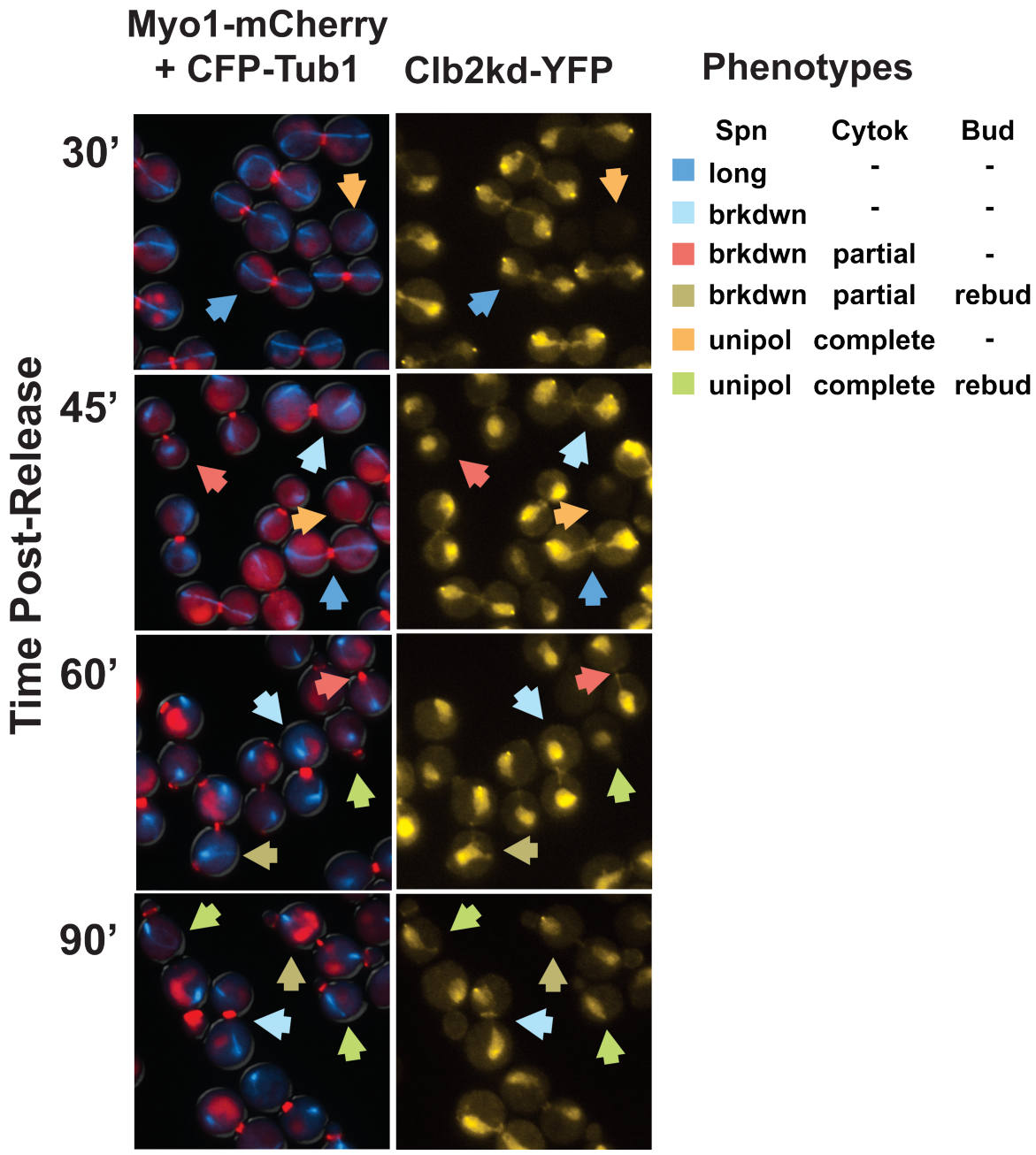
Myo1-mCherry
+ CFP-Tub1
Clb2kd-YFP
Phenotypes
Spn
Cytok
Bud
long
-
-
brkdwn
-
-
brkdwn
partial
-
brkdwn
partial
rebud
unipol
complete
-
unipol
complete
rebud
Time Post-Release
30’
45’
60’
90’

The Clb2 Inhibitory Threshold for Spindle Disassembly

We monitored the disappearance of long spindles and Myo1 rings at 15-minute intervals after release from cdc20 arrest with or without a pulse of Clb2kd-YFP. In unpulsed cultures, anaphase spindles were detected between 15 and 30 minutes after induction of Cdc20, and were not detected 45 min post-release **(figure 11, figure 13A)**. Therefore, any long spindles present at this time could be attributed to the effects of persistent Clb2 activity. To assess the dosage of Clb2kd necessary to prevent or delay spindle disassembly, we plotted the fraction of cell bodies with anaphase spindles versus Clb2kd-YFP concentration at 45 minutes post-release or later **(figure 13B)**.

In the population as a whole, spindle disassembly was delayed by approximately 15 min by the pulse of Clb2kd-YFP (figure 13A). At 45 min post-release, a cell-by-cell analysis revealed that peak-equivalent Clb2kd gave little or no detectable delay compared to unpulsed cells **(figure 13B)**. Only significant hyper-accumulation of Clb2 resulted in a detectable delay of spindle disassembly; for example, 2-fold peak-equivalent Clb2kd caused about a 15 min delay in spindle disassembly. There were almost no long spindles present 60 min post-release in response to any tested Clb2 concentration. Therefore, within the concentration range of our experiment, Clb2 did not delay spindle disassembly longer than 30 minutes. This concentration range appears to cover the physiological range of endogenous Clb2 accumulation even in cells without APC-mediated degradation (Chapter 1); assessment of the effects of much

higher levels is only examining pathological overexpression, and we have avoided this in most experiments.

The fact that the population level of long spindles was much higher at 30 min post release than the unpulsed control (~95% vs. ~25%), with a mean pulse level of Clb2kd that was 1.2 peak-equivalent, suggests that peak-equivalent Clb2kd does likely delay spindle disassembly, but by less than 15 min.

The Clb2 Inhibitory threshold for Cytokinesis

In unpulsed cultures, cytokinesis occurs 30 to 45 minutes after induction of Cdc20. The use of the Myo1-mCherry ring to assess cytokinesis is particularly helpful since the ring contracts over ~5 min (S. DiTalia, pers. comm.), so that intermediate states of partial contraction without complete disappearance can be monitored. As noted above, we assume that Myo1 ring disappearance corresponds to complete cytokinesis, although we lack direct evidence that this is the case.

Approximately 90% of unpulsed cells have initiated cytokinesis (i.e., begun Myo1 ring contraction) at 30 minutes post-release, and completed cytokinesis (i.e., lost any detectable focus of Myo1 signal at the former bud neck) after 45 minutes **(figure 11, figure 14B)**. Following the same logic as for spindles, any significant number of full-sized Myo1 rings present after 45 minutes, and Myo1 rings (or spots in the case of rings that have essentially fully contracted but not disassembled) of any size present after 60 minutes, can be specifically attributed

Figure 13. Peak Clb2p delays but does not block spindle disassembly.
(A) Spindle disassembly versus time is plotted for the unpulsed control (gray) and the pulsed culture (red). Average Clb2kd-YFP pulse, as measured by quantitative western, is plotted for the pulsed culture (blue). **(B)** Spindle disassembly versus Clb2kd-YFP concentration is plotted at 45 min post-release.

A

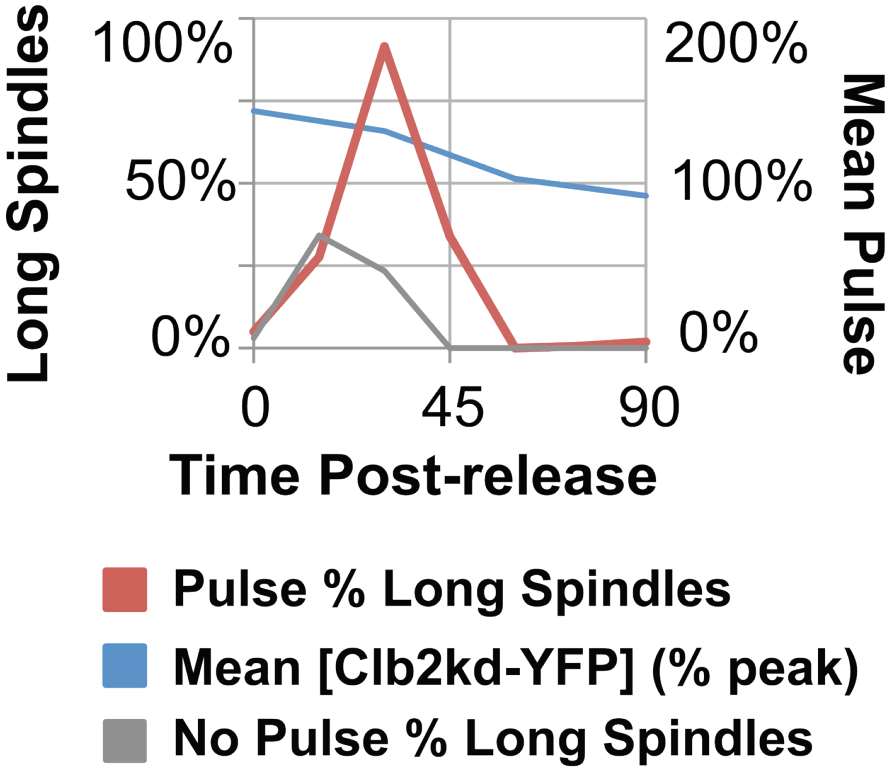
Long Spindles
100%
50%
0%
200%
100%
0%
Mean Pulse
0
45
90
Time Post-release
Pulse % Long Spindles
Mean [Clb2kd-YFP] (% peak)
No Pulse % Long Spindles

B

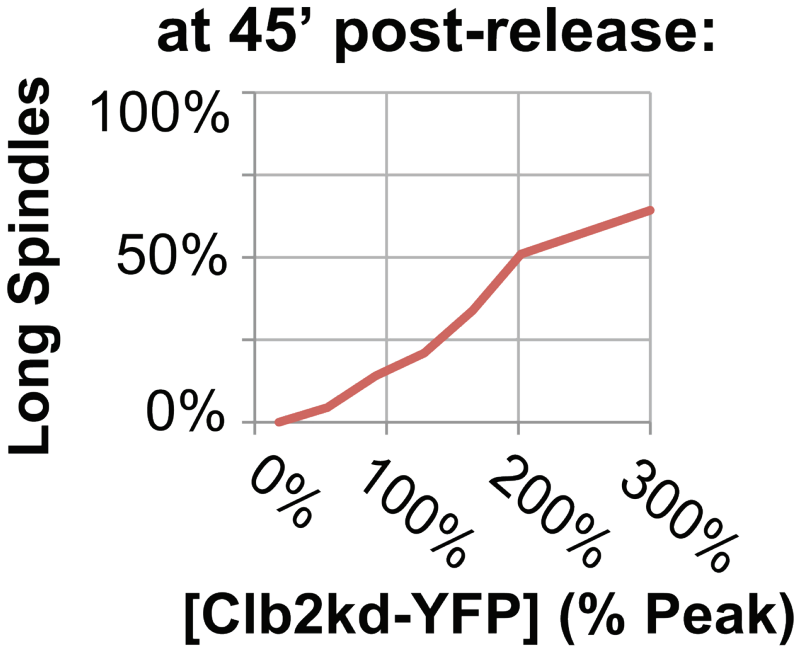
at 45’ post-release:
Long Spindles
100%
50%
0%
0%
100%
200%
300%
[Clb2kd-YFP] (% Peak)

Figure 14. Peak Clb2p delays but does not block cytokinesis and rebudding. **(A)** Cytokinesis and rebudding versus Clb2kd-YFP concentration are plotted at 45, 60, and 90 minutes post-release. Cytokinesis is subdivided into partial or complete phenotypic categories, as described in **figure 11**. % Initiated ring contraction is the sum of % partial and % complete cytokinesis. **(B)** Cytokinesis and rebudding versus time post-release are plotted for four intervals of Clb2kd-YFP concentration as well as the unpulsed control.

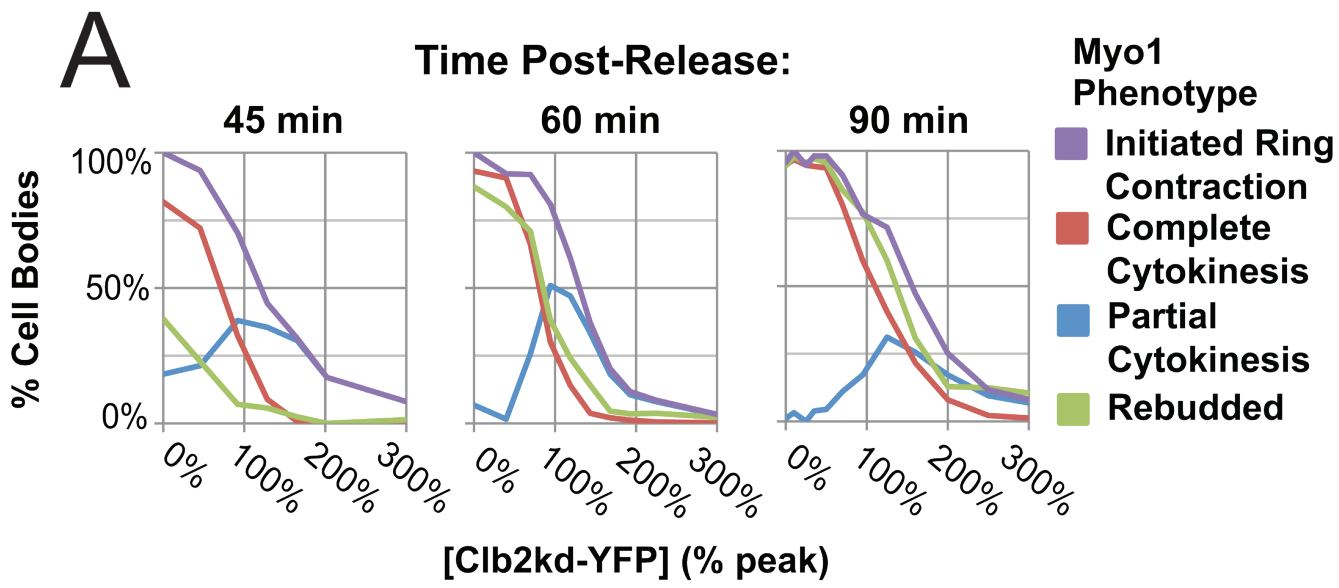
A
Time Post-Release:
45 min
60 min
90 min
Myo1 Phenotype
Initiated Ring Contraction
Complete Cytokinesis
Partial Cytokinesis
Rebudded
% Cell Bodies
100%
50%
0%
0%
100%
200%
300%
[Clb2kd-YFP] (% peak)

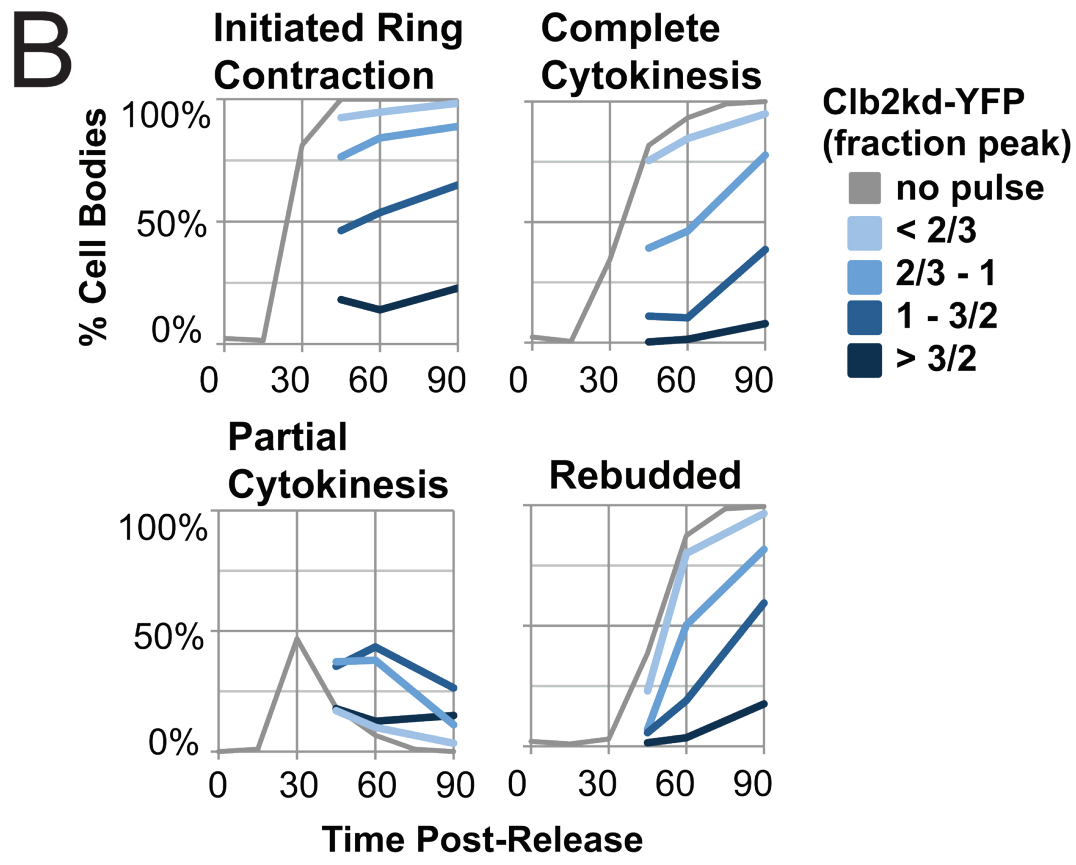
B
Initiated Ring Contraction
Complete Cytokinesis
Partial Cytokinesis
Rebudded
Clb2kd-YFP (fraction peak)
no pulse
< 2/3
2/3 - 1
1 - 3/2
> 3/2
% Cell Bodies
100%
50%
0%
0
30
60
90
Time Post-Release

to the Clb2kd-YFP pulse. To assess the dosage of Clb2 necessary to prevent cytokinesis, we plotted the percentage of cells that underwent partial or complete Myo1 ring breakdown versus Clb2kd-YFP concentration at 45, 60, and 90 minutes post-release **(Figure 14A)**.

Peak-equivalent Clb2kd prevents or delays onset of cytokinesis in at least some cells. At 45 min post-release, when all unpulsed cells have begun cytokinesis, only 65% of the pulsed cells with approximately a peak-equivalent of persistent Clb2kd have initiated ring contraction. This fraction increases to 75% at 60 minutes post-release and remains constant to 90 minutes post-release **(Figure 14A)**. These measurements imply a somewhat heterogeneous response of initiation of cytokinesis to peak levels of Clb2, from essentially no inhibition to a delay of at least 30 min.

While initiation of cytokinesis (Myo1-mCherry ring shrinkage) is inefficiently inhibited by peak Clb2 levels, peak Clb2 inhibits completion of cytokinesis much more efficiently. At 45 minutes post-release, 90% of unpulsed cells have completed cytokinesis; in contrast, only 50% of cells containing peak-equivalent Clb2kd have completed cytokinesis by 90 min post-release **(Figure 14A)**. The dose-response relationship between Clb2kd and events of cytokinesis suggests a dose-dependent delay rather than a stable blockade. (This analysis is obviously complicated to some extent by the fact that initiation of cytokinesis is a prerequisite for its completion; nevertheless, the two phenotypes can be

analyzed separately, and appear to have different responses to peak-equivalent Clb2kd levels).

Overall, peak-equivalent Clb2kd lies at the low end of the inhibitory threshold for cytokinesis onset and at the high end of the inhibitory threshold for cytokinesis completion. As a consequence, a high proportion of cells loaded with peak-equivalent Clb2kd-YFP have partially contracted Myo1 rings well after 30 minutes post-release. In unpulsed cultures, intermediates between full Myo1 rings and complete disassembly occur only transiently, and such cells are only observed in a significant fraction of cells 30 min post-release, just after spindle disassembly **(Figure 14A)**. This agrees with time-lapse microscopy studies that have shown that actomyosin ring contraction takes 3 – 6 minutes (S. DiTalia, pers. comm.). In contrast, 40-50% of cells containing peak-equivalent Clb2kd have partially contracted Myo1 rings for longer than 15 min **(Figure 14A)**. Since to our knowledge Myo1 ring contraction is not reversible, it is unlikely that the persistence of partially contracted rings is due to continuous flux through a transient phenotype. Instead we propose that peak Clb2 delays complete actomyosin ring contraction**.** Partial ring contraction is significant as it does not preclude the presence of a log spindle, as can be seen in the unpulsed control at 30 minutes post-release **(figure 11B)**. A plot of kinetics of partial and complete Myo1 ring breakdown vs. time, for four binned levels of Clb2kd, suggests that persistent Clb2kd generally delays but does not block actomyosin ring contraction **(figure 14B)**.

Overall, these results suggest that peak Clb2 levels attained in a normal cell cycle may not account for delay of initiation of cytokinesis (initial Myo1 ring shrinkage), although if Myo1 ring shrinkage did initiate, peak Clb2 levels would clearly be enough to prevent completion of ring shrinkage, presumably blocking cytokinesis.

The Clb2 Inhibitory Threshold for Bud Formation

Although our primary focus in these experiments was on the amount of Clb2 required to inhibit events of mitotic exit, since this measurement is most directly relevant to the ratchet models, the experimental design also allowed us to measure the effects of persistent Clb2 on events normally occurring in the next cell cycle after mitotic exit. Soon after cytokinesis, unpulsed cells will bud with formation of new Myo1 rings. (These cells are readily distinguishable from the initial blocked cells, even though both have Myo1 rings, due to the very large bud size in the latter). To assess the effects of persistent Clb2kd on budding, we monitored the formation of new Myo1 rings in the same cells examined for spindle disassembly and cytokinesis.

Since over 90% unpulsed cells have formed a new bud and Myo1 ring by 60 min post-release, the Clb2kd inhibitory threshold for bud emergence can be unambiguously scored beginning at this time **(figure 11, figure 14B)**. As with cytokinesis, we plotted the percentage of cells that rebudded versus Clb2kd-YFP concentration at 45, 60, and 90 minutes post-release **(Figure 14A)**. We also

plotted rebudding versus time for four bins of Clb2 concentration and the unpulsed control **(figure 14B)**.

Peak-equivalent Clb2kd did not stably block bud emergence in the next cell cycle, but instead induced a moderate, dose-dependent delay. For example, at 60 minutes post-release, rebudding is complete in 90% unpulsed cells, but in only 40% cells with peak-equivalent Clb2kd; but 15 min later, 75% of cells with peak-equivalent Clb2kd have rebudded **(Figure 14A,B)**. As with completion of cytokinesis, the kinetics of the response of rebudding to Clb2kd implies a dose-dependent delay rather than a stable blockade. At the extremes, Clb2kd concentrations below 2/3 peak have little to no effect on bud formation at any time, and hyper-accumulated Clb2 (2x peak) stably blocks rebudding for at lease 45 min in >80% cells **(figure 14B)**.

Persistent Clb2kd uncouples events of mitotic exit

The relative rate effects of persistent Clb2kd on spindle disassembly, cytokinesis, and bud formation manifest in the emergence of unusual phenotypes in cells with peak-equivalent Clb2kd. These phenotypes are not observed in cells with normal Clb2 degradation and entry into the subsequent cell cycle, (nor, of course, in cells with grossly overexpressed undegradable Clb2 where the events do not occur at all.)

In unpulsed cultures at 30 minutes post-release, cells with long spindles had either partially contracted and uncontracted Myo1 rings, and all cells that had

disassembled spindles at this time had at least begun cytokinesis as indicated by some Myo1 ring contraction **(figure 11)**. In contrast, in pulsed cultures at 45 minutes post-release a large fraction of cells lacked long spindles but possessed uncontracted Myo1 rings **(Figure 12)**. The presence of this aberrant phenotype demonstrates the differential sensitivity of spindle disassembly and cytokinesis to Clb2 concentration. A similar uncoupling of spindle breakdown and cytokinesis was noted previously in cells strongly overexpressing wild-type Clb2, using septin rings instead of Myo1 rings to assess cytokinesis (Cross et al., 2002).

The Clb2 inhibitory threshold for rebudding at 45 minutes post-release is significantly less than that for completion of cytokinesis. In contrast, at 60 and 90 minutes post-release, Clb2 blocks completion of cytokinesis at a lower concentration than it blocks budding **(Figure 14A)**, meaning that cells with lower amounts of Clb2kd can bud without completing cytokinesis. This is an aberrant phenotype essentially never observed in wild-type cells. A significant proportion (~15%) of cells with peak-equivalent Clb2kd form a new bud without completing cytokinesis at 60 min post-release **(Figure 12)**. Since Clb2kd does not prevent rebudding to the same degree that it inhibits cytokinesis, it is unlikely that the relative order of cytokinesis and bud formation is determined by B-cyclin concentration, as could be required by the simplest version of ratchet models (see Introduction).

Super-peak-equivalent but not peak-equivalent Clb2kd stably inhibits mitotic exit and rebudding

Peak-equivalent Clb2kd present from anaphase through mitosis delays, but does not stably inhibit, spindle disassembly, cytokinesis and rebudding, and the durations of these delays are different for each process. The delay in rebudding at a given Clb2 concentration is less than that for cytokinesis, but greater than that for spindle disassembly. Thus the ranking of sensitivities of processes to Clb2 inhibition is: cytokinesis > rebudding > spindle disassembly. Cytokinesis can be subdivided into onset of ring breakdown and rate of ring breakdown, with Clb2 slowing rate more than onset. These differential effects are not obviously reconcilable with a biological advantage, and may simply reflect the underlying biochemistry of inhibition, which is unknown at present for these processes.

Levels of Clb2kd substantially (2-3-fold) higher than peak-equivalent still only delay spindle disassembly, but can block cytokinesis and rebudding almost indefinitely. It is interesting that similar levels to these can likely be attained physiologically, upon activation of the spindle integrity checkpoint, which inhibits Cdc20 activity (see Introduction), a situation we mimic with Cdc20 depletion. Thus, in cells blocked by the spindle integrity checkpoint, B-type cyclin accumulation might indeed be responsible for the prolonged block to mitotic exit that these cells exhibit.

Control of DNA replication: the Clb2kd inhibitory threshold for DNA replication is at least the level that blocks completion of cytokinesis.

To prevent aneuploidy, replication of every segment of DNA must occur once and only once per cell division, and replication must alternate with mitosis and cytokinesis. In eukaryotes, the origin-licensing requirement separates DNA replication into two mechanically coupled steps, licensing and initiation. Pre-RC formation and origin firing are differentially regulated. Specifically, B-Cyclin/CDK activity inhibits Pre-RC formation but promotes origin firing through separate sets of phosphorylations (see Introduction).

Both Clb2- and Clb5-CDK activity can promote origin firing. However, Clb5 is expressed well before Clb2, and DNA replication has already begun by the time Clb2 is normally expressed (Epstein and Cross, 1992). Furthermore, Clb5 activates both early and late-firing origins, whereas Clb2 can only activate early origins (Donaldson et al., 1998). For these reasons, Clb5 is considered the principal cyclin responsible for promoting DNA replication. The ability of Clb5 to bind directly to fired origins and inhibit reinitiation from these origins (Wilmes et al., 2004) suggests that Clb5 may also be the primary physiological mediator of inhibition of re-replication.

Nevertheless, it is reasonable to assess the capacity of persistent Clb2 to prevent initiation after mitotic exit, since it has been shown that sufficient Clb2 expressed in G1 cells will block origin loading (Detweiler and Li, 1998). In wild-type cells, Cdc20 degrades Clb5 before mitotic exit (Wäsch and Cross, 2002),

while Clb2 persists at a reasonably high level for a longer time. Since Clb2 can promote DNA replication in the absence of other B-type cyclins (Hu and Aparicio, 2005), there is a window in wild-type cells between Clb5 degradation and Clb2 degradation during which re-replication might need to be prevented, and it is of interest to know how much Clb2 is required for this inhibitory activity.

Unpulsed cells underwent cytokinesis between 30 and 45 minutes post-release from metaphase arrest, resulting in near-quantitative accumulation of cells with 1C DNA content in this 15 min interval (Fig. 15A). Replication in these cells then proceeded nearly synchronously, being essentially complete 30 min later at 75 min. (A second mitosis in these cells was prevented by depletion of Cdc20).

It is notable that the propidium iodide (PI) signal staining DNA in the unpulsed cells that had newly replicated after division (at 75 min post-release) was significantly lower than that observed initially in metaphase-arrested cells (time 0). This is due to the long 2C arrest that precedes the time course, and probably represents background PI staining of these very large cells. This is a well-known and generally irritating artifact, but useful in this case, as cells that divide and replicate DNA can be distinguished from those that have not yet divided.

We then wanted to assess the effects of persistent Clb2kd on the ability of cells to replicate DNA after release of a *cdc20* block. Single-cell correlation of Clb2 concentration and DNA replication was not possible because we did not have a single-cell reporter for DNA content that was compatible with YFP

fluorescence measurement. However, DNA flow cytometry of cells released from metaphase arrest can to some extent independently score cytokinesis and DNA replication: 1C cells result from cytokinesis without replication, and 4C cells result from DNA replication without cytokinesis. 2C cells appear to be ambiguous (arising from failure of both DNA replication and cytokinesis, or from occurrence of both); fortunately, a well-known DNA flow cytometry artifact allows us to make this distinction as well (see below).

Two cultures were pulsed with Clb2kd-YFP and released as in **(figure 2)**. One culture was pulsed with dCort for 30 minutes, resulting in a mean concentration that dropped from 5/2 to 3/2 peak concentration during the 90 minute time course, and the other was pulsed for 15 minutes, resulting in a pulse that dropped from 2/3 to 1/3 peak during the time course. These cultures were sampled every 15 minutes post-release for DNA content by FACS analysis, and compared to an unpulsed control **(figure 15)**.

Surprisingly, we find that most cells that complete cytokinesis in the short-pulsed culture can also undergo DNA replication. The short pulse of undegradable Clb2 delays completion of cytokinesis by 15 to 30 minutes, as shown by a delay in accumulation of 1C cells. These 1C cells, once generated, then shift from 1C to 2C with kinetics close to the un-pulsed control **(Figure 15B)**. Comparison with previous results (Figure 14) suggests that these cells include cells with near-peak-equivalent Clb2kd, accounting for the cytokinesis delay. This implies that this level of Clb2kd is unlikely to inhibit DNA replication in

the succeeding cell cycle; by implication, then, peak-equivalent Clb2kd is unlikely to be efficient at blocking pre-RC formation.

The longer pulse time generates enough Clb2kd to permit few cells to complete cytokinesis by the conclusion of the time course by the Myo1 ring assay, and essentially no 1C cells, nor newly generated 2C cells, are observed in the timecourse. In addition, there was no evidence that the cells that failed to divide were able to execute DNA replication, since this should have yielded a PI-staining peak in flow cytometry even higher than the initial one. Thus, levels of Clb2kd greater than peak-equivalence bock both cytokinesis and DNA replication.

Overall, we conclude that Clb2 levels that permit cytokinesis (including both Myo1 ring breakdown and cell separation in the DNA flow cytometry assay) are also permissive for DNA replication. Since peak-equivalent Clb2kd levels are at least semi-permissive for cytokinesis, this suggests that peak-equivalent Clb2kd levels may not be enough to prevent DNA replication, and the lack of re-replication initiation between Clb5 and Clb2 breakdown may require another explanation than inhibition of re-replication by Clb2. This poses a difficulty for the ratchet model for control of DNA replication.

Figure 15. Peak Clb2p does not block DNA replication (with Andrea Geoghegan). DNA content histograms, as measured by FACS of PI stained cells, are plotted versus time post-release for three cdc20 block-release-block time courses: two Clb2kd-YFP pulses, one high (**C**, 5/2 → 3/2 peak) and the other low (**B**, 2/3 → 1/3 peak) and an unpulsed control (**A**). Samples were taken at 15-minute intervals for 90 minutes. To the right of each trace is the fraction of cells at that time point that have completed Myo1 ring breakdown. Of note, the initially blocked cells, all presumed to be 2C, have an apparently significantly higher DNA content based on PI staining and flow cytometry than the 'authentic' 2C cells produced in the control block-release (**A**, 90 min; 2nd metaphase arrest). This problem is presumably due to PI background staining of the initial cdc20-arrested cells. For unknown reasons, the first division reduces the PI signal by much more than 2-fold; in subsequent replication the PI signal doubles (see (**A)** control timecourse). This feature is useful in distinguishing cells that have progressed through cytokinesis and subsequent replication from those that have not completed cytokinesis.

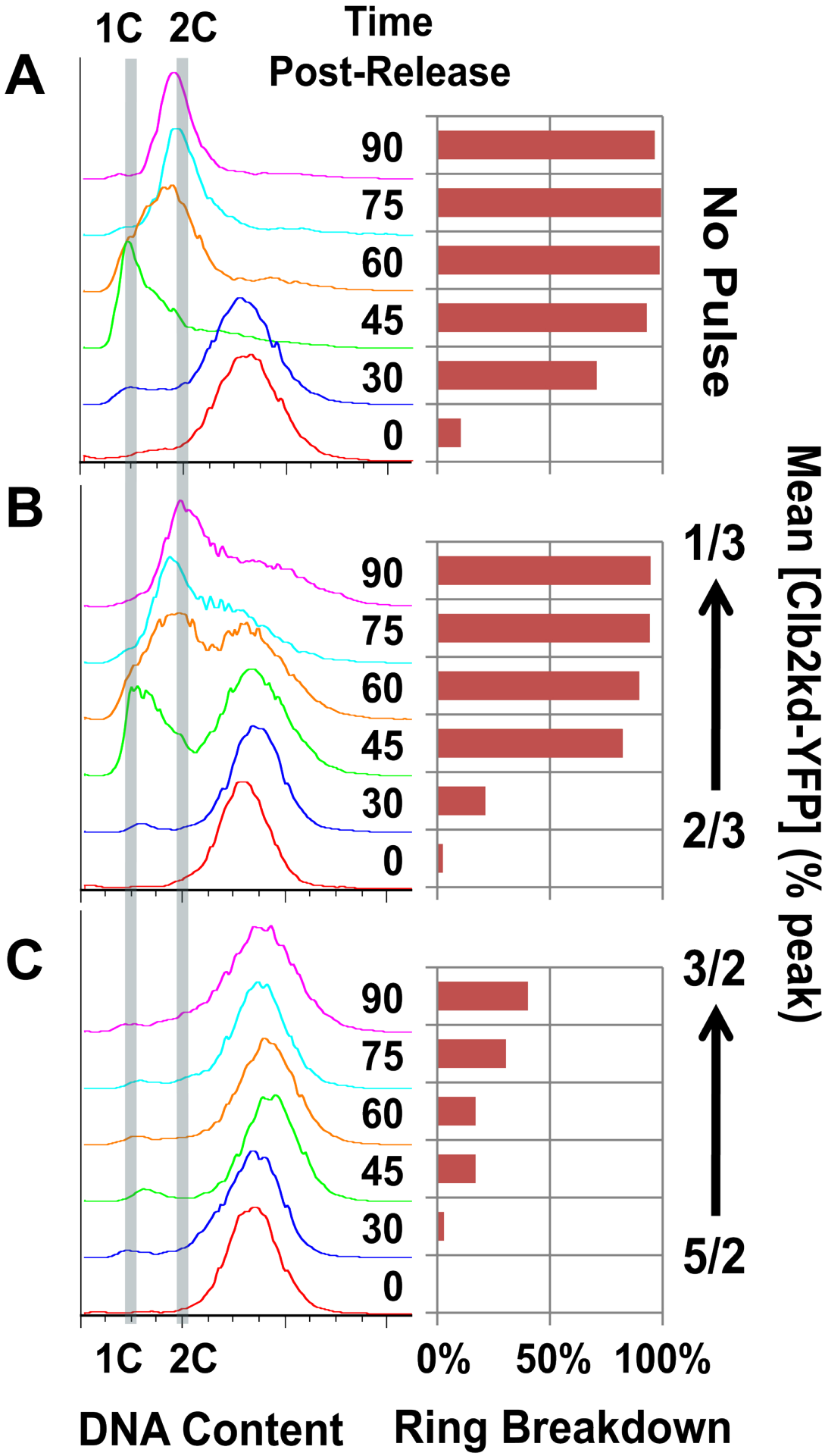
A
B
C
1C
2C
Time
Post-Release
90
75
60
45
30
0
No Pulse
1/3
2/3
3/2
5/2
Mean [Clb2kd-YFP] (% peak)
1C
2C
0%
50%
100%
DNA Content
Ring Breakdown

The Clb2 inhibitory threshold for SPB duplication and separation is at least the level that blocks cytokinesis

As with chromosomes, each cell inherits a single spindle pole body, which it must duplicate in order to form a bipolar spindle. Therefore, SPB duplication and segregation are tightly regulated. B-cyclin/CDK activity may inhibit the early stages of SPB duplication, but is required for separation and function. (This situation is analogous to the licensing/firing model for control of DNA replication, as noted in the Introduction). SPBs first duplicate, but remain very close (probably too close to resolve reliably by light microscopy). Subsequently, the two SPBs separate, forming a bipolar spindle between them that eventually spans the nucleus (the 'bar' or metaphase spindle (Figure 16). In these experiments using light microscopy, we can score only SPB separation. Presumably, separation implies previous duplication.

While strong overexpression of Clb2 inhibits generation of a new separated SPB, the level required for this inhibition has not been determined. We examined this question with cells containing both Myo1-mCherry and SPB29-CFP. Two Clb2kd-YFP inductions, one high (starting at 5/2 peak) and the other low (starting at 2/3 peak), were analyzed as in **Figure 15**. These cultures were sampled every 15 minutes post-release for SPB duplication and separation, and compared to an unpulsed control.

SPBs were counted using Spc29-CFP. SPB count was interpreted based on completion of cytokinesis. A count of two distinct Spc29-CFP dots in a cell that

had completed cytokinesis, or ≥3 dots with incomplete cytokinesis, was scored as SPB duplication and separation (**Figure 16)**.

In the unpulsed control, SPB separation follows cytokinesis, with SPB separation starting between 15 and 30 min after cytokinesis and completing by 45 min after cytokinesis (90 min post-release) (**Figure 16,** right**)**. The kinetics of SPB separation were very similar in the low-pulsed culture, despite the expected delay in cytokinesis (**Figure 16, middle**). In the high-pulsed culture, very few cells complete either cytokinesis or SPB separation (**Figure 16, left**).

The observation that SPB separation completes essentially on schedule even in cells with enough Clb2kd to significantly delay cytokinesis suggests that the inhibitory threshold for SPB separation is higher than that for cytokinesis. Thus, SPBs in cells that exit mitosis are capable of duplication and separation, even in the presence of near-peak-equivalent Clb2kd; this result suggests that peak Clb2 in a normal cell cycle might not be sufficient to restrain SPB duplication and separation.

Bipolar spindle formation is inhibited by sub-peak-equivalent Clb2kd

The finding that persistent peak-equivalent Clb2kd permits duplication and separation of SPBs does not establish functionality of the separated SPBs. Therefore, we examined the effects of persistent Clb2kd on bipolar spindle formation. In cells labeled with CFP-tubulin, we induced high and low Clb2kd-

Figure 16. Peak Clb2p does not block spindle pole body duplication and separation (with Andrea Geoghegan).

SPB duplication and separation (red) and completion of cytokinesis (gray) are plotted versus time post-release for three cdc20 block-release-block time courses: two Clb2kd-YFP pulses, one high (5/2 → 3/2 peak) and the other low (2/3 → 1/3 peak) and an unpulsed control. Below each graph are fluorescence microscopy images of cells 90 min post-release. Upper pictures depict merged Spc29-CFP and Myo1-mCherry fluorescence, and lower panels depict the Clb2kd-YFP pulse. Scoring criteria for SPB duplication and separation depend on completion of cytokinesis. Cells that have completed cytokinesis are scored as having duplicated and separated SPBs if at least 2 Spc29-CFP dots can be resolved (red), whereas cells that have not completed cytokinesis are scored as having at least one pair of duplicated and separated SPBs if at least 3 Spc29-CFP dots can be resolved (orange).

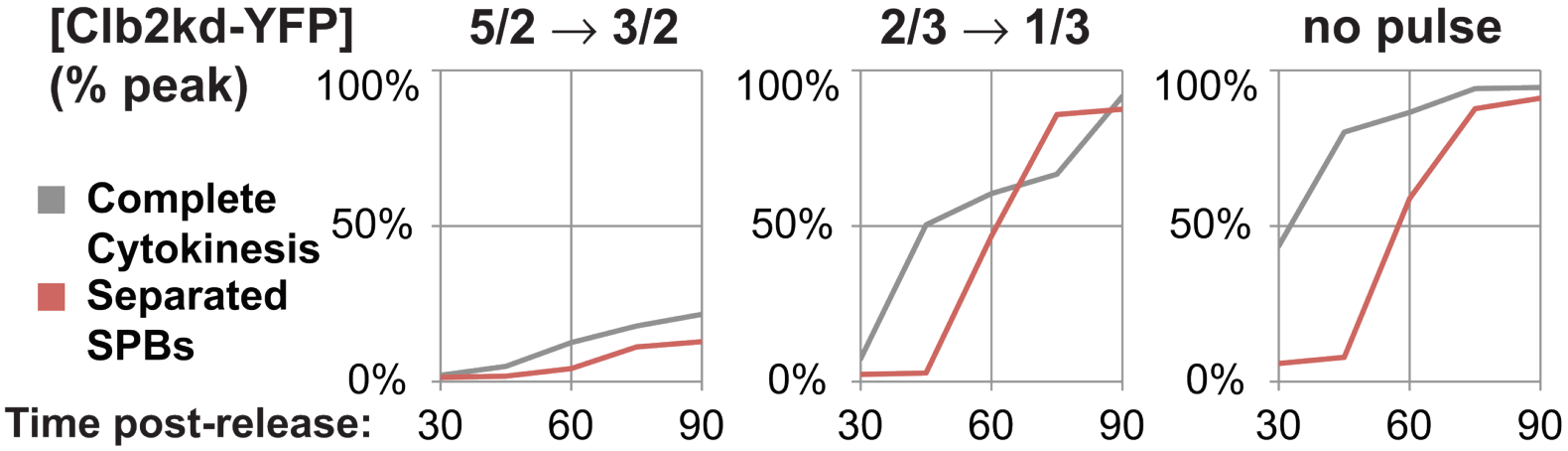
[Clb2kd-YFP]
(% peak)
5/2 → 3/2
2/3 → 1/3
no pulse
100%
50%
0%
Complete Cytokinesis
Separated SPBs
Time post-release:
30
60
90

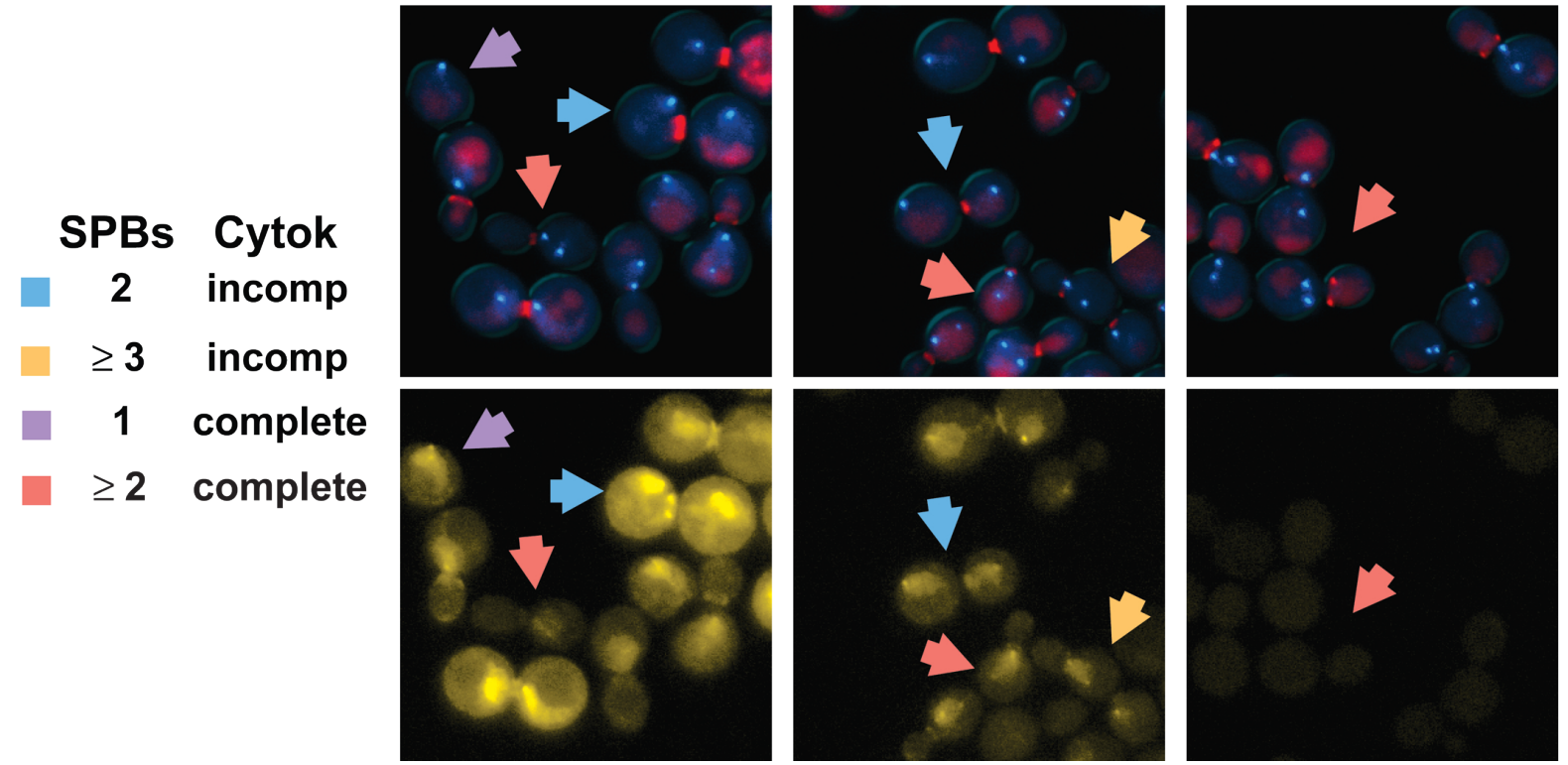
SPBs
Cytok
2
incomp
≥ 3
incomp
1
complete
≥ 2
complete

YFP pulses at a cdc20 block, released the block, reapplied the *cdc20* block in the succeeding cell cycle, and monitored bipolar spindle formation using CFP-tubulin.

In the unpulsed control, approximately 90% of cells have formed bipolar spindles at 90 minutes post-release, at which time they have reached the second cdc20 (metaphase) block (**Figure 17 A, right)**. (We define a bipolar spindle as a 'bar' of tubulin of uniform thickness and a length clearly between the tubulin 'spots' in G1 cells and long anaphase spindles). Surprisingly, in a culture exposed to an initial average of 2/3 peak-equivalent Clb2kd, only 40% of cells had formed a bipolar spindle at 90 min post-release, even though the previous experiment (Fig. 16) suggested that a large majority of such cells had two SPBs based on SPC29 staining.

We plotted the tubulin-CFP phenotypes versus Clb2kd-YFP concentration in individual cells, pooling the results from the low and high pulses, (**Figure 17B)**. Cells with bipolar spindles were almost completely restricted to those cells with significantly less than peak-equivalent Clb2kd; consistent with this level of Clb2kd, almost all of these cells had completed cytokinesis.

At the other extreme, cells with super-peak-equivalent Clb2kd-YFP concentration had almost all failed to complete or even initiate cytokinesis, and these cells almost all had one small tubulin focus in each cell body.

An interesting third category was observed in cells that had completed cytokinesis, with peak-equivalent or sub-peak-equivalent Clb2kd levels: cells that contained two discontinuous tubulin foci; one or both of these foci were clearly

shorter than the bipolar spindles in the control. We named this the '2-dot' phenotype (dark blue arrows in Figure 17A, dark blue lines in Figure 17B, right).

We determined that the two tubulin clusters in these 'two-dot' cells both colocalized with SPBs, by pulsing a strain with untagged Clb2kd, in order to use the YFP channel to localize the SPB component Spc42 relative to CFP-Tub1. We found that the two separated tubulin foci co-localize with the two separated SPBs **(Figure 18A)**.

We next investigated the reason for the discontinuous tubulin fluorescence between the two SPBs. Two explanations seemed plausible. The first was that although persistent Clb2 permits DNA replication, it could disrupt sister chromatid cohesion, resulting in premature chromosome separation; without tension from sister cohesion, a bipolar spindle cannot be maintained (see Introduction). The second possibility was that the duplicated and separated SPBs formed in the presence of persistent Clb2kd was defective for spindle formation. To test the first explanation, we induced a low pulse of untagged Clb2kd in cells that contained GFP-labeled chromosome dots (Michaelis et al., 1997) and Myo1-mCherry. Peak-equivalent levels or lower of Clb2kd are partially permissive for cytokinesis and DNA replication (see above); if such levels prevent sister chromatid cohesion, then we would expect a significant population of post-cytokinetic cells with two chromosome dots due to the Clb2kd pulse. Such cells were never observed (Fig. 18B). Therefore, it appears unlikely that persistent Clb2kd interferes with sister chromatid cohesion.

Figure 17. Peak Clb2p prevents metaphase spindle formation (with Andrea Geoghegan).

(A) Metaphase spindle formation (red) and completion of cytokinesis (gray) are plotted versus time post-release for three cdc20 block-release-block time courses: two Clb2kd-YFP pulses, one high (5/2 → 3/2 peak) and the other low (2/3 → 1/3 peak) and an unpulsed control. Below each graph are fluorescence microscopy images of cells 90 min post-release. Upper pictures depict merged CFP-Tub1 and Myo1-mCherry fluorescence, and lower panels depict the Clb2kd-YFP pulse. Spindle morphogenesis categories depend on completion of cytokinesis. Cells that have not completed cytokinesis may have long continuous anaphase spindles (purple), disassembled spindles consisting of two concentrations of CFP fluorescence on opposite sides of the Myo1 ring (light blue), or multipolar spindles with at least 3 concentrations of CFP fluorescence (orange). Cells that have completed cytokinesis may have bar-shaped metaphase spindles (red), unipolar spindles (green) or short discontinuous "2-dot" spindles (blue). Multipolar spindles and 2-dot short spindles are not observed during the unpulsed time course. Bar-shaped metaphase spindles are not observed in cells that have not completed cytokinesis. **(B)** Spindle morphology versus Clb2kd-YFP concentration among cells that have either completed (right) or not completed (left) cytokinesis at 90 min post-release. Phenotypes charted are described in **figure 17A** above. The percentage of cells with complete or incomplete cytokinesis versus Clb2kd-YFP concentration is plotted in gray.

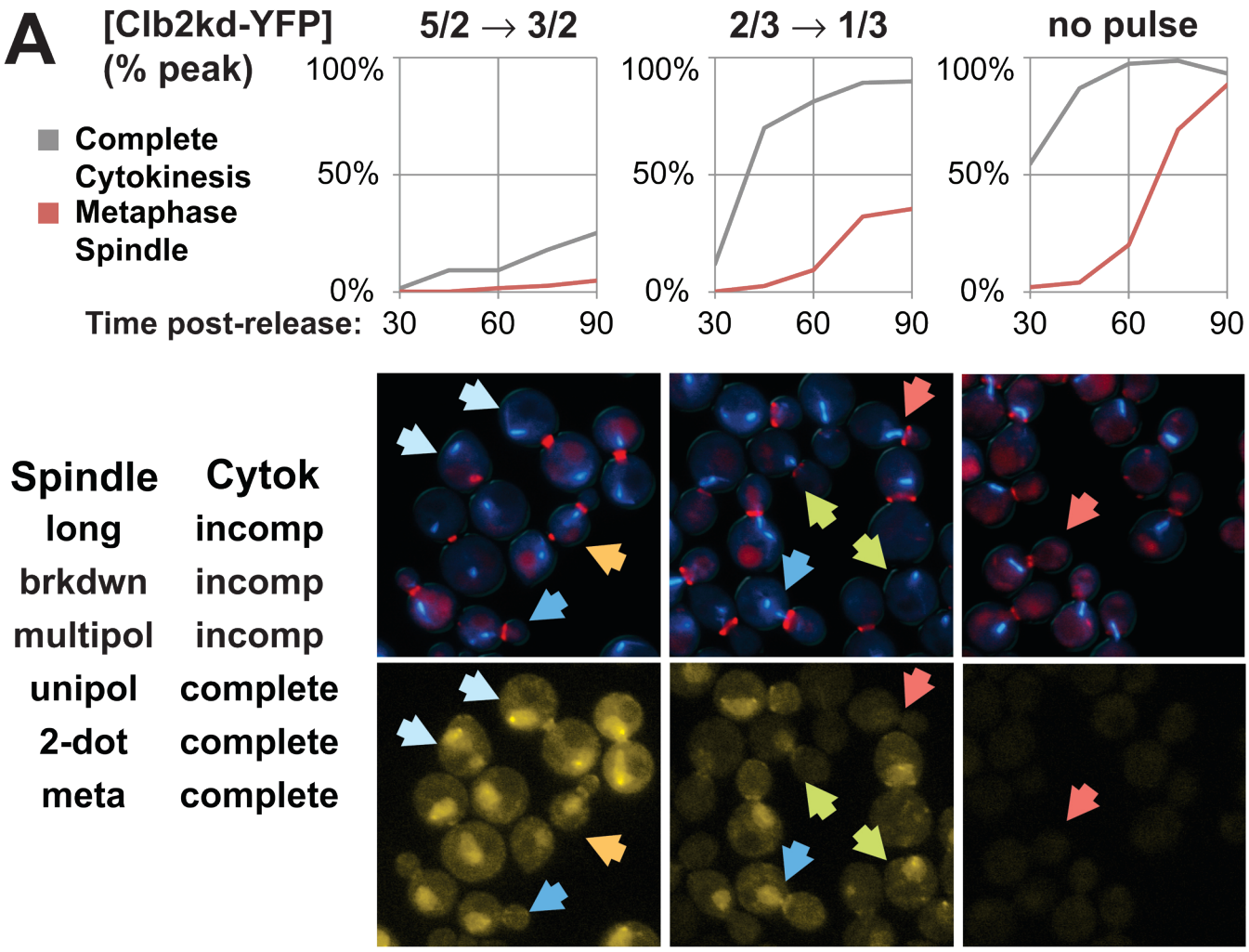
A
[Clb2kd-YFP]
(% peak)
5/2 → 3/2
2/3 → 1/3
no pulse
Complete Cytokinesis
Metaphase Spindle
100%
50%
0%
Time post-release: 30 60 90
Spindle Cytok
long incomp
brkdwn incomp
multipol incomp
unipol complete
2-dot complete
meta complete

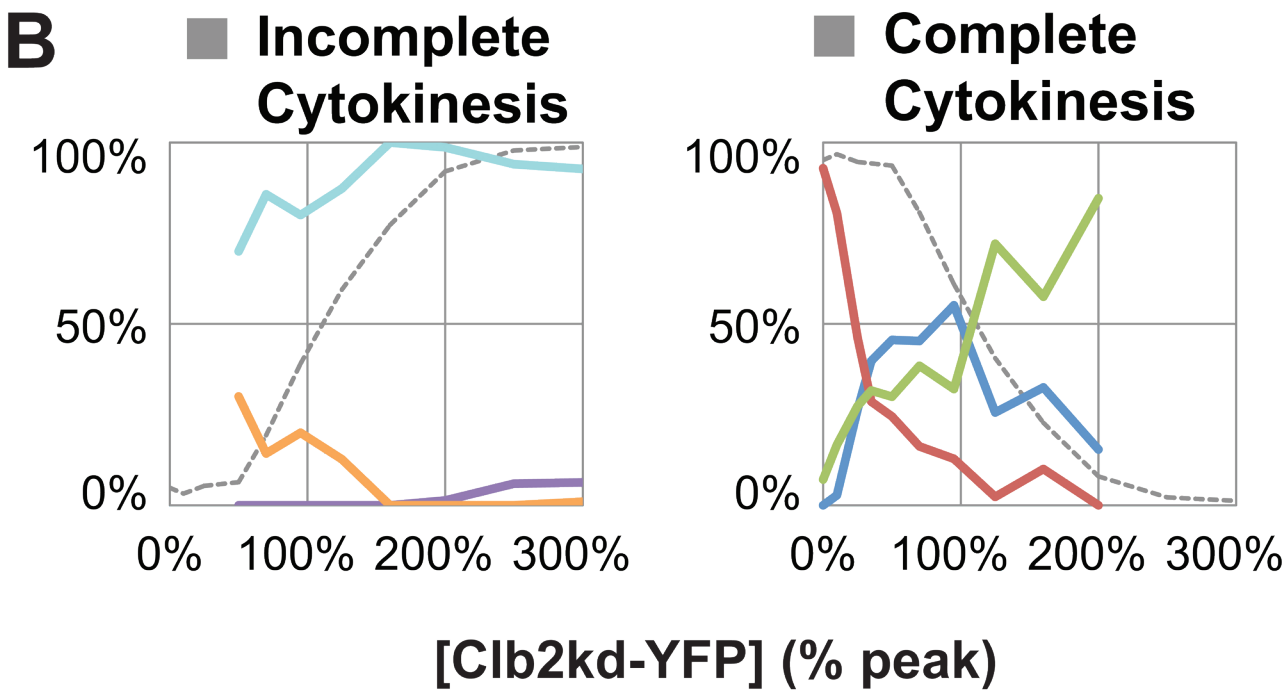
B
Incomplete Cytokinesis
Complete Cytokinesis
100%
50%
0%
0% 100% 200% 300%
[Clb2kd-YFP] (% peak)

Figure 18. Persistent Clb2kd causes accumulation of separated SPBs unattached to a bipolar spindle (Courtesy of Ying Lu).

(A,B) *MET-CDC20 GAL4-rMR* cells bearing an untagged Clb2kd allele under the *GAL1* promoter (P_{GAL}→*CLB2kd*) and the fluorescent marker alleles *SPC29-YFP*, *CFP-TUB1*, and *MYO1-mCherry* (**A**), or *MYO1-mCherry* and GFP-labeled chromosome V dots (**B**) were treated as described in **figure 2**, and examined at 0 and 90 minutes post-release for Clb2kd-pulsed and unpulsed control cells.

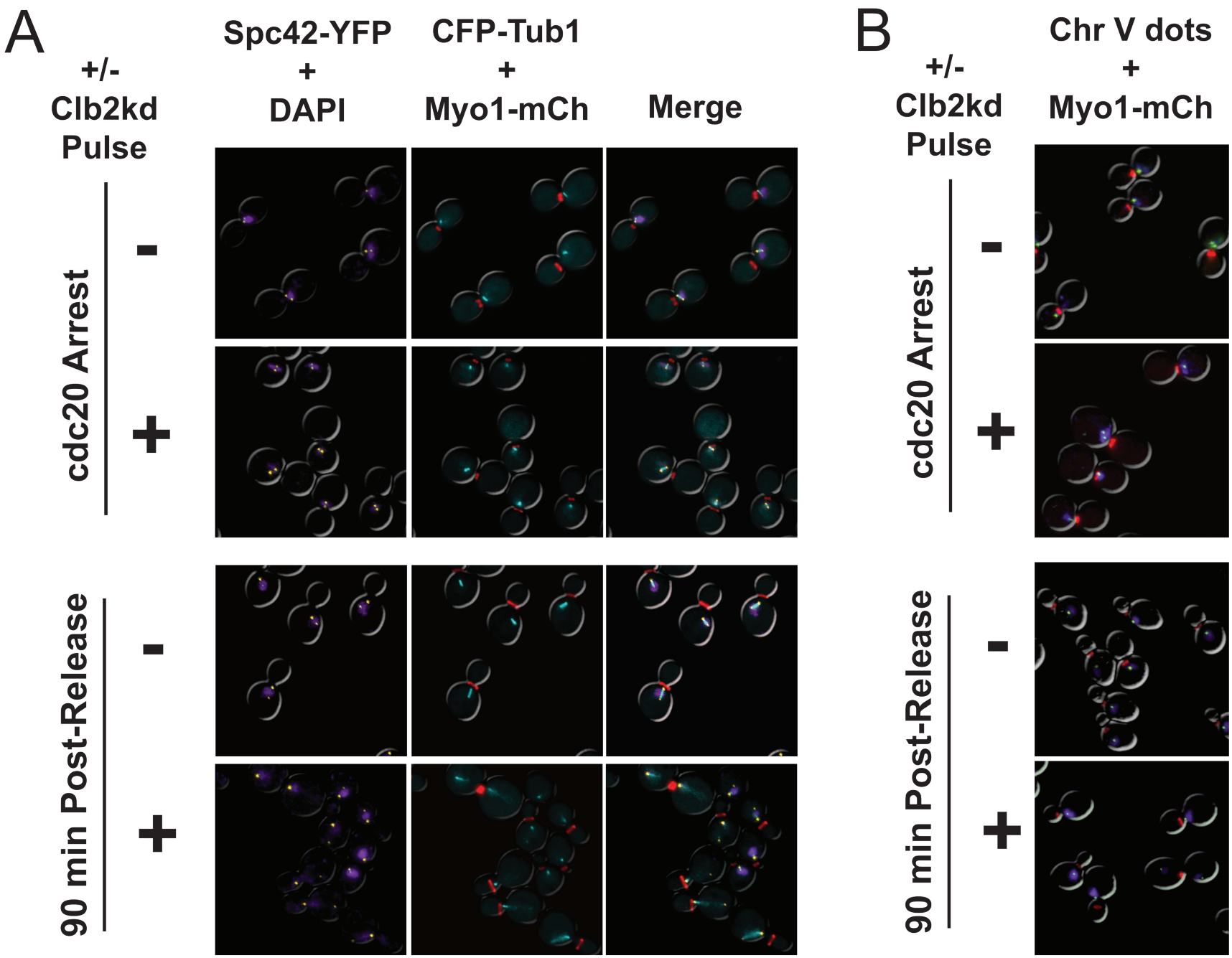
A
+/-
Clb2kd
Pulse
Spc42-YFP
+
DAPI
CFP-Tub1
+
Myo1-mCh
Merge
cdc20 Arrest
-
+
90 min Post-Release
-
+
B
+/-
Clb2kd
Pulse
Chr V dots
+
Myo1-mCh
cdc20 Arrest
-
+
90 min Post-Release
-
+

To address the possibility of defective SPB synthesis, we examined the cells containing Spc29-YFP and CFP-Tub1 in greater detail. We observed that one Spc29-YFP dot was usually brighter than the other. Since YFP takes some time to mature after synthesis, the dim YFP dot could represent the newly synthesized SPB. However, we observed that the tubulin fluorescence was also frequently asymmetric, with less tubulin co-localized with the dim, probably newly synthesized SPB **(Figure 18A)**. Furthermore, this SPB was frequently distant from the main chromosomal density as revealed by DAPI staining. Combined, these results suggest that although persistent Clb2kd permits SPB duplication and separation, one of the SPBs (most likely the new one) is not functional unless Clb2kd is well below peak-equivalent levels. This defective SPB may fail to efficiently nucleate microtubules that engage in kinetochore capture, leading to its migration away from the bulk of the DNA.

Sub-peak-equivalent Clb2kd disrupts normal G1 arrest response to α-factor.

S. cerevisiae haploids can conjugate to form diploids only between exit from mitosis and Start. Without such restriction, mating could result in polyploidy. The point after birth at which cells could no longer be arrested by α-factor (the classical definition of Start) coincides with commitment to budding and DNA replication (Johnston et al., 1977). The coincidence of these events can be explained by the same underlying mechanism, the rapid increase of G1 cyclin

activity that follows, and promotes, SBF- and MBF-mediated transcription (Skotheim et al., 2008).

We studied the quantitative effects of persistent Clb2kd on α-factor arrest by releasing cells from metaphase *cdc20* arrest into medium containing α-factor with or without a prior pulse of Clb2kd-YFP. The control unpulsed strain had its endogenous *CLB2* gene labeled with YFP, while the pulsed strain expressed unlabeled endogenous Clb2, and expressed Clb2kd-YFP in response to the dCort pulse.

In the unpulsed control, anaphase (as judged using Clb2-YFP localization to nuclei) was observed 20 minutes post-release, and cytokinesis was nearly complete in all cells after 40 minutes. By 60 minutes post-release, all unpulsed cells had completed cytokinesis and 95% appeared as 'shmooed', unbudded cells characteristic of α-factor arrest **(figure 19)**. As expected, these cells completely lacked Clb2-YFP.

Among the pulsed cells, at 60 minutes post-release, cells with >150% peak-equivalent Clb2kd-YFP mostly exhibited large-budded arrest, indicating failure of mitotic exit, as expected. At lower Clb2kd-YFP levels, we not only observed complete or partial cytokinesis as described above, but also we observed frequent rebudding (i.e., failure to follow the rule that α-factor blocks budding). The only pulsed cells that both completed cytokinesis and then arrested as

typical unbudded 'shmooed' cells had <25% peak-equivalent Clb2kd-YFP **(figure 19B)**. This result reveals an unanticipated consequence of persistent Clb2kd through mitotic exit: inability to block budding in response to α-factor.

Cells exposed to persistent sub-peak-equivalent Clb2kd concentrations can progress significantly through the subsequent cell cycle in the presence of α-factor.

To further examine disruption of the α-factor response by Clb2kd, we examined spindle formation, *CLN2* promoter activation (*CLN2* is a G1 cyclin activated by SBF, that drives budding), and endogenous Clb2 synthesis in pulsed cells that rebudded in the presence of α-factor.

Since the α-factor arrest threshold was demonstrated to be below peak-equivalent Clb2kd, a low pulse of untagged Clb2kd was sufficient to allow rebudding in the presence of α-factor. Cells that rebudded in a-factor also activated SBF-mediated transcription, as demonstrated by increased GFP signal in rebudded cells containing the P_{CLN2}→*GFP* allele **(figure 20A)**. Endogenous Clb2p first was degraded upon mitosis, but then re-accumulated in these cells, as measured by western blot of untagged endogenous Clb2p in cells pulsed with Clb2kd-YFP **(figure 20B)**. Reciprocally, using pulsed untagged Clb2kd and YFP-tagged endogenous Clb2p, we found microscopically that Clb2p re-accumulation occurred specifically in cells that rebudded **(figure 20C)**. Large-budded cells that failed to exit mitosis, presumably due to containing very high concentrations

of undegradable Clb2p, contain very low levels of endogenous Clb2-YFP. Finally, cells exposed to a low pulse that complete cytokinesis and rebudded in the presence of α-factor could also duplicate spindle-pole bodies, forming either continuous bipolar spindles or 2-dot spindles at 90 minutes post-release **(figure 20D)**. These results are similar to those obtained in the absence of α-factor, while in control unpulsed cells all of these events (rebudding, *CLN2* promoter turn-on, Clb2 reaccumulation, and SPB separation) are completely inhibited in α-factor-treated cells. Thus, overall, going through mitosis in the presence of relatively low sub-peak-equivalent levels of persistent Clb2kd prevents cell cycle arrest by α-factor.

A surprising corollary of these observations is that while shutoff of the *CLN2* promoter is a well-characterized function of endogenous levels of Clb2 (Amon et al., 1993), the *CLN2* promoter fires effectively in cells that go through mitosis with persistent Clb2kd, probably even at peak-equivalent levels, and even in the presence of α-factor.

Chapter 2 Summary

We found that the inhibitory threshold for Clb2kd-mediated stable blockade of mitotic exit was greater than the peak level attained during an unperturbed cell cycle. At close to peak-equivalent Clb2kd levels, Clb2kd persisting through mitotic exit caused a dose-dependent delay in mitotic exit. The delay as a function of amount of Clb2kd is process-specific, resulting in generation of

Figure 19. Peak-equivalent persistent Clb2kd inhibits α-factor arrest.
(A) Phenotypic progression of a *bar1Δ* strain released from cdc20 arrest to a-factor arrest with or without a Clb2kd-YFP pulse. The protocol is the same as that described in **figure 2** up to the point of cdc20 release. Upon release the culture was resuspended in medium lacking methionine and containing 100nM a-factor. Cultures were sampled every 20 minutes for 60 minutes, at which point unpulsed cells were >95% unbudded and visibly shmooed, due to completion of mitosis and arrest due to α-factor in the subsequent cell cycle. Top panels: unpulsed culture Myo1-mCherry fluorescence. Middle panels: pulsed culture Myo1-mCherry fluorescence. Bottom panels: pulsed culture Clb2kd-YFP fluorescence. **(B)** Left graph: Cytokinesis and budding versus time post-release for unpulsed culture. Whereas budding (green) and cytokinesis (blue and red) are scored independently within the same cell, and may be found in any combination in pulsed cultures, unbudded arrest (black) refers to a specific cell type with a combination of completed cytokinesis and no new bud formation. Right graph: Cytokinesis and budding phenotype versus Clb2kd-YFP concentration at 60 min post-release to a-factor arrest. Traces represent the average results of three experiments. Shaded areas represent the 95% confidence interval for the mean percentage of a phenotype at a specific Clb2kd-YFP concentration.

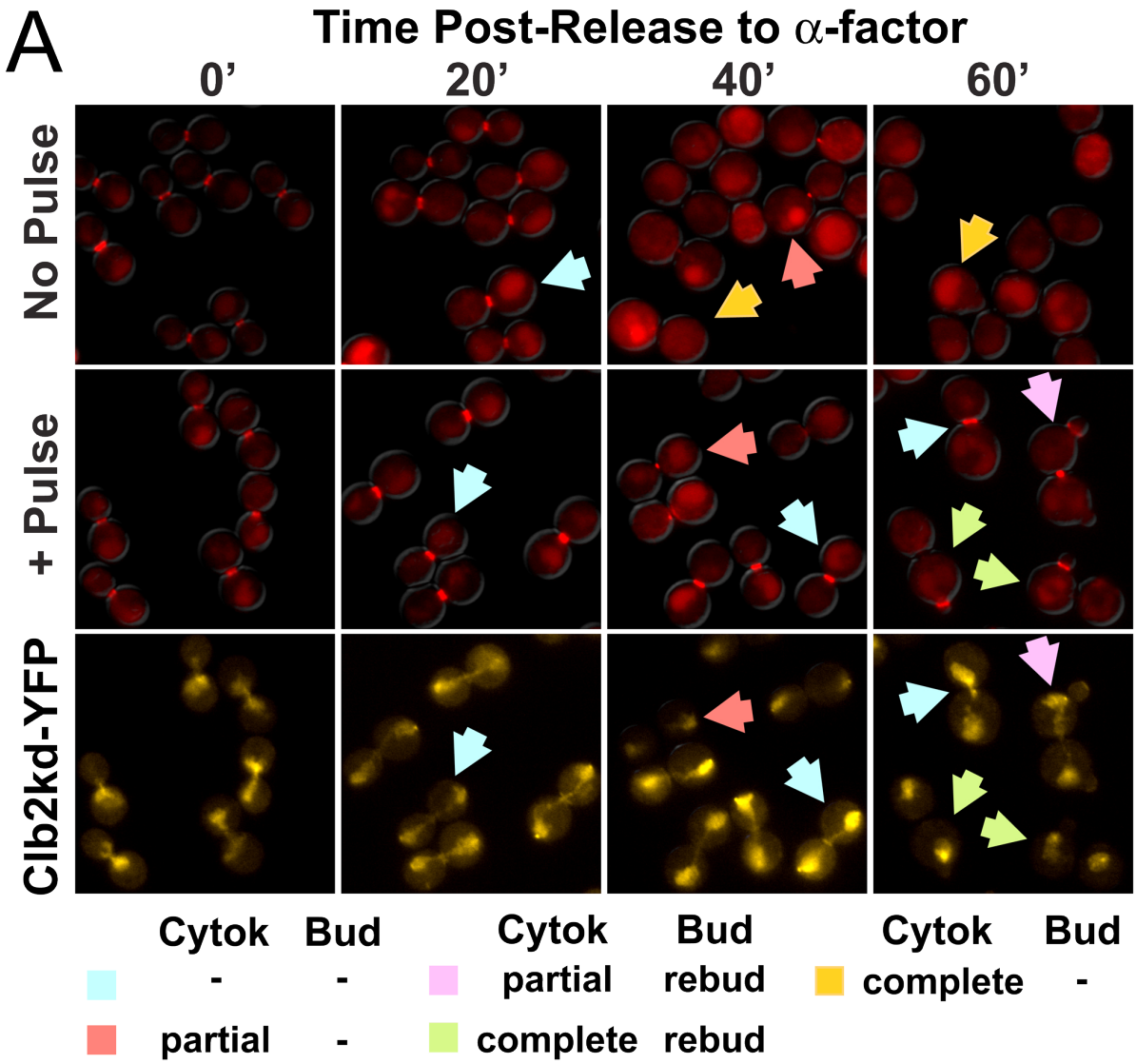
A
Time Post-Release to α-factor
0’
20’
40’
60’
No Pulse
+ Pulse
Clb2kd-YFP
Cytok Bud
- -
partial -
Cytok Bud
partial rebud
complete rebud
Cytok Bud
complete -

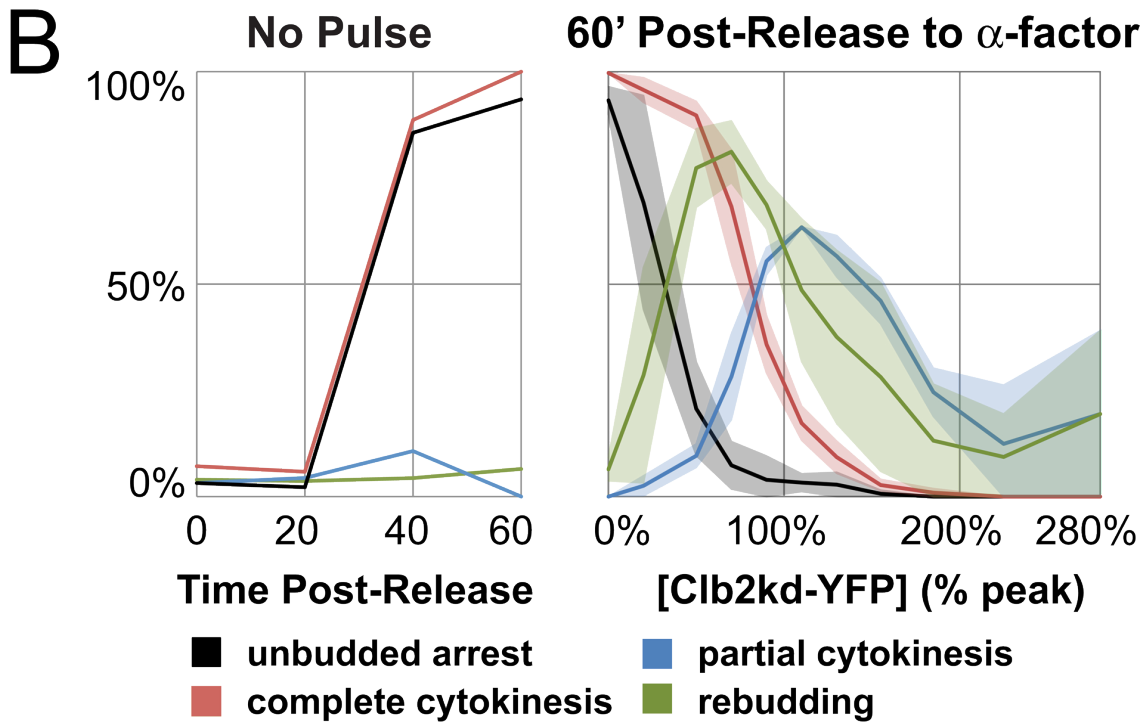
B
No Pulse
60’ Post-Release to α-factor
100%
50%
0%
0
20
40
60
Time Post-Release
0%
100%
200%
280%
[Clb2kd-YFP] (% peak)
unbudded arrest
complete cytokinesis
partial cytokinesis
rebudding

Figure 20. Sub-peak-equivalent persistent Clb2kd permits significant cell cycle progression despite the presence of α-factor.

(A) *P_{GAL}→CLB2kd GAL4-rMR MET-CDC20 bar1Δ* cells bearing *MYO1-mCherry* and GFP fused to the Cln2 degron under the *CLN2* promoter (*CLN2::P_{CLN2}→GFP-deg*) were treated as in figure 19A. Microscopy samples were taken at 0 and 75 minutes post release. Myo1-mCherry and GFP florescence images are merged to distinguish *CLN2* promoter activity in budded and unbudded cells. **(B)** Degradation and re-accumulation of endogenous Clb2p upon release to α-factor in cells pulsed with Clb2kd-YFP, as measured by western blot. **(C)** Re-accumulation of endogenous Clb2-YFP in cells pulsed with unlabeled Clb2kd upon release to α-factor. Pictures at 0' and 90' post-release for pulsed and unpulsed cells. Top panels show spindle and bud morphology. Bottom panels show Clb2-YFP. **(D)** CFP-Tub1 spindle morphology at 0 and 90 minutes post release to a-factor arrest for pulsed and unpulsed cultures. Cells that complete cytokinesis and rebud in a-factor also may duplicate and separate spindle pole bodies, with a similar variety of phenotypes to that observed in **figure 17A**. **(E)** DNA content of cells pulsed with Clb2kd-YFP and released from cdc20-arrest to α-factor.

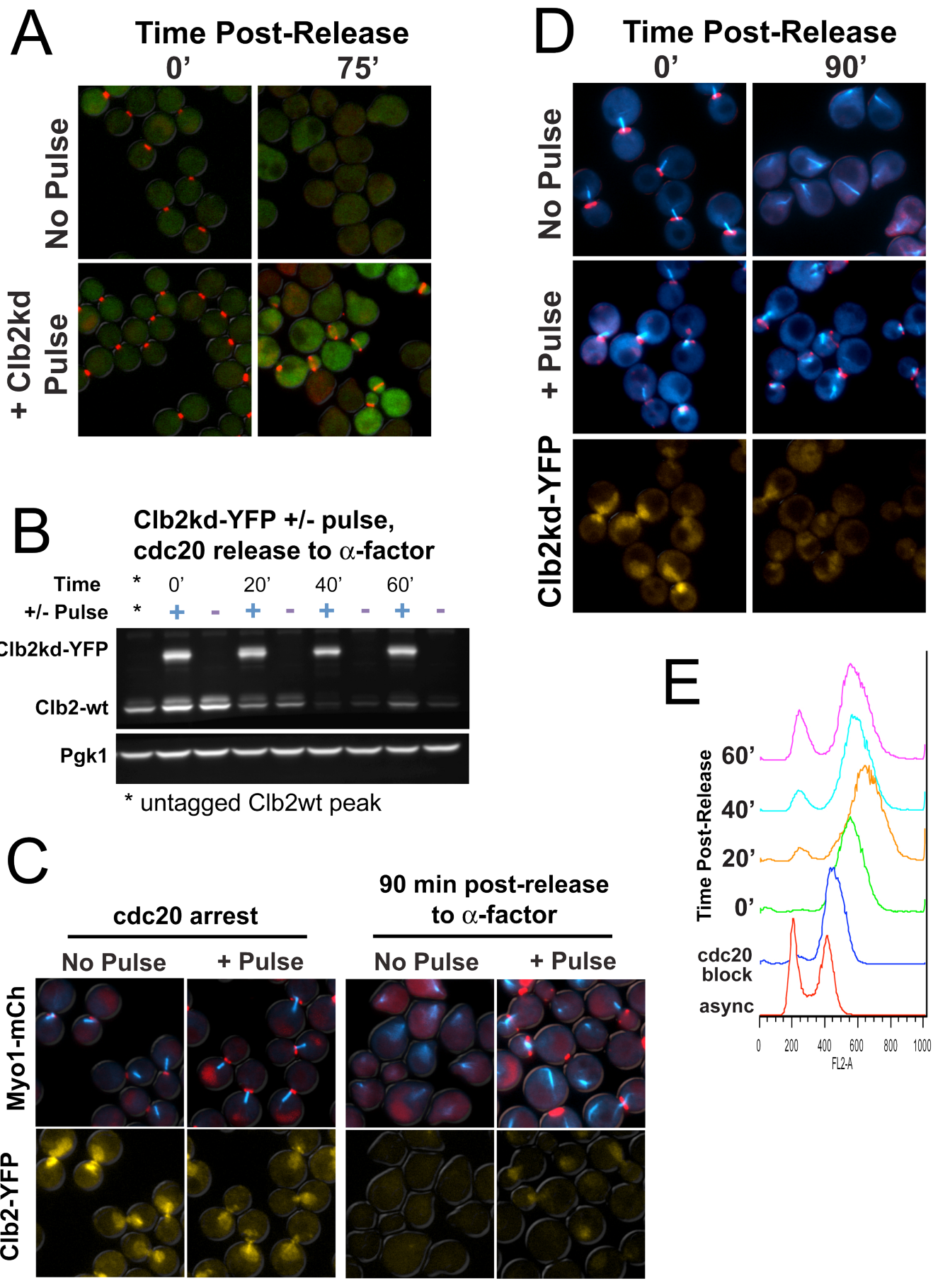
A
Time Post-Release
0'
75'
No Pulse
+ Clb2kd Pulse
B
Clb2kd-YFP +/- pulse,
cdc20 release to α-factor
Time
* 0' 20' 40' 60'
+/- Pulse
* + - + - + - + -
Clb2kd-YFP
Clb2-wt
Pgk1
* untagged Clb2wt peak
C
cdc20 arrest
90 min post-release to α-factor
No Pulse
+ Pulse
No Pulse
+ Pulse
CFP-Tub1 Myo1-mCh
Clb2-YFP
D
Time Post-Release
0'
90'
No Pulse
+ Pulse
Clb2kd-YFP
E
Time Post-Release
60'
40'
20'
0'
cdc20 block
async
0
200
400
600
800
1000
FL2-A

aberrant cell phenotypes at approximately peak-equivalent levels of persistent Clb2kd. Furthermore, following the delayed mitotic exit into the subsequent cell cycle, peak-equivalent Clb2kd permits bud formation, DNA replication and SPB duplication. However, persistent Clb2kd well below peak-equivalent levels prevents bipolar metaphase spindle assembly, possibly because persistent Clb2kd causes defects in the newly formed SPB made in its presence. Furthermore, persistent Clb2kd disrupts α-factor arrest in the subsequent cell cycle at a threshold well below peak-equivalence. These results suggest that peak Clb2 levels are at most barely sufficient to restrain mitotic exit, but these levels or even lower levels cause severe disruption of the subsequent cell cycle if maintained throughout mitosis. Thus, while mitotic cyclin degradation to below the normal peak level may not be required for mitotic exit, as is commonly assumed, mitotic cyclin degradation to well below peak levels may be required for normal execution of the ensuing cell cycle; this is a novel concept for the reason for mitotic cyclin degradation.

These results effectively rule out the simplest version of the ratchet model for control of mitosis, in which mitotic cyclin level is the only relevant regulator. However, as discussed in the Introduction, the cell has other means to inhibit cyclin-Cdk activity besides cyclin degradation. Therefore, we next examine the degree of CDK activity produced by the Clb2kd pulse in our protocol.

Chapter 3: Translation of Clb2p Inhibitory Thresholds to Clb2-CDK Activity Thresholds

In this chapter we examine the relationship between Clb2p inhibitory thresholds and Clb2-CDK activity thresholds for inhibition of events that occur after spindle elongation. First, we assess whether or not endogenous mitotic cyclin activity causes underestimation of the Clb2kd inhibitory thresholds. Then we evaluate the degree to which post-translational inhibition of the Clb2kd-YFP pulse causes overestimation of the Clb2kd inhibitory thresholds, with respect to Clb2kd-Cdk protein kinase activity. We conclude with an analysis of the effect of Clb2kd on the release of Cdc14 phosphatase, which reverses CDK-mediated phosphorylation. Cdc14 directly affects CDK activity through activation of Cdh1 and Sic1, and also probably directly dephosphorylates many Clb-Cdk targets, thus altering the 'net phosphorylation potential' for CDK substrates.

Completion of mitotic exit events in the presence of undegradable Clb2 is independent of the effects of endogenous B-cyclins.

Our analysis of inhibitory thresholds (Chapter 2) is ambiguous unless all inhibitory activity that we observe is due to the Clb2kd-YFP that we measure; for this to be the case, endogenous mitotic Clbs cannot make a major contribution to

the Clb pool compared to Clb2kd during mitotic exit, under the conditions of our experiment.

To test the contributions of Clb1, 3, and 4, we carried out a genetic experiment. Cells deleted for *CLB1, CLB3,* and *CLB4* are viable, and *clb1,3,4Δ* cells exited mitosis with kinetics very similar to WT based on timing of re-accumulation of G1 cells after release from a G1 block **(figure 8A)**. Therefore, we could assess the contribution of these cyclins to the Clb2kd-YFP inhibitory thresholds by measuring these thresholds in the *clb1,3,4Δ* background (Figure 21A) compared to the measurements already made in the *CLB1,3,4* background **(Figure 19)**. This comparison showed clearly that the presence or absence of *CLB1,3,4* did not affect any measured thresholds **(figure 21A)**.

We next measured the effect of pulsed Clb2kd-YFP on endogenous Clb2 degradation by Western blot. In pulsed or unpulsed cultures released from metaphase arrest to either α-factor or a second *cdc20* arrest, endogenous Clb2p is completely degraded by 30 – 40 minutes post-release, while the exogenous Clb2kd-YFP remained stable. Furthermore, in cells with the endogenous *CLB2* locus tagged with YFP and pulsed with untagged Clb2kd, endogenous Clb2-YFP is degraded even in cells that cannot initiate cytokinesis; such cells presumably have the highest levels of Clb2kd. This suggests that even high levels of Clb2kd do not block endogenous Clb2 degradation **(figure 21B,C)**. Complete Clb2 degradation requires Cdh1 in WT cells (Schwab et al., 1997; Visintin et al., 1997). Although Cdh1 is inhibited by cyclin-Cdk activity (Zachariae et al., 1998), this

inhibition might be inefficient by Clb2kd-Cdk, at least up to 2X peak-equivalence (roughly the maximum level we measure in most experiments). This speculation is consistent with the inference that Clb5-Cdk activity is primarily responsible for inactivating Cdh1 (Shirayama et al., 1999).

Since endogenous wild-type Clb2 is degraded despite pulsed Clb2kd even at high levels, and Clb1,3,4 share the same degradation pathways as Clb2, they are also likely to be degraded in pulsed cells (Baumer et al., 2000). This would explain the absence of an effect of deletion of *CLB1,3,4* on Clb2kd inhibitory thresholds. Overall, the evidence suggests that undetected extra cyclin beyond the labeled Clb2kd-YFP is unlikely to contribute significantly to the measured thresholds.

It is worth noting in any case that even if there is extra undetected cyclin contributing to the inhibitory thresholds, this only strengthens our conclusion that it takes surprisingly high mitotic cyclin levels to significantly inhibit many events of mitotic exit.

Deletions of *SWE1* or does not significantly reduce the mitotic exit inhibitory thresholds.

In *S. pombe*, entry into mitosis is regulated by inhibitory phosphorylation of cdc2 at Y15, regulated by wee1 kinase and cdc25 phosphatase (Dunphy, 1994). In *S. cerevisiae*, homologous proteins, Swe1 kinase and Mih1 phosphatase, perform similar biochemical functions in regulating phosphorylation of Cdc28 at

Figure 21. Endogenous Clb1-4 activity does not affect threshold measurements; endogenous Clb2 destruction proceeds regardless of a Clb2kd pulse. (A) Cytokinesis and budding phenotype versus Clb2kd-YFP concentration at 60 min post-release to a-factor arrest in *CLB1,3,4*^{WT} (black) and *clb1,3,4Δ* (red) backgrounds. The time course was performed as described in **figure 19A**. WT traces and confidence intervals (gray) are the same as those presented in figure 19B, but are graphed separately for ease of comparison with *clb1,3,4Δ*. **(B)** Degradation of endogenous Clb2p measured by western blot upon release to a second cdc20 arrest in cultures with or without a Clb2kd-YFP pulse. **(C)** Degradation of endogenous Clb2-YFP in cells pulsed with unlabeled Clb2kd upon release to a second cdc20 arrest. Pictures at 0', 45', and 90' post-release for pulsed and unpulsed cells. Left panels show spindle and bud morphology, and right panels show Clb2-YFP.

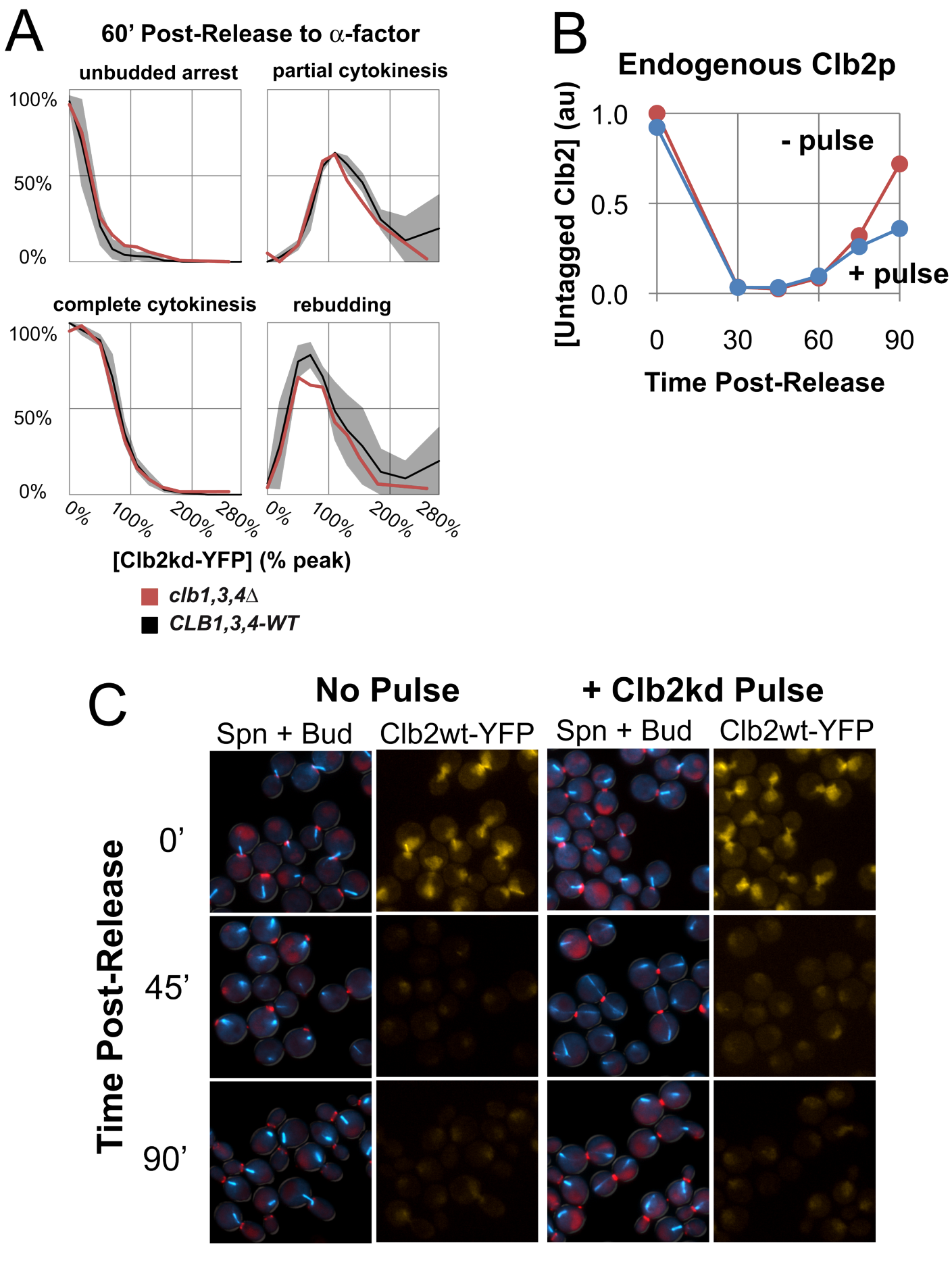
A
60' Post-Release to α-factor
unbudded arrest
partial cytokinesis
complete cytokinesis
rebudding
100%
50%
0%
0%
100%
200%
280%
[Clb2kd-YFP] (% peak)
clb1,3,4Δ
CLB1,3,4-WT
B
Endogenous Clb2p
[Untagged Clb2] (au)
1.0
0.5
0.0
- pulse
+ pulse
0
30
60
90
Time Post-Release
C
No Pulse
+ Clb2kd Pulse
Spn + Bud
Clb2wt-YFP
Spn + Bud
Clb2wt-YFP
Time Post-Release
0'
45'
90'

Y19 (Booher et al., 1993), but regulation of mitotic entry does not require Y19 phosphorylation (Amon et al., 1992). Instead, Y19 phosphorylation has been implicated in a surveillance mechanism for proper bud formation (Sia et al., 1996). Recent work claims that although not essential for regulation of mitosis, Swe1 restrains mitotic entry (Harvey and Kellogg, 2003). This claim is controversial (McNulty and Lew, 2005**)**.

Swe1 has been demonstrated to have a greater effect on Clb2-Cdc28 complexes than on Clb5 or Clb3 complexes. Hence, along with transcriptional regulation, it has been proposed that Swe1 activity contributes to the order of activation of different Clb-Cdc28 species (Hu and Aparicio, 2005; Keaton et al., 2007). Furthermore, Clb2-Cdk may activate Swe1 (Harvey et al., 2005). However, Swe1 degradation is promoted by Clb-CDK activity, possibly through direct phosphorylation (McMillan et al., 2002). These complicated interactions made it difficult to predict whether Swe1 should have an effect on Clb2kd-Cdk kinase activity.

To test this, we measured the effect of *SWE1* deletion on Clb2kd-YFP inhibitory thresholds. At 45 minutes post-release from metaphase arrest, deletion of *SWE1* has no measureable effect on the concentration of Clb2 necessary to delay spindle disassembly **(figure 22)**. *swe1Δ* cells show a small reduction in the Clb2 inhibitory thresholds for initiation of actomyosin ring shrinkage, completion of cytokinesis, and rebudding. Cytokinesis thresholds were reduced by <10%

peak Clb2 at 45' post-release, the earliest time at which a cytokinesis threshold can be measured. Cytokinesis completion and rebudding thresholds were reduced by 10% peak-equivalent Clb2kd 'units' at 60' post-release, the earliest time at which a rebudding threshold can be unambiguously measured. Based on these measurements, we conclude that Swe1 does not significantly reduce the activity of the Clb2kd-YFP pulse, suggesting that under our experimental conditions, Swe1 does not significantly inactivate Clb2kd-YFP-Cdk complexes.

Deletion of *SWI5* potentiates Clb2kd inhibition of cytokinesis

Clb2kd expressed from its endogenous promoter is lethal. This lethality can be rescued by overexpression of Sic1 (Archambault et al., 2003; Wäsch and Cross, 2002). Furthermore, *10xSIC1* bypasses the need for APC-mediated degradation of mitotic cyclin (Thornton and Toczyski, 2003). However, Sic1, like Swe1, is negatively regulated by Clb-CDK activity (Verma et al., 1997). Direct phosphorylation of Sic1 by CDK induces Sic1 degradation. Cells deleted for *SIC1* are viable, but undergo aberrant cell cycle progression, resulting in genomic instability and significant inviability (Mendenhall et al., 1995). We found in preliminary experiments that these cells exhibit too high a proportion of aberrant or inviable cells to reliably ascribe any phenotype to *CLB2kd* expression, as opposed to damage incurred prior to the pulse. Therefore we pursued other strategies to evaluate whether or not Sic1 affected the activity of the Clb2kd-YFP pulse.

Figure 22. Deletion of *SWE1* does not significantly reduce the mitotic exit inhibitory thresholds. Mitotic exit and rebudding versus Clb2kd-YFP concentration in $SWE1^{WT}$ and *swe1Δ* backgrounds was assayed in a cdc20 time course released to a second cdc20 arrest, as described in figure 2. Spindle disassembly versus Clb2kd-YFP concentration is plotted at 45 min post-release, and cytokinesis and budding phenotype versus Clb2kd-YFP concentration are plotted at 60 min post-release.

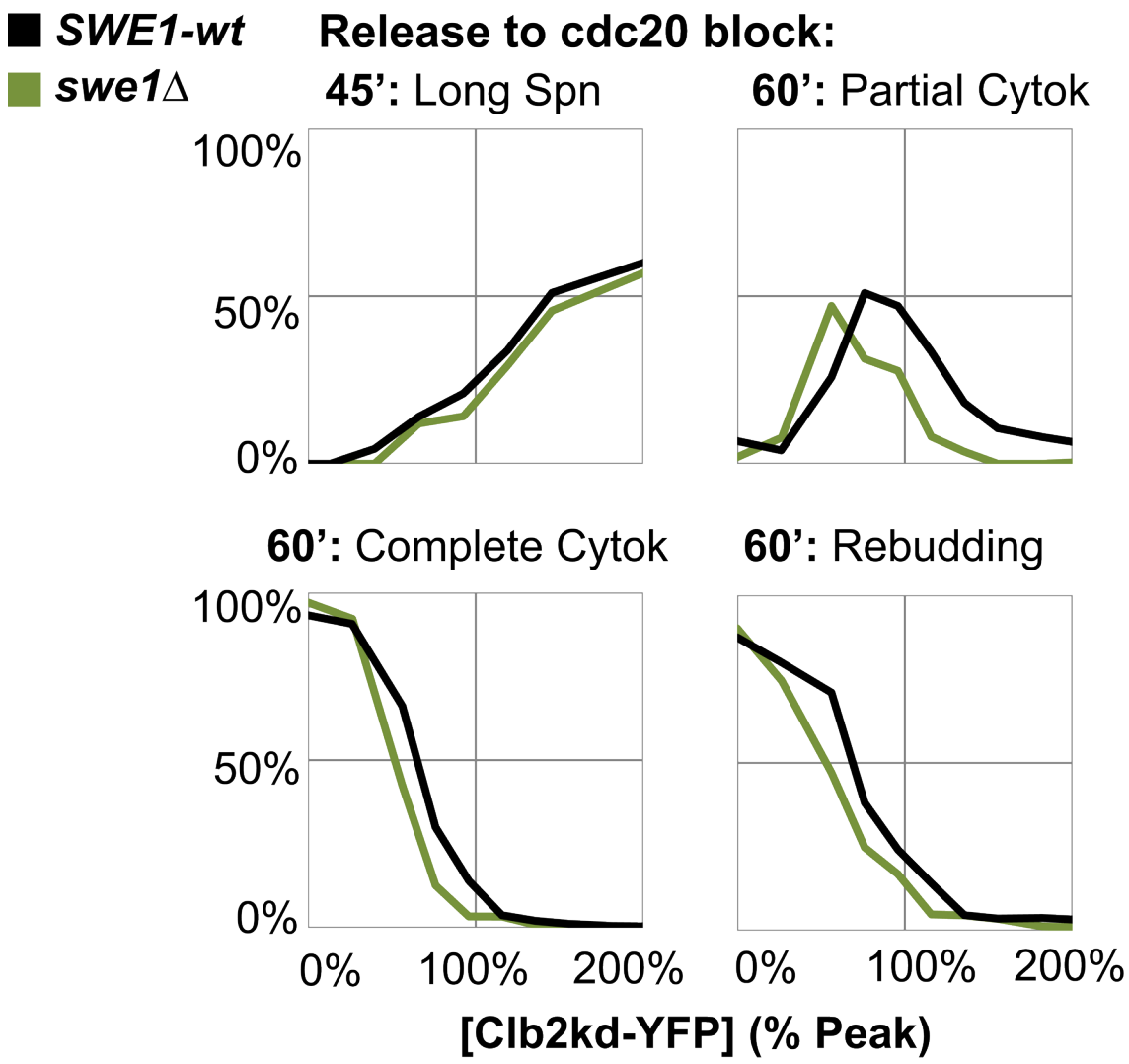
SWE1-wt
swe1Δ
Release to cdc20 block:
45': Long Spn
60': Partial Cytok
60': Complete Cytok
60': Rebudding
100%
50%
0%
0%
100%
200%
[Clb2kd-YFP] (% Peak)

To test the potential effect of Sic1 on the activity on the Clb2kd-YFP pulse, we first measured inhibitory thresholds in a *swi5Δ* background. Swi5 is a transcription factor activated by Cdc14 and inactivated by CDK activity (Moll et al., 1991; Visintin et al., 1998). Swi5 induces *SIC1* transcription upon exit from mitosis, but deletion of *SWI5* does not eliminate basal *SIC1* transcription or Ace2-dependent transcription in daughter cells (Knapp et al., 1996). Consequently, *swi5Δ* cells do not suffer the same growth defects as *sic1Δ* cells, and can be studied using our methods.

We released *swi5Δ* cultures with or without a Clb2kd-YFP pulse from metaphase arrest to a second arrest with Cdc20 depletion. Unpulsed *swi5Δ* cultures exhibited a brief delay in cytokinesis and bud formation relative to $SWI5^{WT}$ cells, but no delay in spindle disassembly **(figure 23A)**. Deletion of *SWI5* had no effect on the spindle disassembly threshold for Clb2kd_YFP in pulsed cells, measured 45 minutes post-release **(figure 23B)**. However, *swi5Δ* cells had a moderately lower threshold for inhibition of bud formation, and a markedly lower threshold for completion of cytokinesis **(figure 23C)**. This difference in thresholds was measured at 45 and 60 minutes post-release. Therefore we conclude that Swi5 potentiates Clb2-CDK inhibition of cytokinesis and bud formation, but not spindle disassembly.

One way in which Swi5 could affect Clb2kd activity is through induction of *SIC1* transcription. Therefore, inhibition of Cdk activity by Sic1 might significantly

affect the inhibitory threshold measurements, explaining the effects of *SWI5* deletion. However, Swi5 has transcriptional targets other than Sic1. One target is Cdc6, which has the potential to inhibit Clb2-Cdk somewhat similarly to Sic1. However, Cdc6 appears to be a weaker promoter of mitotic exit than Sic1 (Archambault et al., 2003); additionally, since Cdc6 binds stably to Clb2-Cdk complexes, its possible effect can be assayed by *in vitro* kinase assay (see below).

Other transcriptional targets of Swi5 might also increase Clb2 inhibitory thresholds without direct Clb2-CDK inhibition. Recent microarray analysis reveals that transcription of *CYK3* is reduced in *swi5Δ* cells (Stefano DiTalia personal communication). Cyk3 associates with the actin ring at the bud neck and contributes to cytokinesis (Ko et al., 2007). Therefore, further experiments were therefore required to evaluate the effect of Sic1 on Clb2kd inhibitory thresholds.

Doubling *SIC1* gene dosage and transcription does not increase the mitotic exit inhibitory thresholds.

We reasoned that measurement of the quantitative effect of increased *SIC1* expression would shed light on whether endogenous Sic1p inhibits the Clb2kd-YFP pulse. We generated strains with two or six stably integrated copies of *SIC1*, as measured by quantitative PCR **(figure 24A)**. We next tested these

Figure 23. Deletion of *SWI5* does not reduce the spindle disassembly inhibitory threshold, but potentiates Clb2kd inhibition of cytokinesis and rebudding. (Courtesy of Andrea Geoghegan).

Mitotic exit and rebudding versus Clb2kd-YFP concentration in $SWI5^{WT}$ (blue) and *swi5Δ* (red) backgrounds was assayed in a cdc20 time course released to a second cdc20 arrest, as described in figure 2. **(A)** Spindle disassembly versus time is plotted for unpulsed controls (circles) and pulsed cultures (squares). **(B)** Spindle disassembly versus Clb2kd-YFP concentration is plotted at 45 min post-release. **(C)** Cytokinesis and budding phenotype versus Clb2kd-YFP concentration are plotted at 45 min and 60 min post-release. Cytokinesis initiation is the sum of cells that have partial or complete Myo1 ring contraction.

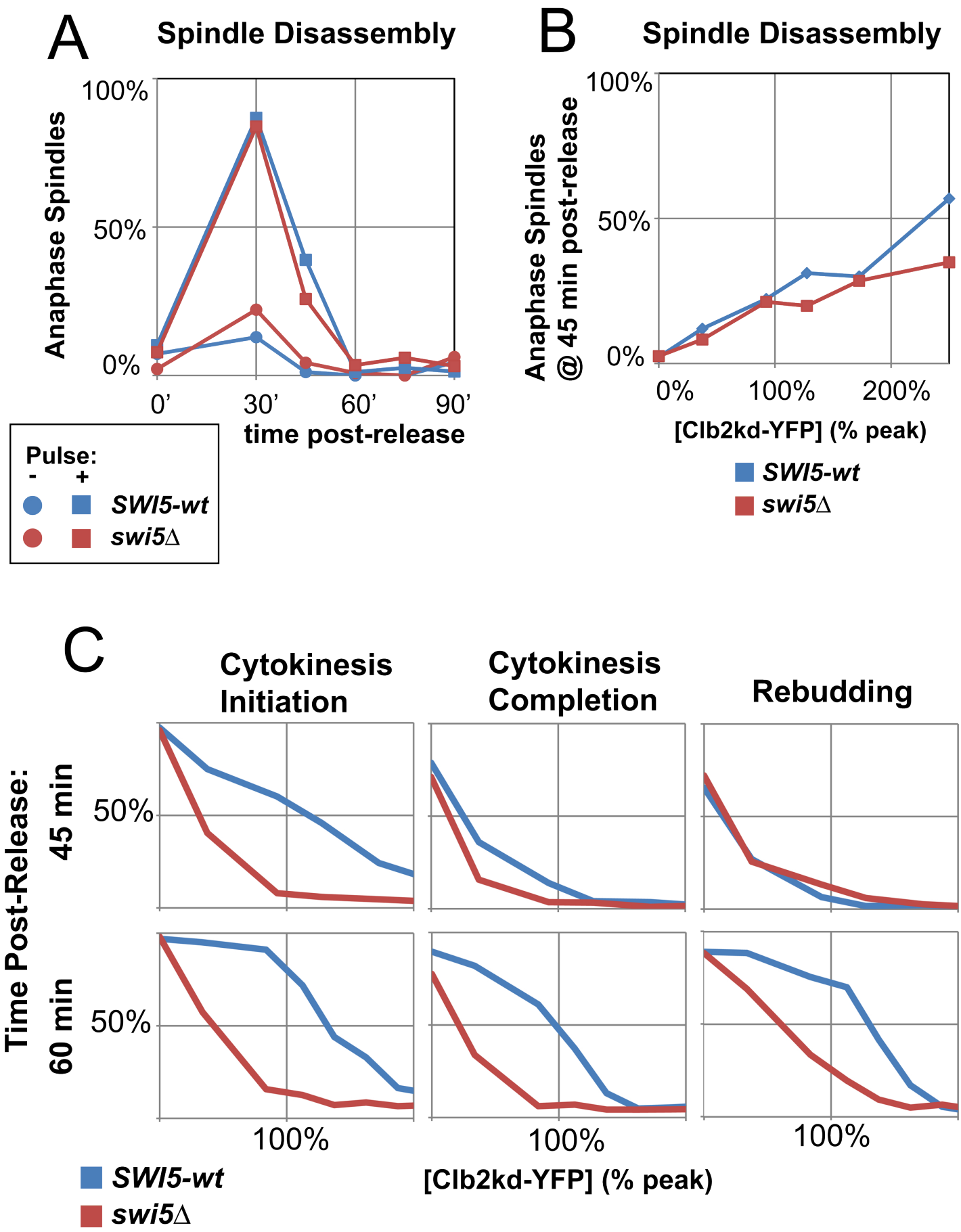
A
Spindle Disassembly
100%
50%
0%
Anaphase Spindles
0'
30'
60'
90'
time post-release
Pulse:
-
+
SWI5-wt
swi5Δ
B
Spindle Disassembly
Anaphase Spindles @ 45 min post-release
100%
50%
0%
0%
100%
200%
[Clb2kd-YFP] (% peak)
SWI5-wt
swi5Δ
C
Cytokinesis Initiation
Cytokinesis Completion
Rebudding
Time Post-Release:
45 min
60 min
50%
50%
100%
100%
100%
SWI5-wt
swi5Δ
[Clb2kd-YFP] (% peak)

Figure 24. Doubling *SIC1* gene dosage and transcription does not increase the mitotic exit inhibitory thresholds. *SIC1* gene copy numbers **(A)** and expression levels **(B)** for two multi-copy *SIC1* alleles relative to wild-type. The gene copy number was assayed by quantitative PCR using *CLN2* as a single-copy control. The expression level is measured by RTqPCR performed on samples from a cdc20 time course released to a-factor arrest. The *SIC1* RNA signal was standardized to *ACT1* RNA in the same sample, and is expressed as a ratio of peak *SIC1* expression in the wild-type background, 20 min post-release. **(C)** Cytokinesis and budding phenotype versus Clb2kd-YFP concentration at 60 min post-release to a-factor arrest in $SIC1^{WT}$, *2xSIC1*, and *6xSIC1* backgrounds. WT traces and error bars are the same as those presented in figure 19B, and presented in the same format as **figure 21A.**

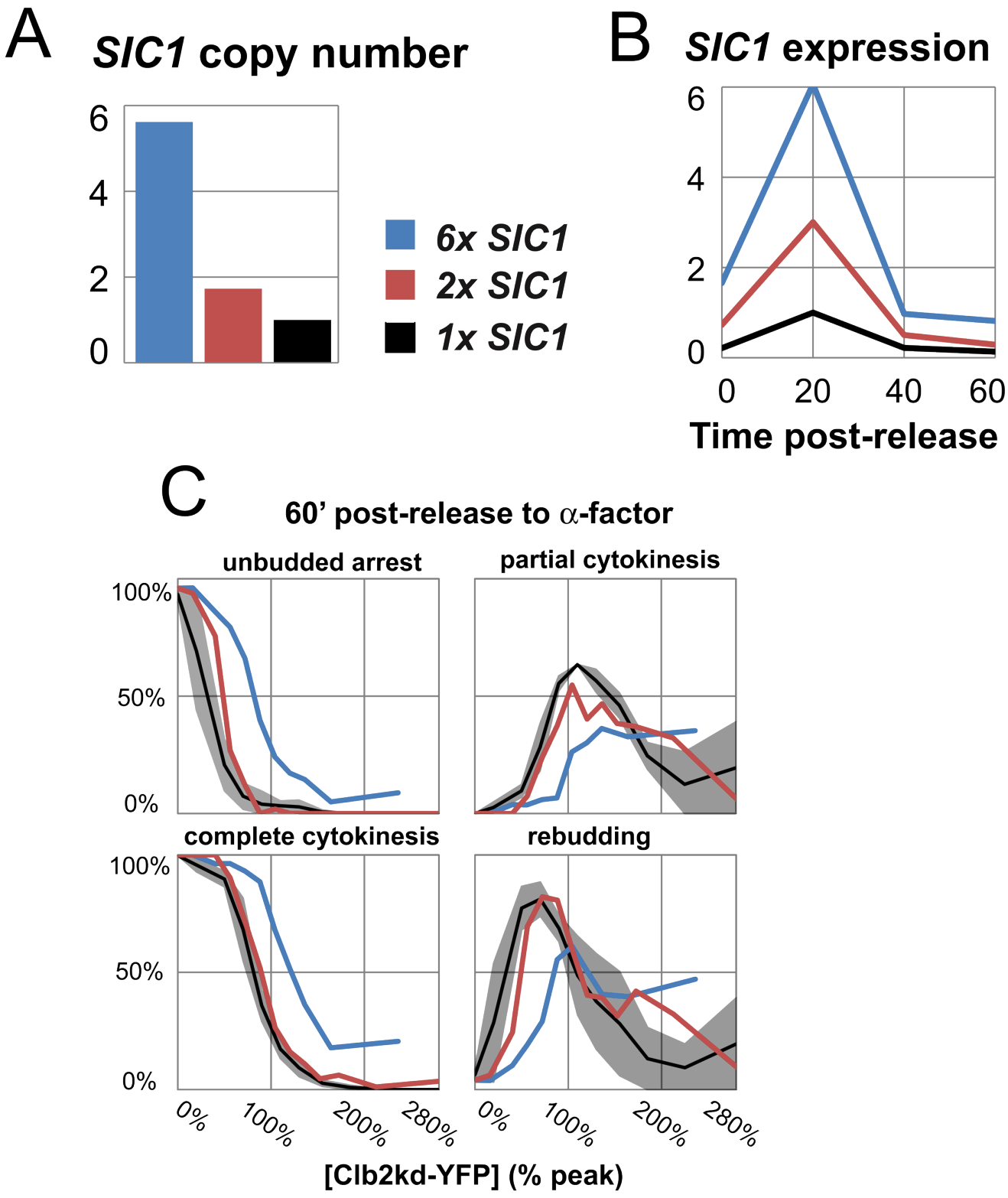
A
SIC1 copy number
6
4
2
0
6x SIC1
2x SIC1
1x SIC1
B
SIC1 expression
6
4
2
0
0
20
40
60
Time post-release
C
60' post-release to α-factor
unbudded arrest
partial cytokinesis
complete cytokinesis
rebudding
100%
50%
0%
0%
100%
200%
280%
[Clb2kd-YFP] (% peak)

strains to make sure that transcript level was proportional to gene copy number. We blocked strains with one, two, or six copies of *SIC1* at a metaphase arrest, released to α-factor, and sampled the culture every 20 minutes for 60 minutes. At each time point we measured *SIC1* mRNA relative to *ACT1* mRNA by RTqPCR. Transcript level in all cultures began low, peaked at 20 minutes post-release, coincident with anaphase, dropped to near baseline level or below at 40 minutes post release, and remained low to the end of the time course. At the 20-minute post-release peak, *2xSIC1* produces roughly twice the *SIC1* transcript as the wild-type allele, and *6xSIC1* yields six times the wild-type transcript level **(figure 24B)**. We therefore conclude that transcript level reflects gene copy number for multi-copy *SIC1* alleles.

Sic1p is a stoichiometric inhibitor of Clb2-Cdk. If Sic1 levels are setting the Clb2kd inhibitory thresholds, then doubling the Sic1 synthesis rate by doubling its mRNA level should approximately double the Clb2kd inhibitory thresholds by forcing a requirement for nearly twice as much Clb2kd to saturate the doubled amount of Sic1. On the other hand, Sic1p degradation is induced by Clb2-Cdk activity, so high levels of Clb2kd might prevent accumulation of Sic1p. If this were the case, then doubling the synthesis rate would have little effect on Sic1p accumulation or the activity of the Clb2kd-YFP pulse. To distinguish these possibilities, we measured the post-anaphase Clb2kd-YFP inhibitory thresholds in cells with 2 or 6 copies of *SIC1*, and compared these thresholds to those

derived from wild-type cells with *1xSIC1.* We measured these inhibitory thresholds 60 minutes post-release to α-factor arrest.

We found that *2xSIC1* did not affect the higher Clb2 inhibitory thresholds for cytokinesis or rebudding, but modestly increased the amount of Clb2kd necessary to disrupt α-factor arrest **(figure 24C)**. This threshold remains well below peak-equivalent levels of Clb2kd. *6xSIC1*, in contrast, permits α-factor arrest in cells pulsed with ¾ peak Clb2, and significantly increases the cytokinesis and rebudding inhibitory thresholds. Because *2xSIC1* does not increase the concentration at which Clb2 inhibits cytokinesis or rebudding, we propose that Sic1 activity has little to do with setting these thresholds. Six copies of *SIC1* may be sufficient to begin to overwhelm the Clb2kd pulse, but this is a highly non-physiological level – 10 copies of *SIC1* will bypass the requirement for the APC for Clb-CDK inhibition (Thornton and Toczyski, 2003). It remains possible that a homeostatic mechanism exists to regulate Sic1 protein concentration such that doubling transcription does not affect translation, and this mechanism compensates for *2xSIC1* but not *6xSIC1*, but this possibility seems unlikely. These genetic results suggest that endogenous Sic1 does not affect Clb2kd activity at near-peak Clb2 concentration.

The undegradable Clb2p pulse is fully active throughout the time course as measured by *in-vitro* kinase assay.

To further evaluate the role of post-translational CDK inhibition in setting the inhibitory thresholds, we directly assessed the activity of the Clb2kd-YFP pulse by *in-vitro* kinase assay. We released four cultures from arrest due to Cdc20 depletion; after release, we depleted Cdc20 again to capture cells at a second metaphase arrest. The first culture contained the *CLB2-YFP* allele as its sole source of Clb2-CDK activity. Cultures two through four contained the single- or multi-copy *SIC1* strains analyzed above, with untagged endogenous Clb2 and the P_{GAL1}→*CLB2kd-YFP* allele. All four cultures were exposed to deoxycorticosterone for 25 minutes to produce a Clb2kd-YFP pulse with a mean concentration slightly below peak Clb2. Samples were taken every 15 minutes for 90 minutes and analyzed for DNA content, YFP-tagged Clb2 concentration, and YFP-associated kinase activity.

As observed previously, the Clb2-YFP protein concentration in cells arrested by Cdc20 depletion was twice the endogenous peak level of expression. Protein concentration remained high fifteen minutes after release, then plummeted to near undetectable levels 30 and 45 minutes after release, and slowly recovered to the Cdc20-depleted arrest level during the remainder of the time course. Kinase activity in the *CLB2-YFP* strain was even more tightly regulated than Clb2-YFP protein levels, most likely due to the well-established inhibitory effect of Sic1 (Schwob et al., 1994) **(figure 25A).**

Pulsed Clb2kd-YFP activity in cells with one copy of *SIC1* remained approximately constant throughout the time course **(figure 25B)**, and possessed a similar activity when standardized to Clb2 protein level as the Clb2-YFP in Cdc20-depleted cells. That the activity remained so stable was somewhat surprising because although the mean concentration began near peak level of expression, some cells should contain little undegradable Clb2. Consequently, even if cells with high Clb2 levels inhibited Sic1 accumulation, cells with low expression during the pulse might accumulate Sic1. If this Sic1 were in excess, then it could bind the pulsed Clb2kd-YFP from other cells after cell lysis (post-lysis binding of Sic1 to Clb-Cdk complexes is a well-established phenomenon (Schwob et al., 1994). Post-lysis inhibition of the pulse would artificially lower the *in-vitro* kinase activity. That this did not occur suggests very low levels of Sic1 accumulation in these pulsed cultures at any point in the experiment.

Pulsed Clb2kd-YFP activity in cells with two copies of *SIC1* dropped slightly between 15 and 30 minutes post-release **(figure 25B);** this slight drop could correlate with the slight increase in Clb2kd inhibitory thresholds with *2xSIC1*. In contrast, *6xSIC1* cells showed complete elimination of YFP-associated kinase activity between 15 and 30 minutes post-release **(figure 25B)**. CDK activity in the *6xSIC1* culture returns more quickly than in the *CLB2-YFP* culture, probably because no new synthesis of Clb2kd-YFP is required, merely relief of Sic1-mediated inhibition by Sic1 degradation (likely mediated by Cln-Cdk complexes). The *6xSIC1* time course provides a positive control, demonstrating that this

Figure 25. The Clb2kd-YFP pulse yields active Clb2kd-associated kinase throughout the time course.

Four *MET-CDC20 GAL4-rMR MYO1-mCherry* strains were treated as described in figure 1. The first contained *CLB2^{WT}-YFP* under the endogenous promoter. The other three strains, (the same ones as analyzed in figure 23), contained *CLB2::P$_{GAL1}$→CLB2kd-YFP* and *SIC1^{WT}*, *2xSIC1*, or *6xSIC1*. An abbreviated dCort induction (25 min) was used to generate a Clb2kd-YFP pulse slightly below peak Clb2 concentration. Upon release from cdc20 arrest, cultures were sampled for protein concentration and kinase activity **(A and B)**, as well as for progression of cytokinesis and rebudding by fluorescence microscopy **(C)** and DNA content **(D)**. **(A)** CLB2^{WT}-YFP protein concentration was measured by western blot (blue) and YPF-associated *in vitro* histone H1 (HH1) kinase activity by phosphorimager (red). Protein concentration is standardized to peak Clb2-YFP concentration, as in figure 10C. Kinase activity is standardized to the initial level in the cdc20-arrested cells. **(B)** Clb2kd-YFP concentration and kinase activity were measured as in (**A**) for each of the Sic1 backgrounds.

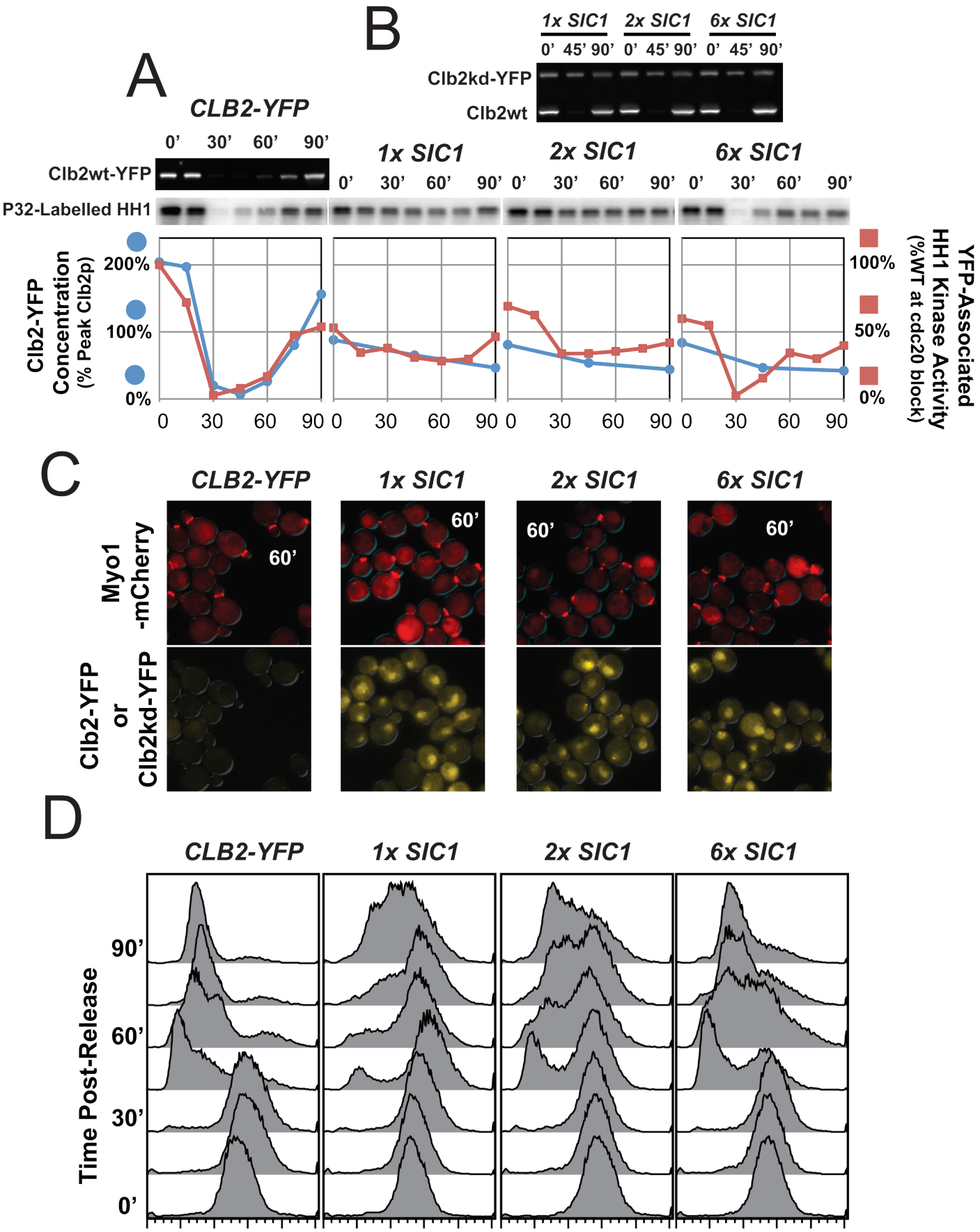
A
CLB2-YFP
0' 30' 60' 90'
Clb2wt-YFP
P32-Labelled HH1
1x SIC1
2x SIC1
6x SIC1
0' 30' 60' 90'
Clb2-YFP Concentration (% Peak Clb2p)
200%
100%
0%
0 30 60 90
YFP-Associated HH1 Kinase Activity (%WT at cdc20 block)
100%
50%
0%
B
1x SIC1
2x SIC1
6x SIC1
0' 45' 90' 0' 45' 90' 0' 45' 90'
Clb2kd-YFP
Clb2wt
C
CLB2-YFP
1x SIC1
2x SIC1
6x SIC1
Myo1 -mCherry
Clb2-YFP or Clb2kd-YFP
60'
D
CLB2-YFP
1x SIC1
2x SIC1
6x SIC1
Time Post-Release
90'
60'
30'
0'

method can detect Sic1-mediated inhibition of Clb2kd-YFP activity, and correlates with the significant shift of Clb2kd inhibitory thresholds by *6x SIC1*. For both the *2x* and *6x SIC1* assays, though, the kinase assay has the potential to overstate the effect of Sic1 due to post-lysis binding.

Comparison of the effect of one, two and six copies of *SIC1* on the activity of the pulse suggests that negative feedback between Clb2 and Sic1 can generate a non-linear, switch-like decrease in CDK activity at a critical concentration of inhibitor. Although inhibitory Clb2 thresholds were not measured for these time courses, fluorescence images and measurement of DNA content by flow cytometry demonstrates that the pulse is near the threshold for preventing cytokinesis in cells with one or two copies of *SIC1*, and reveals the phenotypic effects of *6xSIC1* on this threshold **(figure 25C)**.

The kinase assay results, and the genetic results for *SWE1*deletion and *2xSIC1*, argue that the cellular response to fixed peak endogenous B-cyclin is not significantly affected by post-translational inhibition. Furthermore, preliminary results tracing Sic1-GFP accumulation after release from *cdc20* arrest indicate that a sub-peak concentration of Clb2kd inhibits even transient Sic1 accumulation (Ying Lu, pers. comm.). The *swi5* result argues in a different direction; although not a definitive experiment because Swi5 has many transcriptional targets, these targets do include *SIC1* and *CDC6*, encoding stoichiometric inhibitors of Clb2-Cdk. If these inhibitors were strongly induced in our protocol, though, we expect

that this should be reflected in the *in vitro* kinase assay. The other possibility cited above, that additional Swi5 transcriptional targets such as Cyk3 might directly affect cytokinesis rather than inhibiting Clb2kd-Cdk activity, remains open. On balance, we favor the idea that the protein level of Clb2kd is a fair indicator of Clb2kd-Cdk kinase activity throughout our time-courses.

The kinase assay results have a second important consequence for our interpretation of the Clb2kd-YFP thresholds. Our interpretation depends on the assumption that deletion of the destruction and *KEN* boxes does not affect Clb2-Cdk biological or enzymatic activity. The kinase activity per unit protein of the Clb2kd-YFP pulse is the same as that of $Clb2^{WT}$-YFP **(figure 25A,B)**. This indicates that the db,ken deletions do not reduce Clb2kd-Cdk enzymatic activity compared to Clb2-wt-Cdk. Furthermore, the thresholds we measure are within the threshold range measured by Cross et al for $Clb2^{WT}$ inhibition of mitotic exit (Cross et al., 2005) – that is, close to the normal peak level. Although more approximate, this result suggests similar biological activity of Clb2kd and Clb2-wt, as well as similar enzymatic activity. Thus, overall, we think the evidence suggests that Clb2kd level is a good reporter for Clb2kd-Cdk activity level. If this is correct, the Clb2kd inhibitory thresholds we have measured relative to peak Clb2 are actually also Clb2-Cdk kinase activity thresholds. This poses a problem for the more sophisticated ratchet models that account for Clb-CDK inhibition independent of degradation.

Cdc14 release from the nucleolus occurs regardless of Clb2kd concentration.

Our analysis of Cdk inhibitors indicated that the Clb2kd inhibitory concentration thresholds were similar to Clb2-Cdk activity thresholds. Inhibition of Cdc14 release, which reverses Cdk-dependent phosphorylation, would provide a unified explanation for these findings. Clb-Cdk activity can repress the release of Cdc14 phosphatase through inhibitory phosphorylation of Cdc15 kinase (Jaspersen and Morgan, 2000). However, other results indicate that Clb2 promotes Cdc14 release, through phosphorylation and inhibition of Net1, a Cdc14 inhibitor (Azzam et al., 2004; Queralt and Uhlmann, 2008). Therefore we next investigated whether the effects of pulse activity were a consequence of inhibition of Cdc14 release.

We measured Cdc14 release by live single-cell microscopy as the ratio of the coefficient of variation (CV) of Cdc14-YFP intensity to the CV of Net1-mCherry intensity. Cdc14 is sequestered in the nucleolus and inhibited by Net1 (Shou et al., 1999; Visintin et al., 1999). Therefore this ratio reflects activity of Cdc14. Furthermore, this method controls for both mechanical artifacts, such as changes in focal plane, as well as biological artifacts, such as changes in nucleolar architecture during spindle elongation.

In cycling cells, as Cdc14 releases from Net1 and the nucleolus, its fluorescence becomes diffuse. Net1 remains tightly localized within the nucleolus **(figure 26A)**. Cdc14 is released within 10 minutes of spindle

elongation, as inferred by separation of the Net1-mCherry signal **(figure 26B)**. Cytokinesis occurs within 10 minutes of Cdc14 release, and rebudding occurs 20 minutes after Cdc14 release. Very similar timing is observed upon release from cdc20-arrest **(figure 26C)**. In cells pulsed with Clb2kd, bud formation may precede or follow cytokinesis, or either process may not occur, consistent with previous observations. Although timing of cytokinesis and rebudding is delayed, Cdc14 is released on time regardless of the phenotypic consequences of the pulse **(figure 26C**). We conclude that cytokinesis and rebudding are uncoupled from initial Cdc14 release by the Clb2kd pulse. Therefore, although Cdc14 release is essential for mitotic exit, differential release at different Clb2kd doses does not account for the effects of Clb2kd on mitotic exit or the subsequent cell cycle.

The Clb2kd-YFP thresholds are not explained by Cdk-dependent regulation of Cdc14 release. However, Cdc14 release might explain some of the effects of Clb2kd on post-anaphase events. Interestingly, for unknown reasons Cdc14 release, nucleolar reuptake and re-release can occur cyclically in Clb2kd-pulsed cells. Considering cells with multiple Cdc14 release events, c cytokinesis correlates strongly with Cdc14 release, whereas budding correlates less strongly **(figure 26D)**. Therefore, we propose that cells that cannot undergo cytokinesis during the first Cdc14 release tend to wait for the second release. This result presents a possible mechanistic basis for the difference in response of cytokinesis and bud formation to the same concentration of Clb2kd **(figure 14)**.

Figure 26. Cdc14 release from the nucleolus occurs independent of Clb2kd expression (courtesy of Ying Lu).

MET-CDC20 GAL4-rMR P_{GAL}→*CLB2kd* cells with the fluorescent marker alleles *CDC14-YFP*, *NET1-mCherry*, and *MYO1-GFP* were arrested and pulsed as described in figure 2. Upon release from cdc20-arrest, cells were analyzed by time-lapse fluorescence microscopy for Cdc14 release from Net1, cytokinesis, and bud formation. **(A)** A cdc20-arrested cell (t = 0 min) and a cell undergoing release of Cdc14 from the nucleolus (t = 24 min) are depicted. **(B)** Cdc14 localization versus time post-release for a cycling cell. Cdc14 release status is measured by the ratio of the coefficients of variation (CVs) of pixel intensities over the area of the cell for Cdc14-YFP and Net1-mCherry. Net1 remains localized to the nucleolus throughout the cell cycle, resulting in a high CV at all times; spreading of Cdc14 to a broader distribution lowers the CV; thus Cdc14 release is quantitatively measured by a decrease in the ratio of these CVs. Cytokinesis (red square) and rebudding (green square) are noted along the Cdc14 release trace when they occur. **(C)** Representative Cdc14 release traces for four phenotypic consequences of pulsed Clb2kd, ranked from top to bottom by correlation with increasing Clb2kd concentration: slightly delayed cytokinesis and normal rebudding, rebudding before cytokinesis, delayed rebudding and no cytokinesis, and persistent large-budded arrest. **(D)** Cdc14 release traces for Clb2kd-pulsed cells that do not undergo cytokinesis during the first release. First release (blue) and second release (green) are plotted with t=0 at the time of release. Cytokinesis (red squares) and rebudding (green squares) are noted.

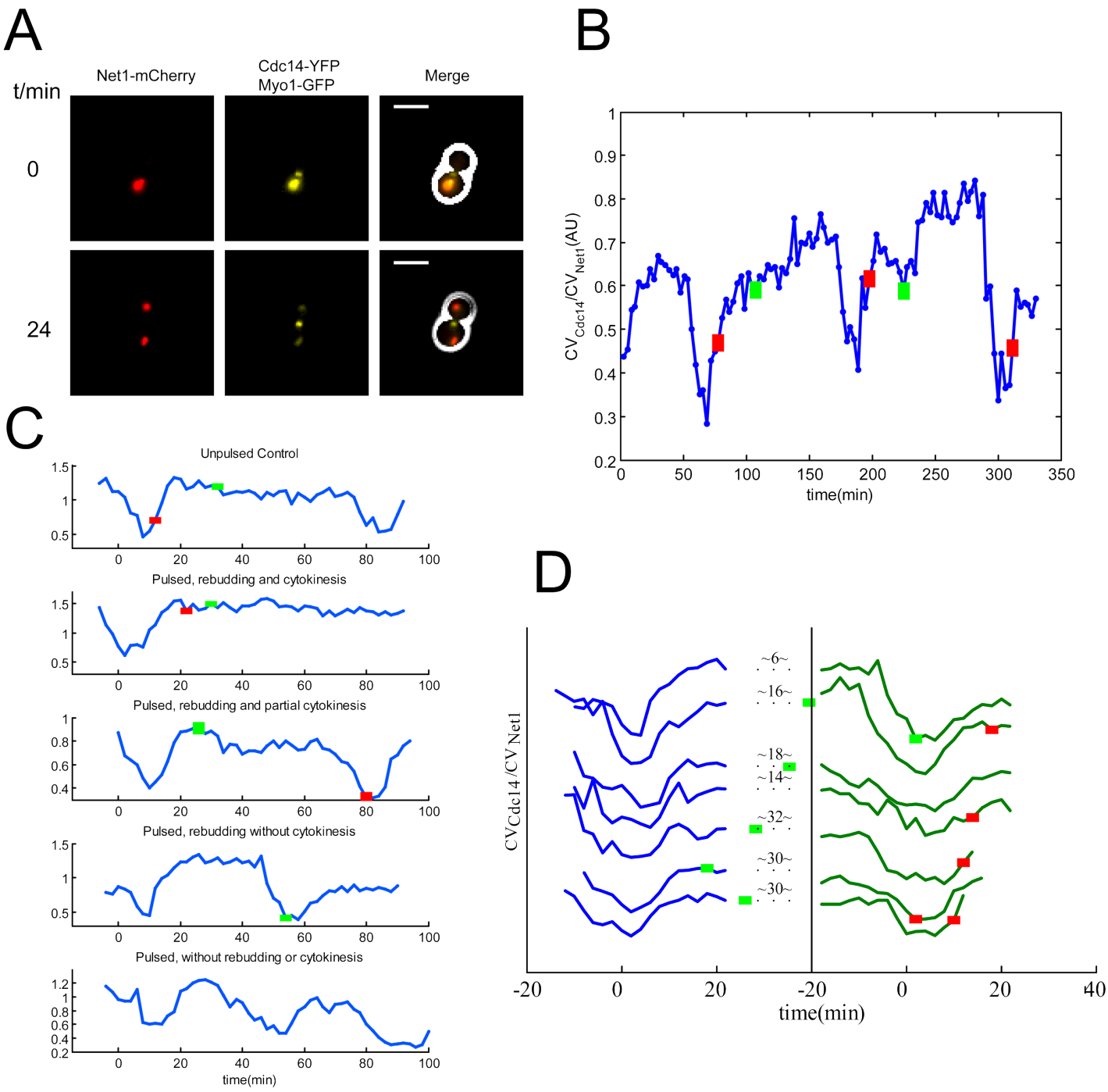
A
t/min
Net1-mCherry
Cdc14-YFP
Myo1-GFP
Merge
0
24
B
CVCdc14/CVNet1(AU)
time(min)
C
Unpulsed Control
Pulsed, rebudding and cytokinesis
Pulsed, rebudding and partial cytokinesis
Pulsed, rebudding without cytokinesis
Pulsed, without rebudding or cytokinesis
time(min)
D
CVCdc14/CVNet1
~6~
~16~
~18~
~14~
~32~
~30~
~30~
time(min)

Discussion

Cell division requires a precise sequence of processes, particularly with respect to chromosome duplication and segregation. The regulatory motifs that coordinate this sequence may be intrinsic or extrinsic to the processes involved. Chief among the extrinsic regulators of cell division is cyclin-dependent kinase (Cdk), which must bind cyclin to be active. Cyclin-Cdk complexes have been demonstrated to regulate many or all cell cycle processes (Morgan, 1997). For example, cyclin B-Cdk activity promotes DNA replication and entry into mitosis, but inhibits mitotic exit and several early steps in cell division.

The interpretations of Cdk-dependent cell cycle control are based mostly on comparison of strong overexpression to the absence of Cdk activity. Complete inhibition of cyclin B-Cdk activity prevents DNA replication and mitotic spindle synthesis. Over-accumulation of B-cyclin prevents cells from exiting mitosis or, if expressed just after mitotic exit, licensing origins and entering the subsequent cell cycle. Little is known about the relationship between amount of activity and the occurrence (i.e. thresholds), rate, and coordination of these processes. Therefore we titrated a fixed Clb2p level (Clb2kd) in metaphase-arrested cells, from super-physiological through peak and below, and monitored the events that occurred after release from arrest.

Caveats to the method.

The procedure used to determine Clb2 inhibitory thresholds is complicated, and as a result there are unavoidable uncertainties; we discussed these problems as they came up throughout the previous three chapters. We do not believe these problems invalidate the conclusions reached, but they need to be considered. To recapitulate:

First, our method necessarily makes heavy use of YFP-tagged versions of Clb2, which appear to somewhat alter activity and abundance; we do not consider these effects major and the experiments are appropriately controlled, but it is a deviation from wild-type.

Second, we assume that the *ken,db* mutations that stabilize Clb2kd do not also affect its activity compared to Clb2-wt. We know this assumption is true with respect to Clb2kd-Cdk vs. Clb2-Cdk enzymatic activity; biological activity is harder to evaluate, and the complete stabilization of Clb2 by these mutations is obviously essential for our method.

Third, we assume that the induced stable Clb2kd is the only relevant mitotic cyclin for inhibition of events of mitotic exit. We have both biochemical and genetic evidence that this is the case, but this evidence is somewhat incomplete.

Fourth, our method necessarily makes use of cell cycle block-release protocols, especially *cdc20* block-release. There could be many aspects of this procedure that perturb results relative to wild-type; one perturbation that is obvious is that the cells throughout the experiment are approximately two-fold

larger than asynchronous wild-type cells, due to continued cell growth at the *cdc20* block. We really have no way to evaluate how much this size difference may distort the measured inhibitory thresholds; one favorable point may be that we are measuring Clb2kd concentration rather than number of molecules per cell in all cases, making it more likely that cell size effects are neutralized.

Fifth, our method requires the use of strains in which the normal *CDC20* gene is replaced by a *MET3-CDC20* gene; thus this critical mitotic regulator is under abnormal control. For a variety of reasons discussed in detail in previous chapters, we do not consider this likely to cause any problems in interpretation.

Sixth, we assume that our *in vitro* kinase assay faithfully reflects *in vivo* enzymatic activity of Clb2kd-YFP-Cdk. Inhibitory proteins whose association is labile, or modifications that are labile *in vitro*, will not be detected in this assay. We have supported these observations with genetic experiments for significant known inhibitors (Sic1, Swe1), but any *in vitro* assay needs to be interpreted with caution before applying it quantitatively to the *in vivo* situation.

Seventh, our biological experiments necessarily measured Clb2kd-YFP levels in individual cells; we lack a single-cell assay for Clb2-Cdk enzymatic activity, though, and we cannot be sure that the single-cell level of Clb2kd directly varies with enzymatic activity. The analysis in Chapter 3 suggests, though, that overall, Clb2kd level is likely to be a good reporter for Clb2kd-Cdk enzymatic activity.

Eighth, our estimate of normal peak Clb2 levels is derived from synchronized populations, and thus is subject to various (probably minor) quantitative artifacts.

Two last points with respect to these caveats: first, the potential sources of error do not all point in the same direction with respect to accurate estimate of Clb2kd inhibitory thresholds, and hence may cancel each other out to some extent; second, some of the potential problems, if true, would only strengthen one of our main conclusions, that inhibitory thresholds for Clb2 in mitotic exit are surprisingly high, since some of the problems cited would only raise the 'true' threshold above our estimate.

Clb2 inhibitory thresholds are process-specific.

We measured multiple inhibitory dose-response relationships for Clb2kd, demonstrating that Clb2-Cdk does not inhibit all post-anaphase events to the same degree. Inhibition of spindle disassembly required the highest Clb2kd concentration of all processes studied, well above peak **(figure 13)**. Long-term inhibition (>45 min) of the initiation of cytokinesis also required high Clb2kd concentration, although less than spindle disassembly. Next in rank of sensitivity was bud formation, followed by completion of cytokinesis **(figure 14)**.

Peak-equivalent Clb2kd permitted cytokinesis with some delay. Cells that completed cytokinesis also replicated DNA and SPBs, demonstrating that the inhibitory Clb2kd thresholds for these processes were at least the cytokinesis threshold **(figure 15, 16)**. Since the Clb2kd pulse did not result in the accumulation of cells with 4C DNA content, DNA replication may share the same threshold as cytokinesis, or cytokinesis itself may inhibit DNA replication **(figure**

15). In contrast, a Clb2kd pulse that delayed cytokinesis did not delay SPB duplication **(figure 16)**. Hence inhibition of SPB duplication may require a higher concentration of Clb2. SPB duplication and bud formation both require activation of G1 cyclins. The inhibitory threshold for bud formation is greater than the cytokinesis threshold. Therefore we speculate that Clb2 could inhibit both SPB duplication and bud formation primarily through inhibition of SBF and G1 cyclin accumulation.

Metaphase spindle synthesis after SPB duplication and separation was inhibited at very low doses of Clb2kd **(figure 19)**. Spindle pole body maturation is interconnected with specific Clb function in complex ways, though (Haase et al., 2001), so persistent low-level Clb2 through the early stages of SPB maturation may have unexpected negative effects. Paradoxically, Clb2 normally promotes mitotic spindle synthesis (Fitch et al., 1992). Aberrant spindle formation in the presence of Clb2kd may be due to defective synthesis of the new SPB when carried out in the presence of Clb2kd **(figure 18)**. It is unlikely that a mechanism that causes defective SPB formation would confer a selective advantage. Therefore we propose that this is a deleterious consequence of persistent Clb2 in the subsequent cell cycle, which would select for complete mitotic cyclin degradation.

Sub-peak levels of Clb2kd inhibit α-factor arrest in the subsequent cell cycle of cells that complete mitotic exit (**figure 17).** This is surprising given that Clb2 has no known role in regulating the α-factor arrest response pathway, and very

little Clb2kd was required for this inhibition. Cells containing low levels of Clb2kd, after completing mitosis, could activate the *CLN2* promoter, rebud, duplicate SPBs and express endogenous Clb2 in the presence of α-factor **(figure 20)**. The mechanism by which Clb2kd disrupts α-factor arrest remains unclear; again, though, this observation could provide a rationale for complete mitotic cyclin degradation at the end of mitosis. Additionally, one could speculate that this inhibition is part of a mechanism to prevent α-factor arrest response during periods when Clb2 is being synthesized, since mating factor responsiveness is only biologically appropriate in G1.

Because of the diversity of these inhibitory thresholds, fixed Clb2p levels uncoupled post-mitotic events; for example, pulsed cells disassembled spindles without initiating cytokinesis, or rebudded without completing cytokinesis **(figure 12)**. These aberrant phenotypes are a manifestation of the varying inhibitory thresholds, and the occurrence of such cells represents internally controlled confirmation of our measurements of the thresholds, at least with respect to their relative magnitudes.

Clb2 induces a dose-dependent delay in process execution

The concept of an inhibitory threshold implies that below a certain level an event occurs and above this level it does not. However, we found that Clb2kd inhibition of post-mitotic events was not all-or-none. Instead, Clb2kd induced a

delay in process execution, and this delay scaled with concentration. Furthermore, the magnitude of the delay per unit Clb2kd was process-specific.

During mitotic exit, endogenous Clb2 is not fixed, but rapidly degraded by the APC. Therefore, it is unlikely that the differences in dose-dependent delays provide gross regulation of event timing. Instead, these rate effects may fine-tune the sequence of mitotic exit events. For instance, spindle disassembly exhibits a lesser delay per unit Clb2 than actomyosin ring contraction; this difference in sensitivity could contribute to these events occurring sequentially (the biologically appropriate order) during a single drop in Clb2 level, especially if this drop is unusually slow in some cells. In cases where Clb2 proteolysis in wild-type cells is generally complete before an event occurs, the threshold level for regulation may not be under tight selection. For example, the rate-effects on budding or subsequent events may not be calibrated to confer a selective advantage, since bud formation normally occurs considerably after Clb2 has been completely degraded.

The level of Clb2kd necessary to inhibit Pre-RC formation may be greater than that sufficient to promote DNA replication

Bipartite regulation of DNA replication has long been considered to be strong evidence for ratchet models (Nasmyth, 1996). In the absence of Clb5-Cdk activity, Clb2 can promote DNA replication without over-replication. We have indirectly evaluated the role of Clb2-Cdk inactivation in permitting Pre-RC

formation. Population analysis of the pulsed cultures revealed that cells that could execute cytokinesis, which is not stably inhibited by peak-equivalent Clb2kd, could also replicate DNA. Since the Clb2kd pulse is normally distributed and remains active throughout the time course, and Pre-RC formation is a prerequisite for DNA replication, we infer that peak Clb2-Cdk activity does not prevent Pre-RC formation. Therefore, it is unlikely that a Clb2-Cdk activity ratchet prevents re-replication.

Clb2 is not the principal cyclin responsible for driving DNA replication. Clb5 levels rise before Clb2, and Clb5-Cdk activates DNA replication more efficiently. Therefore, in order to thoroughly test the DNA replication ratchet model, Clb5-Cdk activity thresholds for inhibition of DNA replication would need to be measured and to be compared to peak Clb5 expression. Since unlike Clb2, Clb5 does not directly inhibit mitotic exit (Wäsch and Cross, 2002), a similar protocol to that described in **figure 1** could be employed to study the effects of highly overexpressed undegradable Clb5 on the subsequent cell cycle. Indeed, highly overexpressed undegradable Clb5 does appear to block replication after mitosis (Jacobson et al., 2000).

However, in the process of demonstrating that Clb5 does not inhibit mitotic exit, Wäsch and Cross have already presented data suggesting that persistent over-accumulated Clb5 does not prevent DNA replication. They employed an allele of *CLB5* that lacked a destruction box (*CLB5*Δ*db*), expressed from its endogenous promoter. Unlike *CLB2Δdb* cells, which arrest in telophase,

CLB5Δdb cells are viable despite over-accumulation of Clb5Δdb. Surprisingly, even in the absence of CKI-mediated inhibition, *CLB5Δdb sic1Δ* cells released from telophase arrest can exit mitosis and replicate DNA in the subsequent cycle, although the efficiency may have been lower based on an indirect plasmid retention assay (Wäsch and Cross, 2002). Therefore, high Clb5-Cdk activity may not prevent Pre-RC formation. Combined with the Clb2kd results presented here, these findings contradict control of DNA replication via a global Cdk activity ratchet. It is difficult to reconcile these findings with the results on the critical timing of pulses of Cdc6 on the ability to replicate (Piatti et al., 1996); however, the inference that Cdc6 had to be present before endogenous accumulation of Clb kinase was based largely on a correlational analysis, and on the potentially pleiotropic effects of a *clb5,6* deletion.

In contrast, our results, and the results of Wäsch and Cross 2002, suggest that endogenous peak levels of Clb2 or Clb5 do not efficiently block pre-RC formation; these experiments were performed without perturbing timing or levels of expression of the essential pre-RC component Cdc6.

Our data pose serious challenges to ratchet models involving global B-cyclin concentration and activity ratchet models for control of mitosis and mitotic exit.

The abilities of Cdks to both activate and inhibit different steps in cell division, combined with Cdk activity oscillation, have suggested a class of models, which

we call “ratchet” models. Ratchet models describe how the order of cell cycle events can be coupled to an oscillating regulator by precise quantitative coordination of activating and inhibiting thresholds. The relevant regulatory unit for a Cdk-dependent ratchet model may be cyclin concentration, Cdk activity, or Cdk substrate phosphorylation potential (sum of kinase and phosphatase activities). The relevant frame of reference may be whole-cell regulator level (global) or the level within a sub-cellular compartment (local).

Ratchet models concisely explain the effects of the absence, excess, or aberrant timing of cyclin B expression or Cyclin B / Cdk activity on DNA replication, mitosis and mitotic exit. However, the models make critical and precise predictions about inhibitory thresholds, and these thresholds have never been measured to our knowledge.

We measured several inhibitory thresholds for global Clb2kd concentration. Our indirect analysis of Clb2kd pulse activity suggests that concentration thresholds near peak Clb2 expression closely approximate activity thresholds. We compared these thresholds to peak Clb2 expression in order to evaluate the possible contribution of a regulatory ratchet to ordering cell cycle events.

We found that the level of Clb2kd necessary to inhibit mitotic exit is greater than that sufficient to promote mitosis. Complete inactivation of Clb2-Cdk is not required for mitotic exit. In fact, many elements of mitotic exit can proceed without any reduction from peak Clb2-Cdk activity. In addition to these problems

for ratchet control of mitosis, our results also pose problems for ratchet models for control of DNA replication (see above).

However, it is notable that while the inhibitory thresholds appear too high for ratchet models to operate, they are not too high by a large factor; a few-fold increase over peak-equivalent level is sufficient for Clb2kd to provide a major delay to mitotic exit. Given the number of caveats to our conclusions (see above), it is possible that a straightforward ratchet model might barely survive. Still, the measurements we have made leave very little room for this model to operate; we consider this unlikely.

Ratchet-like models that can accommodate our results

Our results, interpreted literally, formally contradict the global Clb2 concentration and activity ratchets for coordinating mitosis and mitotic exit. However, peak-equivalent Clb2kd does delay some aspects of mitotic exit. This finding suggests three possibilities that are not mutually exclusive:

1. **Mitotic exit events may require only a brief extrinsically imposed delay in order to follow mitosis.** Clb2kd does not inhibit mitotic exit at an all-or-none dosage threshold, but instead delays mitotic exit in proportion to its concentration. Furthermore, Clb2kd causes a greater delay per unit concentration for cytokinesis than for spindle disassembly, with bud formation falling in between. These findings suggest the specific

mitotic events may require different degrees of Cdk-dependent extrinsic delay in order to occur at the correct time. Much of the coordination of the timing of these events may be either intrinsic or mediated by Cdk-independent checkpoints. For example, if Myo1 ring contraction is possible as soon as budding occurs, then regulation of cytokinesis requires a substantial extrinsic delay. On the other hand, if construction of a contractile ring requires the majority of the budded period, or is inhibited by a surveillance mechanism that monitors spindle elongation, then little extrinsic delay is required for the ratchet model to be satisfied. Therefore, the relevant consideration may not be whether a regulatory ratchet controls these events, but how much of a regulatory ratchet these events require given their intrinsic timing and Cdk-independent regulation.

2. **Mitosis and mitotic exit may be coordinated by the summed activity of Cyclin B/Cdk-mediated phosphorylation and Cdc14-mediated dephosphorylation of specific targets.** In *cdc15-2* arrested cells, which cannot release Cdc14 from the nucleolus, APC^{Cdc20} activity reduces Clb2p concentration to approximately 1/3 peak. This level of Clb2 can maintain a telophase arrest in the absence of Cdc14 activity, but the block reverses rapidly upon Cdc14 release, even in the absence of Cdh1-dependent Clb2 degradation or Sic1 inhibition (Wäsch and Cross, 2002). Consistently, *cdc15-2* arrested cells can be induced to exit mitosis by overexpression of

Sic1 (Yeong et al., 2000). Cdc14 is released regardless of Clb2kd concentration **(figure 26)**. Therefore Cdc14 may play a significant role in dephosphorylating Cdk substrates to permit mitotic exit. Cdc14 is released periodically in cells inhibited by Clb2kd from completing mitotic exit **(figure 26C)**. Interestingly, in cells that could not complete cytokinesis after the first Cdc14 release, completion of cytokinesis correlated tightly with the second release **(figure 26D)**. This finding is consistent with co-regulation of mitotic exit substrate phosphorylation by Clb2-Cdk and Cdc14.

3. **Mitosis and mitotic exit may be coordinated by the local oscillation of Clb2-Cdk activity near their relevant substrates.** Neither Clb2 nor Cdc14 are evenly distributed throughout the cell, nor are their local concentrations constant. Therefore, it is likely that local activity near substrates is the relevant unit of regulation. However, it is not known whether Clb2-Cdk activity in all sub-cellular locations oscillates in proportion to global activity. Therefore, local regulatory ratchets are difficult to evaluate at present.

Conclusions.

How is the order of cell cycle events established? The simplest version of the ratchet model as it pertains to cyclin levels appears to be invalidated by the

present results. Our experiments measuring Clb2-Cdk activity levels, and genetically manipulating known Clb2-Cdk activity regulators, imply that a more sophisticated ratchet involving Cyclin-Cdk activity is also unlikely. A substrate-level phosphorylation ratchet can still function provided that phosphatase levels are cell-cycle-regulated, as is the case for Cdc14, due to regulated release from the nucleolus. This kind of ratchet may require a considerable degree of evolutionary tuning of phosphorylation-dephosphorylation kinetics of individual substrates to be robust, as well as spatial regulation of kinase-phosphatase balance.

It may be that the original formulation of Hartwell, in which coordination of timing of events is due to a combination of mechanical dependency and intrinsic time to complete a process, is largely sufficient to account for cell-cycle periodicity, especially when reinforced by checkpoint mechanisms in the rare events when uncoupling occurs (Hartwell and Weinert, 1989).

The demonstrated ability of Clb2-Cdk to inhibit mitotic exit at super-peak-equivalent levels may be relevant to checkpoint controls. It is striking that *cdc20*-blocked cells, which are presumably mimics of spindle-checkpoint-inhibited cells since Cdc20 is the target of this checkpoint, accumulate a super-peak level of Clb2 (about 2-fold the normal peak), sufficient for a very extended delay of mitotic exit according to our data. This may be the main biological function of the ability of Clb2 to inhibit mitotic exit, more than to regulate timing in the unperturbed cell cycle.

Bibliography

Amon, A., S. Irniger, and K. Nasmyth. 1994. Closing the cell cycle circle in yeast: G2 cyclin proteolysis initiated at mitosis persists until the activation of G1 cyclins in the next cycle. *Cell*. 77:1037-50.

Amon, A., U. Surana, I. Muroff, and K. Nasmyth. 1992. Regulation of p34CDC28 tyrosine phosphorylation is not required for entry into mitosis in S. cerevisiae. *Nature*. 355:368-71.

Amon, A., M. Tyers, B. Futcher, and K. Nasmyth. 1993. Mechanisms that help the yeast cell cycle clock tick: G2 cyclins transcriptionally activate G2 cyclins and repress G1 cyclins. *Cell*. 74:993-1007.

Archambault, V., C.X. Li, A.J. Tackett, R. Wäsch, B.T. Chait, M.P. Rout, and F.R. Cross. 2003. Genetic and biochemical evaluation of the importance of Cdc6 in regulating mitotic exit. *Mol Biol Cell*. 14:4592-604.

Azzam, R., S.L. Chen, W. Shou, A.S. Mah, G. Alexandru, K. Nasmyth, R.S. Annan, S.A. Carr, and R.J. Deshaies. 2004. Phosphorylation by cyclin B-Cdk underlies release of mitotic exit activator Cdc14 from the nucleolus. *Science*. 305:516-9.

Bailly, E., S. Cabantous, D. Sondaz, A. Bernadac, and M.N. Simon. 2003. Differential cellular localization among mitotic cyclins from Saccharomyces cerevisiae: a new role for the axial budding protein Bud3 in targeting Clb2 to the mother-bud neck. *J Cell Sci*. 116:4119-30.

Baumer, M., G.H. Braus, and S. Irniger. 2000. Two different modes of cyclin clb2 proteolysis during mitosis in Saccharomyces cerevisiae. *FEBS Lett*. 468:142-8.

Beach, D., B. Durkacz, and P. Nurse. 1982. Functionally homologous cell cycle control genes in budding and fission yeast. *Nature*. 300:706-9.

Bean, J.M., E.D. Siggia, and F.R. Cross. 2005. High functional overlap between MluI cell-cycle box binding factor and Swi4/6 cell-cycle box binding factor in the G1/S transcriptional program in Saccharomyces cerevisiae. *Genetics*. 171:49-61.

Bean, J.M., E.D. Siggia, and F.R. Cross. 2006. Coherence and timing of cell cycle start examined at single-cell resolution. *Mol Cell*. 21:3-14.

Bi, E., P. Maddox, D.J. Lew, E.D. Salmon, J.N. McMillan, E. Yeh, and J.R. Pringle. 1998. Involvement of an actomyosin contractile ring in Saccharomyces cerevisiae cytokinesis. *J Cell Biol*. 142:1301-12.

Biggar, S.R., and G.R. Crabtree. 2001. Cell signaling can direct either binary or graded transcriptional responses. *EMBO J*. 20:3167-76.

Bloom, J., and F.R. Cross. 2007a. Multiple levels of cyclin specificity in cell-cycle control. *Nat Rev Mol Cell Biol*. 8:149-60.

Bloom, J., and F.R. Cross. 2007b. Novel role for Cdc14 sequestration: Cdc14 dephosphorylates factors that promote DNA replication. *Mol Cell Biol*. 27:842-53.

Booher, R.N., R.J. Deshaies, and M.W. Kirschner. 1993. Properties of Saccharomyces cerevisiae wee1 and its differential regulation of p34CDC28 in response to G1 and G2 cyclins. *EMBO J*. 12:3417-26.

Broek, D., R. Bartlett, K. Crawford, and P. Nurse. 1991. Involvement of p34cdc2 in establishing the dependency of S phase on mitosis. *Nature*. 349:388-93.

Calzada, A., M. Sacristan, E. Sanchez, and A. Bueno. 2001. Cdc6 cooperates with Sic1 and Hct1 to inactivate mitotic cyclin-dependent kinases. *Nature*. 412:355-8.

Ciosk, R., W. Zachariae, C. Michaelis, A. Shevchenko, M. Mann, and K. Nasmyth. 1998. An ESP1/PDS1 complex regulates loss of sister chromatid cohesion at the metaphase to anaphase transition in yeast. *Cell*. 93:1067-76.

Cohen-Fix, O., and D. Koshland. 1999. Pds1p of budding yeast has dual roles: inhibition of anaphase initiation and regulation of mitotic exit. *Genes Dev*. 13:1950-9.

Cohen-Fix, O., J.M. Peters, M.W. Kirschner, and D. Koshland. 1996. Anaphase initiation in Saccharomyces cerevisiae is controlled by the APC-dependent degradation of the anaphase inhibitor Pds1p. *Genes Dev*. 10:3081-93.

Correa-Bordes, J., and P. Nurse. 1995. p25rum1 orders S phase and mitosis by acting as an inhibitor of the p34cdc2 mitotic kinase. *Cell*. 83:1001-9.

Costanzo, M., J.L. Nishikawa, X. Tang, J.S. Millman, O. Schub, K. Breitkreuz, D. Dewar, I. Rupes, B. Andrews, and M. Tyers. 2004. CDK activity antagonizes Whi5, an inhibitor of G1/S transcription in yeast. *Cell*. 117:899-913.

Cross, F.R. 1988. DAF1, a mutant gene affecting size control, pheromone arrest, and cell cycle kinetics of Saccharomyces cerevisiae. *Mol Cell Biol*. 8:4675-84.

Cross, F.R. 2003. Two redundant oscillatory mechanisms in the yeast cell cycle. *Dev Cell*. 4:741-52.

Cross, F.R., V. Archambault, M. Miller, and M. Klovstad. 2002. Testing a mathematical model of the yeast cell cycle. *Mol Biol Cell*. 13:52-70.

Cross, F.R., L. Schroeder, M. Kruse, and K.C. Chen. 2005. Quantitative characterization of a mitotic cyclin threshold regulating exit from mitosis. *Mol Biol Cell*. 16:2129-38.

Cross, F.R., and A.H. Tinkelenberg. 1991. A potential positive feedback loop controlling CLN1 and CLN2 gene expression at the start of the yeast cell cycle. *Cell*. 65:875-83.

D'Amours, D., and A. Amon. 2004. At the interface between signaling and executing anaphase--Cdc14 and the FEAR network. *Genes Dev*. 18:2581-95.

Dahmann, C., J.F. Diffley, and K.A. Nasmyth. 1995. S-phase-promoting cyclin-dependent kinases prevent re-replication by inhibiting the transition of replication origins to a pre-replicative state. *Curr Biol*. 5:1257-69.

de Bruin, R.A., W.H. McDonald, T.I. Kalashnikova, J. Yates, 3rd, and C. Wittenberg. 2004. Cln3 activates G1-specific transcription via phosphorylation of the SBF bound repressor Whi5. *Cell*. 117:887-98.

Detweiler, C.S., and J.J. Li. 1998. Ectopic induction of Clb2 in early G1 phase is sufficient to block prereplicative complex formation in Saccharomyces cerevisiae. *Proc Natl Acad Sci U S A*. 95:2384-9.

Di Talia, S., J.M. Skotheim, J.M. Bean, E.D. Siggia, and F.R. Cross. 2007. The effects of molecular noise and size control on variability in the budding yeast cell cycle. *Nature*. 448:947-51.

Diffley, J.F., J.H. Cocker, S.J. Dowell, and A. Rowley. 1994. Two steps in the assembly of complexes at yeast replication origins in vivo. *Cell*. 78:303-16.

Dirick, L., T. Bohm, and K. Nasmyth. 1995. Roles and regulation of Cln-Cdc28 kinases at the start of the cell cycle of Saccharomyces cerevisiae. *EMBO J*. 14:4803-13.

Dirick, L., and K. Nasmyth. 1991. Positive feedback in the activation of G1 cyclins in yeast. *Nature*. 351:754-7.

Donaldson, A.D., M.K. Raghuraman, K.L. Friedman, F.R. Cross, B.J. Brewer, and W.L. Fangman. 1998. CLB5-dependent activation of late replication origins in S. cerevisiae. *Mol Cell*. 2:173-82.

Dunphy, W.G. 1994. The decision to enter mitosis. *Trends Cell Biol*. 4:202-7.

Elledge, S.J. 1996. Cell cycle checkpoints: preventing an identity crisis. *Science*. 274:1664-72.

Elsasser, S., F. Lou, B. Wang, J.L. Campbell, and A. Jong. 1996. Interaction between yeast Cdc6 protein and B-type cyclin/Cdc28 kinases. *Mol Biol Cell*. 7:1723-35.

Enoch, T., K.L. Gould, and P. Nurse. 1991. Mitotic checkpoint control in fission yeast. *Cold Spring Harb Symp Quant Biol*. 56:409-16.

Epstein, C.B., and F.R. Cross. 1992. CLB5: a novel B cyclin from budding yeast with a role in S phase. *Genes Dev*. 6:1695-706.

Evans, T., E.T. Rosenthal, J. Youngblom, D. Distel, and T. Hunt. 1983. Cyclin: a protein specified by maternal mRNA in sea urchin eggs that is destroyed at each cleavage division. *Cell*. 33:389-96.

Fisher, D.L., and P. Nurse. 1996. A single fission yeast mitotic cyclin B p34cdc2 kinase promotes both S-phase and mitosis in the absence of G1 cyclins. *EMBO J*. 15:850-60.

Fitch, I., C. Dahmann, U. Surana, A. Amon, K. Nasmyth, L. Goetsch, B. Byers, and B. Futcher. 1992. Characterization of four B-type cyclin

genes of the budding yeast Saccharomyces cerevisiae. *Mol Biol Cell*. 3:805-18.

Gautier, J., C. Norbury, M. Lohka, P. Nurse, and J. Maller. 1988. Purified maturation-promoting factor contains the product of a Xenopus homolog of the fission yeast cell cycle control gene cdc2+. *Cell*. 54:433-9.

Gerhart, J., M. Wu, and M. Kirschner. 1984. Cell cycle dynamics of an M-phase-specific cytoplasmic factor in Xenopus laevis oocytes and eggs. *J Cell Biol*. 98:1247-55.

Glotzer, M., A.W. Murray, and M.W. Kirschner. 1991. Cyclin is degraded by the ubiquitin pathway. *Nature*. 349:132-8.

Haase, S.B., M. Winey, and S.I. Reed. 2001. Multi-step control of spindle pole body duplication by cyclin-dependent kinase. *Nat Cell Biol*. 3:38-42.

Hartwell, L.H., J. Culotti, J.R. Pringle, and B.J. Reid. 1974. Genetic control of the cell division cycle in yeast. *Science*. 183:46-51.

Hartwell, L.H., and T.A. Weinert. 1989. Checkpoints: controls that ensure the order of cell cycle events. *Science*. 246:629-34.

Harvey, S.L., A. Charlet, W. Haas, S.P. Gygi, and D.R. Kellogg. 2005. Cdk1-dependent regulation of the mitotic inhibitor Wee1. *Cell*. 122:407-20.

Harvey, S.L., and D.R. Kellogg. 2003. Conservation of mechanisms controlling entry into mitosis: budding yeast wee1 delays entry into mitosis and is required for cell size control. *Curr Biol*. 13:264-75.

Hayles, J., D. Fisher, A. Woollard, and P. Nurse. 1994. Temporal order of S phase and mitosis in fission yeast is determined by the state of the p34cdc2-mitotic B cyclin complex. *Cell*. 78:813-22.

Holloway, S.L., M. Glotzer, R.W. King, and A.W. Murray. 1993. Anaphase is initiated by proteolysis rather than by the inactivation of maturation-promoting factor. *Cell*. 73:1393-402.

Hu, F., and O.M. Aparicio. 2005. Swe1 regulation and transcriptional control restrict the activity of mitotic cyclins toward replication proteins in Saccharomyces cerevisiae. *Proc Natl Acad Sci U S A*. 102:8910-5.

Huang, J.N., I. Park, E. Ellingson, L.E. Littlepage, and D. Pellman. 2001. Activity of the APC(Cdh1) form of the anaphase-promoting complex persists until S phase and prevents the premature expression of Cdc20p. *J Cell Biol*. 154:85-94.

Hwang, L.H., L.F. Lau, D.L. Smith, C.A. Mistrot, K.G. Hardwick, E.S. Hwang, A. Amon, and A.W. Murray. 1998. Budding yeast Cdc20: a target of the spindle checkpoint. *Science*. 279:1041-4.

Irniger, S., S. Piatti, C. Michaelis, and K. Nasmyth. 1995. Genes involved in sister chromatid separation are needed for B-type cyclin proteolysis in budding yeast. *Cell*. 81:269-78.

Jacobson, M.D., S. Gray, M. Yuste-Rojas, and F.R. Cross. 2000. Testing cyclin specificity in the exit from mitosis. *Mol Cell Biol*. 20:4483-93.

Jaspersen, S.L., J.F. Charles, and D.O. Morgan. 1999. Inhibitory phosphorylation of the APC regulator Hct1 is controlled by the kinase Cdc28 and the phosphatase Cdc14. *Curr Biol*. 9:227-36.

Jaspersen, S.L., and D.O. Morgan. 2000. Cdc14 activates cdc15 to promote mitotic exit in budding yeast. *Curr Biol*. 10:615-8.

Johnston, G.C., J.R. Pringle, and L.H. Hartwell. 1977. Coordination of growth with cell division in the yeast Saccharomyces cerevisiae. *Exp Cell Res*. 105:79-98.

Keaton, M.A., E.S. Bardes, A.R. Marquitz, C.D. Freel, T.R. Zyla, J. Rudolph, and D.J. Lew. 2007. Differential susceptibility of yeast S and M phase CDK complexes to inhibitory tyrosine phosphorylation. *Curr Biol*. 17:1181-9.

King, R.W., P.K. Jackson, and M.W. Kirschner. 1994. Mitosis in transition. *Cell*. 79:563-71.

King, R.W., J.M. Peters, S. Tugendreich, M. Rolfe, P. Hieter, and M.W. Kirschner. 1995. A 20S complex containing CDC27 and CDC16 catalyzes the mitosis-specific conjugation of ubiquitin to cyclin B. *Cell*. 81:279-88.

Kleppe, K., E. Ohtsuka, R. Kleppe, I. Molineux, and H.G. Khorana. 1971. Studies on polynucleotides. XCVI. Repair replications of short synthetic DNA's as catalyzed by DNA polymerases. *J Mol Biol*. 56:341-61.

Knapp, D., L. Bhoite, D.J. Stillman, and K. Nasmyth. 1996. The transcription factor Swi5 regulates expression of the cyclin kinase inhibitor p40SIC1. *Mol Cell Biol*. 16:5701-7.

Ko, N., R. Nishihama, G.H. Tully, D. Ostapenko, M.J. Solomon, D.O. Morgan, and J.R. Pringle. 2007. Identification of yeast IQGAP (Iqg1p) as an anaphase-promoting-complex substrate and its role in actomyosin-ring-independent cytokinesis. *Mol Biol Cell*. 18:5139-53.

Levine, K., K. Huang, and F.R. Cross. 1996. Saccharomyces cerevisiae G1 cyclins differ in their intrinsic functional specificities. *Mol Cell Biol*. 16:6794-803.

Lew, D.J., and S.I. Reed. 1993. Morphogenesis in the yeast cell cycle: regulation by Cdc28 and cyclins. *J Cell Biol*. 120:1305-20.

Lohka, M.J., M.K. Hayes, and J.L. Maller. 1988. Purification of maturation-promoting factor, an intracellular regulator of early mitotic events. *Proc Natl Acad Sci U S A*. 85:3009-13.

MacKay, V.L., B. Mai, L. Waters, and L.L. Breeden. 2001. Early cell cycle box-mediated transcription of CLN3 and SWI4 contributes to the proper timing of the G(1)-to-S transition in budding yeast. *Mol Cell Biol*. 21:4140-8.

Mattioni, T., J.F. Louvion, and D. Picard. 1994. Regulation of protein activities by fusion to steroid binding domains. *Methods Cell Biol*. 43 Pt A:335-52.

McMillan, J.N., C.L. Theesfeld, J.C. Harrison, E.S. Bardes, and D.J. Lew. 2002. Determinants of Swe1p degradation in Saccharomyces cerevisiae. *Mol Biol Cell*. 13:3560-75.

Mcnulty, J.J. and Lew D.J. 2005. Swe1p responds to cytoskeletal perturbation, not bud size, in S. cerevisiae. *Curr Biol.* 20;15(24):2190-8.

Mendenhall, M.D., W. al-Jumaily, and T.T. Nugroho. 1995. The Cdc28 inhibitor p40SIC1. *Prog Cell Cycle Res*. 1:173-85.

Michaelis, C., R. Ciosk, and K. Nasmyth. 1997. Cohesins: chromosomal proteins that prevent premature separation of sister chromatids. *Cell*. 91:35-45.

Miller, M.E., and F.R. Cross. 2001. Cyclin specificity: how many wheels do you need on a unicycle? *J Cell Sci*. 114:1811-20.

Minshull, J., J. Pines, R. Golsteyn, N. Standart, S. Mackie, A. Colman, J. Blow, J.V. Ruderman, M. Wu, and T. Hunt. 1989. The role of cyclin synthesis, modification and destruction in the control of cell division. *J Cell Sci Suppl*. 12:77-97.

Moll, T., G. Tebb, U. Surana, H. Robitsch, and K. Nasmyth. 1991. The role of phosphorylation and the CDC28 protein kinase in cell cycle-regulated nuclear import of the S. cerevisiae transcription factor SWI5. *Cell*. 66:743-58.

Moreno, S., K. Labib, J. Correa, and P. Nurse. 1994. Regulation of the cell cycle timing of Start in fission yeast by the rum1+ gene. *J Cell Sci Suppl*. 18:63-8.

Morgan, D.O. 1996. The dynamics of cyclin dependent kinase structure. *Curr Opin Cell Biol*. 8:767-72.

Morgan, D.O. 1997. Cyclin-dependent kinases: engines, clocks, and microprocessors. *Annu Rev Cell Dev Biol*. 13:261-91.

Murray, A.E., and T. Hunt. 1993. The Cell Cycle. W. H. Freeman, New York.

Murray, A.W., and M.W. Kirschner. 1989a. Cyclin synthesis drives the early embryonic cell cycle. *Nature*. 339:275-80.

Murray, A.W., and M.W. Kirschner. 1989b. Dominoes and clocks: the union of two views of the cell cycle. *Science*. 246:614-21.

Murray, A.W., M.J. Solomon, and M.W. Kirschner. 1989. The role of cyclin synthesis and degradation in the control of maturation promoting factor activity. *Nature*. 339:280-6.

Nash, R., G. Tokiwa, S. Anand, K. Erickson, and A.B. Futcher. 1988. The WHI1+ gene of Saccharomyces cerevisiae tethers cell division to cell size and is a cyclin homolog. *EMBO J*. 7:4335-46.

Nasmyth, K. 1996. At the heart of the budding yeast cell cycle. *Trends Genet*. 12:405-12.

Nguyen, V.Q., C. Co, and J.J. Li. 2001. Cyclin-dependent kinases prevent DNA re-replication through multiple mechanisms. *Nature*. 411:1068-73.

Noton, E., and J.F. Diffley. 2000. CDK inactivation is the only essential function of the APC/C and the mitotic exit network proteins for origin resetting during mitosis. *Mol Cell*. 5:85-95.

Orr-Weaver, T.L. 1999. The ties that bind: localization of the sister-chromatid cohesin complex on yeast chromosomes. *Cell*. 99:1-4.

Pfleger, C.M., and M.W. Kirschner. 2000. The KEN box: an APC recognition signal distinct from the D box targeted by Cdh1. *Genes Dev*. 14:655-65.

Piatti, S., T. Bohm, J.H. Cocker, J.F. Diffley, and K. Nasmyth. 1996. Activation of S-phase-promoting CDKs in late G1 defines a "point of no return" after which Cdc6 synthesis cannot promote DNA replication in yeast. *Genes Dev*. 10:1516-31.

Piatti, S., C. Lengauer, and K. Nasmyth. 1995. Cdc6 is an unstable protein whose de novo synthesis in G1 is important for the onset of S phase and for preventing a 'reductional' anaphase in the budding yeast Saccharomyces cerevisiae. *EMBO J*. 14:3788-99.

Potapova, T.A., J.R. Daum, B.D. Pittman, J.R. Hudson, T.N. Jones, D.L. Satinover, P.T. Stukenberg, and G.J. Gorbsky. 2006. The reversibility of mitotic exit in vertebrate cells. *Nature*. 440:954-8.

Prinz, S., E.S. Hwang, R. Visintin, and A. Amon. 1998. The regulation of Cdc20 proteolysis reveals a role for APC components Cdc23 and Cdc27 during S phase and early mitosis. *Curr Biol*. 8:750-60.

Queralt, E., and F. Uhlmann. 2008. Separase cooperates with Zds1 and Zds2 to activate Cdc14 phosphatase in early anaphase. *J Cell Biol*.

Rao, P.N., and R.T. Johnson. 1970. Mammalian cell fusion: studies on the regulation of DNA synthesis and mitosis. *Nature*. 225:159-64.

Rudner, A.D., K.G. Hardwick, and A.W. Murray. 2000. Cdc28 activates exit from mitosis in budding yeast. *J Cell Biol*. 149:1361-76.

Rudner, A.D., and A.W. Murray. 2000. Phosphorylation by Cdc28 activates the Cdc20-dependent activity of the anaphase-promoting complex. *J Cell Biol*. 149:1377-90.

Schneider, B.L., Q.H. Yang, and A.B. Futcher. 1996. Linkage of replication to start by the Cdk inhibitor Sic1. *Science*. 272:560-2.

Schwab, M., A.S. Lutum, and W. Seufert. 1997. Yeast Hct1 is a regulator of Clb2 cyclin proteolysis. *Cell*. 90:683-93.

Schwann, T., Schleyden, MJ. 1847. Microscopical researches into the accordance in the structure and growth of animals and plants. Printed for the Sydenham Society, London.

Schwob, E., T. Bohm, M.D. Mendenhall, and K. Nasmyth. 1994. The B-type cyclin kinase inhibitor p40SIC1 controls the G1 to S transition in S. cerevisiae. *Cell*. 79:233-44.

Schwob, E., and K. Nasmyth. 1993. CLB5 and CLB6, a new pair of B cyclins involved in DNA replication in Saccharomyces cerevisiae. *Genes Dev*. 7:1160-75.

Shirayama, M., A. Toth, M. Galova, and K. Nasmyth. 1999. APC(Cdc20) promotes exit from mitosis by destroying the anaphase inhibitor Pds1 and cyclin Clb5. *Nature*. 402:203-7.

Shirayama, M., W. Zachariae, R. Ciosk, and K. Nasmyth. 1998. The Polo-like kinase Cdc5p and the WD-repeat protein Cdc20p/fizzy are regulators and substrates of the anaphase promoting complex in Saccharomyces cerevisiae. *EMBO J*. 17:1336-49.

Shou, W., J.H. Seol, A. Shevchenko, C. Baskerville, D. Moazed, Z.W. Chen, J. Jang, H. Charbonneau, and R.J. Deshaies. 1999. Exit from mitosis is triggered by Tem1-dependent release of the protein phosphatase Cdc14 from nucleolar RENT complex. *Cell*. 97:233-44.

Sia, R.A., H.A. Herald, and D.J. Lew. 1996. Cdc28 tyrosine phosphorylation and the morphogenesis checkpoint in budding yeast. *Mol Biol Cell*. 7:1657-66.

Simmons Kovacs, L.A., C.L. Nelson, and S.B. Haase. 2008. Intrinsic and Cyclin-dependent Kinase-dependent Control of Spindle Pole Body Duplication in Budding Yeast. *Mol Biol Cell*. 19:3243-53.

Skotheim, J.M., S. Di Talia, E.D. Siggia, and F.R. Cross. 2008. Positive feedback of G1 cyclins ensures coherent cell cycle entry. *Nature*. 454:291-6.

Stern, B., and P. Nurse. 1996. A quantitative model for the cdc2 control of S phase and mitosis in fission yeast. *Trends Genet*. 12:345-50.

Straight, A.F., W.F. Marshall, J.W. Sedat, and A.W. Murray. 1997. Mitosis in living budding yeast: anaphase A but no metaphase plate. *Science*. 277:574-8.

Sullivan, M., and F. Uhlmann. 2003. A non-proteolytic function of separase links the onset of anaphase to mitotic exit. *Nat Cell Biol*. 5:249-54.

Surana, U., A. Amon, C. Dowzer, J. McGrew, B. Byers, and K. Nasmyth. 1993. Destruction of the CDC28/CLB mitotic kinase is not required for the metaphase to anaphase transition in budding yeast. *EMBO J*. 12:1969-78.

Surana, U., H. Robitsch, C. Price, T. Schuster, I. Fitch, A.B. Futcher, and K. Nasmyth. 1991. The role of CDC28 and cyclins during mitosis in the budding yeast S. cerevisiae. *Cell*. 65:145-61.

Tanaka, S., T. Umemori, K. Hirai, S. Muramatsu, Y. Kamimura, and H. Araki. 2007. CDK-dependent phosphorylation of Sld2 and Sld3 initiates DNA replication in budding yeast. *Nature*. 445:328-32.

Thornton, B.R., and D.P. Toczyski. 2003. Securin and B-cyclin/CDK are the only essential targets of the APC. *Nat Cell Biol*. 5:1090-4.

Toyn, J.H., A.L. Johnson, J.D. Donovan, W.M. Toone, and L.H. Johnston. 1997. The Swi5 transcription factor of Saccharomyces cerevisiae has a role in exit from mitosis through induction of the cdk-inhibitor Sic1 in telophase. *Genetics*. 145:85-96.

Tyers, M. 1996. The cyclin-dependent kinase inhibitor p40SIC1 imposes the requirement for Cln G1 cyclin function at Start. *Proc Natl Acad Sci U S A*. 93:7772-6.

Tyers, M., G. Tokiwa, and B. Futcher. 1993. Comparison of the Saccharomyces cerevisiae G1 cyclins: Cln3 may be an upstream activator of Cln1, Cln2 and other cyclins. *EMBO J*. 12:1955-68.

Uhlmann, F., F. Lottspeich, and K. Nasmyth. 1999. Sister-chromatid separation at anaphase onset is promoted by cleavage of the cohesin subunit Scc1. *Nature*. 400:37-42.

Uhlmann, F., D. Wernic, M.A. Poupart, E.V. Koonin, and K. Nasmyth. 2000. Cleavage of cohesin by the CD clan protease separin triggers anaphase in yeast. *Cell*. 103:375-86.

Verma, R., R.S. Annan, M.J. Huddleston, S.A. Carr, G. Reynard, and R.J. Deshaies. 1997. Phosphorylation of Sic1p by G1 Cdk required for its degradation and entry into S phase. *Science*. 278:455-60.

Visintin, R., K. Craig, E.S. Hwang, S. Prinz, M. Tyers, and A. Amon. 1998. The phosphatase Cdc14 triggers mitotic exit by reversal of Cdk-dependent phosphorylation. *Mol Cell*. 2:709-18.

Visintin, R., E.S. Hwang, and A. Amon. 1999. Cfi1 prevents premature exit from mitosis by anchoring Cdc14 phosphatase in the nucleolus. *Nature*. 398:818-23.

Visintin, R., S. Prinz, and A. Amon. 1997. CDC20 and CDH1: a family of substrate-specific activators of APC-dependent proteolysis. *Science*. 278:460-3.

Wäsch, R., and F.R. Cross. 2002. APC-dependent proteolysis of the mitotic cyclin Clb2 is essential for mitotic exit. *Nature*. 418:556-62.

Weinert, T., and L. Hartwell. 1989. Control of G2 delay by the rad9 gene of Saccharomyces cerevisiae. *J Cell Sci Suppl*. 12:145-8.

Wilmes, G.M., V. Archambault, R.J. Austin, M.D. Jacobson, S.P. Bell, and F.R. Cross. 2004. Interaction of the S-phase cyclin Clb5 with an "RXL" docking sequence in the initiator protein Orc6 provides an origin-localized replication control switch. *Genes Dev*. 18:981-91.

Wittenberg, C., K. Sugimoto, and S.I. Reed. 1990. G1-specific cyclins of S. cerevisiae: cell cycle periodicity, regulation by mating pheromone, and association with the p34CDC28 protein kinase. *Cell*. 62:225-37.

Wolfe, K.H., and D.C. Shields. 1997. Molecular evidence for an ancient duplication of the entire yeast genome. *Nature*. 387:708-13.

Wuarin, J., V. Buck, P. Nurse, and J.B. Millar. 2002. Stable association of mitotic cyclin B/Cdc2 to replication origins prevents endoreduplication. *Cell*. 111:419-31.

Wuarin, J., and P. Nurse. 1996. Regulating S phase: CDKs, licensing and proteolysis. *Cell*. 85:785-7.

Yeong, F.M., H.H. Lim, C.G. Padmashree, and U. Surana. 2000. Exit from mitosis in budding yeast: biphasic inactivation of the Cdc28-Clb2 mitotic kinase and the role of Cdc20. *Mol Cell*. 5:501-11.

Zachariae, W., and K. Nasmyth. 1996. TPR proteins required for anaphase progression mediate ubiquitination of mitotic B-type cyclins in yeast. *Mol Biol Cell*. 7:791-801.

Zachariae, W., and K. Nasmyth. 1999. Whose end is destruction: cell division and the anaphase-promoting complex. *Genes Dev*. 13:2039-58.

Zachariae, W., M. Schwab, K. Nasmyth, and W. Seufert. 1998. Control of cyclin ubiquitination by CDK-regulated binding of Hct1 to the anaphase promoting complex. *Science*. 282:1721-4.

Zegerman, P., and J.F. Diffley. 2007. Phosphorylation of Sld2 and Sld3 by cyclin-dependent kinases promotes DNA replication in budding yeast. *Nature*. 445:281-5.